

# *Modes of climate variability: synthesis and review of proxy-based reconstructions through the Holocene*

Article

Accepted Version

Creative Commons: Attribution-Noncommercial-No Derivative Works 4.0

Hernández, A., Martin-Puertas, C., Moffa-Sánchez, P., Moreno-Chamarro, E., Ortega, P., Blockley, S., Cobb, K. M., Comas-Bru, L. ORCID: <https://orcid.org/0000-0002-7882-4996>, Giralt, S., Goosse, H., Luterbacher, J., Martrat, B., Muscheler, R., Parnell, A., Pla-Rabes, S., Sjolte, J., Scaife, A. A., Swingedouw, D., Wise, E. and Xu, G. (2020) Modes of climate variability: synthesis and review of proxy-based reconstructions through the Holocene. *Earth Science Reviews*, 209. 103286. ISSN 0012-8252 doi: <https://doi.org/10.1016/j.earscirev.2020.103286> Available at <https://centaur.reading.ac.uk/91739/>

It is advisable to refer to the publisher's version if you intend to cite from the work. See [Guidance on citing](#).

To link to this article DOI: <http://dx.doi.org/10.1016/j.earscirev.2020.103286>

Publisher: Elsevier

All outputs in CentAUR are protected by Intellectual Property Rights law, including copyright law. Copyright and IPR is retained by the creators or other copyright holders. Terms and conditions for use of this material are defined in

the [End User Agreement](#).

[www.reading.ac.uk/centaur](http://www.reading.ac.uk/centaur)

## **CentAUR**

Central Archive at the University of Reading

Reading's research outputs online

**Abstract**

Modes of climate variability affect global and regional climates on different spatio-temporal scales, and they have important impacts on human activities and ecosystems. As these modes are a useful tool for simplifying the understanding of the climate system, it is crucial that we gain improved knowledge of their long-term past evolution and interactions over time to contextualise their present and future behaviour. We review the literature focused on proxy-based reconstructions of modes of climate variability during the Holocene (i.e., the last 11.7 thousand years) with a special emphasis on i) proxy-based reconstruction methods; ii) available proxy-based reconstructions of the main modes of variability, i.e., El Niño Southern Oscillation, Pacific Decadal Variability, Atlantic Multidecadal Variability, the North Atlantic Oscillation, the Southern Annular Mode and the Indian Ocean Dipole; iii) major interactions between these modes; and iv) external forcing mechanisms related to the evolution of these modes. This review shows that modes of variability can be reconstructed using proxy-based records from a wide range of natural archives, but these reconstructions are scarce beyond the last millennium, partly due to the lack of robust chronologies with reduced dating uncertainties, technical issues related to proxy calibration, and difficulty elucidating their stationary impact (or not) on regional climates over time. While for each mode the available reconstructions tend to agree at multidecadal timescales, they show notable disagreement on shorter timescales beyond the instrumental period. The reviewed evidence suggests that the intrinsic variability of modes can be modulated by external forcing, such as orbital, solar, volcanic, and anthropogenic forcing. The review also highlights some modes experience higher variability over the instrumental period, which is partly ascribed to anthropogenic forcing. These features stress the paramount importance of further studying their past variations using long climate-proxy records for the progress of climate science.

## Modes of climate variability: Synthesis and review of proxy-based reconstructions through the Holocene

Armand Hernández<sup>1\*</sup>, Celia Martín-Puertas<sup>2</sup>, Paola Moffa-Sánchez<sup>3</sup>, Eduardo Moreno-Chamarro<sup>4</sup>, Pablo Ortega<sup>4</sup>, Simon Blockley<sup>2</sup>, Kim M. Cobb<sup>5</sup>, Laia Comas-Bru<sup>6</sup>, Santiago Giralt<sup>1</sup>, Hugues Goosse<sup>7</sup>, Jürg Luterbacher<sup>8,9</sup>, Belen Martrat<sup>10</sup>, Raimund Muscheler<sup>11</sup>, Andrew Parnell<sup>12</sup>, Sergi Pla-Rabes<sup>13,14</sup>, Jesper Sjolte<sup>11</sup>, Adam A. Scaife<sup>15,16</sup>, Didier Swingedouw<sup>17</sup>, Erika Wise<sup>18</sup>, Guobao Xu<sup>19,20</sup>

<sup>1</sup> Institute of Earth Sciences Jaume Almera, ICTJA, CSIC, 08028 Barcelona, Spain

<sup>2</sup> Department of Geography, Royal Holloway University of London, TW20 0EX Egham, UK

<sup>3</sup> Department of Geography, Durham University, Durham, UK, DH1 3LE

<sup>4</sup> Barcelona Supercomputing Center (BSC), Barcelona, Spain.

<sup>5</sup> School of Earth and Atmospheric Sciences, Georgia Institute of Technology, Atlanta, GA, USA

<sup>6</sup> School of Archaeology, Geography & Environmental Sciences, University of Reading, RG6 6AH Reading, Berkshire, United Kingdom

<sup>7</sup> Earth and Life Institute, Université catholique de Louvain, Belgium.

<sup>8</sup> World Meteorological Organization (WMO), Department for Science and Innovation, 7bis Avenue de la Paix, 1211 Geneva, Switzerland

<sup>9</sup> Department of Geography, Climatology, Climate Dynamic and Climate Change, And Center of International Development and Environmental Research, Justus Liebig University of Giessen, Germany

<sup>10</sup> Institute of Environmental Assessment and Water Research (IDAEA-CSIC), Barcelona, Spain

<sup>11</sup> Department of Geology – Quaternary Science, Lund University, Sölvegatan 12, 223 62, Lund, Sweden

<sup>12</sup> Hamilton Institute, Insight Centre for Data Analytics, Maynooth University, Kildare, Ireland

<sup>13</sup> CREAM, 08193, Bellaterra (Cerdanyola del Vallès), Spain.

<sup>14</sup> Universitat Autònoma de Barcelona (UAB), Bellaterra (Cerdanyola del Vallès), 08193, Spain.

<sup>15</sup> Met Office Hadley Centre, Exeter, UK

<sup>16</sup> College of Engineering, Mathematics and Physical Sciences, Exeter University, Exeter, UK

<sup>17</sup> Environnements et Paléoenvironnements Océaniques et Continentaux (EPOC), UMR CNRS 5805, EPOC-OASU Université de Bordeaux, Allée Geoffroy Saint-Hilaire, 33615 Pessac, France

<sup>18</sup> Department of Geography, University of North Carolina at Chapel Hill, Chapel Hill, North Carolina 27599, USA

<sup>19</sup> State Key Laboratory of Cryospheric Science, Northwest Institute of Eco-Environment and Resources, Chinese Academy of Sciences, Lanzhou 730000, China

<sup>20</sup> Laboratory of Tree-Ring Research, University of Arizona, Tucson, 85721, USA

\*Corresponding author: armandhernandezh@gmail.com

1  
2  
3 **Abstract**  
4  
5

6 Modes of climate variability affect global and regional climates on different spatio-temporal  
7 scales, and they have important impacts on human activities and ecosystems. As these modes  
8 are a useful tool for simplifying the understanding of the climate system, it is crucial that we gain  
9 improved knowledge of their long-term past evolution and interactions over time to contextualise  
10 their present and future behaviour. We review the literature focused on proxy-based  
11 reconstructions of modes of climate variability during the Holocene (i.e., the last 11.7 thousand  
12 years) with a special emphasis on i) proxy-based reconstruction methods; ii) available proxy-  
13 based reconstructions of the main modes of variability, i.e., El Niño Southern Oscillation, Pacific  
14 Decadal Variability, Atlantic Multidecadal Variability, the North Atlantic Oscillation, the Southern  
15 Annular Mode and the Indian Ocean Dipole; iii) major interactions between these modes; and iv)  
16 external forcing mechanisms related to the evolution of these modes. This review shows that  
17 modes of variability can be reconstructed using proxy-based records from a wide range of  
18 natural archives, but these reconstructions are scarce beyond the last millennium, partly due to  
19 the lack of robust chronologies with reduced dating uncertainties, technical issues related to  
20 proxy calibration, and difficulty elucidating their stationary impact (or not) on regional climates  
21 over time. While for each mode the available reconstructions tend to agree at mutidecadal  
22 timescales, they show notable disagreement on shorter timescales beyond the instrumental  
23 period. The reviewed evidence suggests that the intrinsic variability of modes can be modulated  
24 by external forcing, such as orbital, solar, volcanic, and anthropogenic forcing. The review also  
25 highlights some modes experience higher variability over the instrumental period, which is partly  
26 ascribed to anthropogenic forcing. These features stress the paramount importance of further  
27 studying their past variations using long climate-proxy records for the progress of climate  
28 science.  
29  
30  
31  
32  
33  
34  
35  
36  
37  
38  
39  
40  
41  
42  
43  
44  
45  
46  
47  
48  
49  
50  
51  
52  
53  
54  
55  
56  
57  
58  
59  
60  
61  
62  
63  
64  
65

## **1.- Introduction**

The Earth is a complex system in which climate variability, i.e., variations in the mean state of the climate system, results from intricate interactions between its components (atmosphere, hydrosphere, geosphere, cryosphere, and biosphere). Different geophysical processes are, therefore, capable of contributing to climatic variability on different timescales (Mitchell, 1976). The potential sources of climatic variability are mainly the result of: i) internal processes involving interactions between the different parts of the system; and/or ii) external forcing mechanisms from independent environmental changes. A large proportion of the spatial structure of climate variability follows recurrent patterns, often referred to as modes of climate variability (Stephenson et al., 2004). The term modes of climate variability is, however, ambiguously employed in the climate community, with a range of uses that make its definition difficult (IPCC, 2013). Here, we define modes of climate variability as preferred spatial patterns and their fluctuations across different timescales, which represent a simplification of the complex spatial and temporal evolution of the climate system.

Modes of variability have typically been identified through statistical analysis of observational and model data and are generally described by a characteristic spatial pattern and its associated timeseries (Christensen et al., 2013). While these modes of variability are at most quasiperiodic, they are oscillatory in character, and their state is monitored using so-called climate indices. Empirical orthogonal function analysis is among the most widely and extensively used methods to calculate climate indices (Hannachi et al., 2007). This methodology allows a display of the space-time field that is useful for dimensionality reduction and pattern extraction, although it is not exempt from problems (i.e., bias in the variance) (Beguería et al., 2016). Alternatively, simple indices based on data from fixed meteorological stations have been traditionally used as they can provide continuous timeseries that extend further back in time, in some cases beyond the 20th century (Comas-Bru and Hernández, 2018; Cropper et al., 2015; Hurrell, 1995; Jones et al., 1997; Vinther et al., 2003a; Visbeck, 2009). The main disadvantage of station-based indices is that they are anchored to their locations, and they might not effectively represent the centres of action of some modes. Consequently, modes of variability are usually defined from gridded data (Folland et al., 2009; Moore et al., 2013; Roundy, 2014). The correlation between a given index of a mode of climate variability and a large-scale climate field are often named teleconnections. This concept refers to the ability of modes of climate variability to explain the connections between climate in remote regions through associated atmospheric or oceanic pathways (Barnston and Livezey, 1987; Shaman, 2014).

The impact of some of the best-known modes of variability, i.e., the El Niño–Southern Oscillation (ENSO), the North Atlantic Oscillation (NAO), the Pacific Decadal Variability (PDV), Atlantic Multidecadal Variability (AMV), the Northern and Southern Annular Modes (NAM and SAM) and the Indian Ocean Dipole (IOD), extend over large areas and/or ocean basins. These modes of variability are often associated with severe climate events such as droughts, floods, heat waves and cold spells (e.g., Benito et al., 2015; Cook et al., 2015; Ionita et al., 2012) affecting agriculture, water resources and blue economies, which, in turn, modulate air quality, fire risk, energy availability and human health (Bastos et al., 2016; Jerez et al., 2013; Zubieta et al., 2017). In this context, understanding the evolution of modes of variability and associated

1  
2  
3  
4 teleconnections on a global scale during the last few millennia is essential to i) attribute climate  
5 changes to internal variability versus external forcing factors, ii) evaluate the ability of different  
6 climate models to reproduce them robustly, and iii) constrain uncertainties in future climate  
7 projections and associated hazards.  
8

9  
10 Instrumental measurements of the climatic variables used to characterise these modes have  
11 been available for a couple of centuries in the best case (e.g., Jones, 2001; Luterbacher et al.,  
12 2002; Parker et al., 2007, 1992; Prohom et al., 2016). A better understanding of these modes,  
13 many of which operate from submonthly to multidecadal timescales, requires longer climate  
14 records beyond the limited temporal and spatial coverage of instrumental measurements.  
15 Consequently, the use of indirect climate indicators from natural archives (proxy-based records)  
16 becomes of paramount importance (Gornitz, 2009; Marcott et al., 2013; Neukom et al., 2019).  
17 These indirect climate indicators generally respond to environmental parameters such as  
18 temperature and precipitation, and, in turn, may be indirectly linked to certain modes of  
19 variability, through, for example, their response to the atmospheric circulation (e.g., Bradley,  
20 2015; Jones et al., 2009; Jones and Mann, 2004). Over the last decades, several studies have  
21 attempted to reconstruct a number of modes of climate variability at different timescales using  
22 historical documents and natural archives. Major findings show evidence of the spatio-temporal  
23 variability of these modes and their impacts, interactions and possible links to external forcings  
24 for the Holocene in general (e.g., Chen et al., 2016; Ivanochko et al., 2008; Koutavas and  
25 Joanides, 2012) and the last millennium in particular (e.g., Dätwyler et al., 2018; Mann et al.,  
26 2009; Ortega et al., 2015; Wang et al., 2017). Nevertheless, they are not exempt from  
27 limitations, such as chronological uncertainties, an oversimplification or misinterpretation of  
28 stationarity, and limited capability to attribute observed climate changes to internal variability  
29 and/or external forcing factors (e.g. solar and volcanic activity) (e.g., Evans et al., 2013; Raible  
30 et al., 2014). These limitations may partly be overcome using climate models. There is a  
31 number of approaches based on palaeoclimatic simulations, such as large-multimodel  
32 ensembles (e.g., Lee et al., 2019; Phillips et al., 2014; Terray, 2012) and proxy system modeling  
33 (e.g., Dee et al., 2017; Evans et al., 2013), that have already shown their ability to reproduce  
34 and differentiate external and internal processes affecting the climate system. However, the  
35 obtained results are disparate (Haywood et al., 2019) and their potential to simulate some  
36 aspects (e.g., extreme changes) related to modes of variability is still poor (e.g., Zhang and Sun,  
37 2014).  
38  
39  
40  
41  
42  
43  
44  
45  
46

47 Despite the dramatic increase in the number of proxy-based reconstructions over the past  
48 decades, a synthesis of the main modes of variability and teleconnections in a palaeoclimatic  
49 context is lacking. This paper focuses on reviewing the literature centred on proxy-based  
50 reconstructions of modes of climate variability during our current interglacial, the Holocene (i.e.,  
51 the last 11.7 ka). The article is organised as follows: Section 2 introduces the different  
52 reconstruction methods that are frequently employed and evaluates ongoing work and future  
53 developments. Section 3 provides an account of the proxy-based reconstructions available for  
54 the main modes of climate variability (Fig. 1). Section 4 describes major interactions between  
55 modes of variability, while section 5 focuses on mechanisms driven by external forcing, which  
56 have been related to the changes in modes of variability through the Holocene. Finally, section  
57 6 synthesises the main review outputs and includes future perspectives.  
58  
59  
60  
61  
62  
63  
64  
65

## 2.- Reconstruction methods

### 2.1.- Archives, spatial distributions and sensitivities

Information on past climatic and environmental conditions (i.e., proxy data) is commonly preserved in natural and documentary archives across the globe. To yield reliable reconstructions of a mode of variability, proxy-based records should i) be sensitive to climatic variables (e.g., temperature, precipitation, wind); ii) be continuous and highly-resolved (monthly to decadal), at least, for several hundreds of years to detect decadal-scale variability beyond the instrumental period; iii) maintain a stationary modern proxy-climate relationship over time (the principle of uniformitarianism); and iv) cover a large and homogeneous spatial region that includes the areas influencing the targeted mode of variability (Table 1).

It is important to highlight that high-quality proxy-based climatic records do not reconstruct the temporal evolution of modes of climate variability by themselves but their impacts and interactions on the physical and biogeochemical dynamics of the proxy-based record. The common approach to establish a reliable proxy-climate relationship is to calibrate the proxy signal using modern data (see Section 2.3). However, this can introduce large uncertainties and is not possible when the record does not cover the instrumental period. In addition, some other overarching challenges remain when working with proxy data, presented as follows in approximate order of decreasing importance:

1. The relationship between climate and a given proxy-based record may vary over time. This variation may occur because either the proxy reacts to climate differently under different non-climate related conditions, or because the sensitivity of the proxy to a given set of climate drivers may vary with changes in the mean climate state. This phenomenon may be solved by using mechanistic modelling of the proxy-climate relationship by accounting for these important non-climate variables in the calibration model if available. The climate-proxy linkage may also vary as a function of timescale. For example corals might have a different relationship with climate on annual, interannual and decadal timescales (Gagan et al., 2012).
2. The calibration data do not fully explore the range of proxy/climate behaviours (with few exceptions such as coral archives). This is the so-called 'no modern analogue' problem and can be reduced by increasing the calibration dataset size, or by using mechanistic models of proxy/climate behaviour.
3. A weak relationship between proxies and climate, which may occur where proxies or climate variables are poorly chosen and can be accounted for using a probabilistic modelling approach (such as the Bayesian inverse approach) where the models are sufficiently flexible so that weak relationships yield large uncertainties in reconstructed climates. Employing a multi-proxy approach can identify common climate signals of interest amongst individual proxies that may be only correlated to local climate variables.



1  
2  
3  
4 4. Poor chronological control may occur even if the proxy climate relationship is strong but the  
5 dating methods (or extraction/counting methods for the proxy) are not able to accurately  
6 quantify the information in the archive. This phenomenon can be accounted for by modelling the  
7 uncertainty in the process so that poor data yield large climate uncertainty estimates (e.g.,  
8 Parnell et al., 2015).  
9

10  
11  
12  
13  
14  
15  
16  
17  
18  
19  
20  
21  
22  
23  
24  
25  
26  
27  
28  
29  
30  
31  
32  
33  
34  
35  
36  
37  
38  
39  
40  
41  
42  
43  
44  
45  
46  
47  
48  
49  
50  
51  
52  
53  
54  
55  
56  
57  
58  
59  
60  
61  
62  
63  
64  
65

14  
15  
16  
17  
18  
19  
20  
21  
22  
23  
24  
25  
26  
27  
28  
29  
30  
31  
32  
33  
34  
35  
36  
37  
38  
39  
40  
41  
42  
43  
44  
45  
46  
47  
48  
49  
50  
51  
52  
53  
54  
55  
56  
57  
58  
59  
60  
61  
62  
63  
64  
65

Table 1.- Examples of the most commonly used archives to carry out high-resolution proxy-based reconstruction of modes of climate variability.

Archive	Advantages	Limitations	Proxies used for reconstructions	Mode	Nominal Temporal Resolution	Interpretable Temporal Resolution	Reference
Tree rings	<ul style="list-style-type: none"> <li>- Absolute chronologies (precise calendar year dates)</li> <li>- High-resolution proxy records (sub-annual to annual)</li> <li>- Widespread distribution in both Hemispheres</li> <li>- Strong climate signal</li> <li>- Continuous records</li> </ul>	<ul style="list-style-type: none"> <li>- Climate sensitivity typically reflects a particular season</li> <li>- Concentrated in the mid-latitudes; many trees in tropical regions do not have annual rings</li> <li>- Most records &lt; 1000 years in length.</li> </ul>	Total tree-ring widths, earlywood widths, latewood widths, maximum latewood density, $\delta^{18}\text{O}$	PDO, ENSO, NAO, SAM, AMV	Annual	Sub-annual/Annual/and above	e.g., Abram et al., 2014; Cook et al., 2019; D'Arrigo and Wilson, 2006; Dätwyler et al., 2019; Gray et al., 2004; Li et al., 2013; MacDonald and Case, 2005; Verdon and Franks, 2006
Ice cores	<ul style="list-style-type: none"> <li>- Absolute chronologies (annual-layer counts).</li> <li>- Age uncertainty &lt; <math>\pm</math> 50 years</li> <li>- High-resolution proxy records (annual)</li> <li>- Continuous record &gt; 1000 years in length</li> </ul>	Limited to polar and high-elevation regions	Network of $\delta^{18}\text{O}$ ; $\delta^{18}\text{O}$	NAO	Annual	Annual/Multiannual and above	e.g., Jones et al., 2009; Ortega et al., 2014; Sjolte et al., 2018; Vinther et al., 2010, 2003b
Speleothems	<ul style="list-style-type: none"> <li>- Absolute chronologies (radiometric methods and annual layer counts)</li> <li>- Age uncertainty &lt; <math>\pm</math> 50 years</li> <li>- High-resolution proxy records (sub-annual)</li> </ul>	<ul style="list-style-type: none"> <li>- Possible presence of growth hiatuses</li> <li>- Variable water transit time: difficult to quantify.</li> <li>- Potential non-equilibrium isotopic deposition (kinetic effects)</li> </ul>	Sr/Ca; $\delta^{18}\text{O}$ ; $\delta^{13}\text{C}$ ; growth rate of laminae	NAO, ENSO	Sub-Annual to multi-centennial	Sub-Annual to multi-centennial	e.g., Chen et al., 2016; Frappier et al., 2002; Lachniet et al., 2004; Smith et al., 2016a; Trouet et al., 2009; Wassenburg et al., 2016

14  
15  
16  
17  
18  
19  
20  
21  
22  
23  
24  
25  
26  
27  
28  
29  
30  
31  
32  
33  
34  
35  
36  
37  
38  
39  
40  
41  
42  
43  
44  
45  
46  
47  
48  
49  
50  
51  
52  
53  
54  
55  
56  
57  
58  
59  
60  
61  
62  
63  
64  
65

		- Most continuous records > 1000 years in length - Distribution in a large range of hydroclimatic conditions						
Corals		- Absolute chronologies (radiometric methods and annual layer counts) - Age uncertainty < 1 year - High-resolution proxy records (sub-annual)	- Limited to tropical regions - Record < 1000 years in length	$\delta^{18}\text{O}$ ; Sr/Ca	ENSO, PDO, IOD, AMV	Monthly to seasonal	Seasonal and above	e.g., Abram et al., 2020; Cobb et al., 2013; Gong and Luterbacher, 2008; McGregor et al., 2010; Verdon and Franks, 2006; Wilson et al., 2010
Marine sediments		- Continuous record > 1000 years in length - Widespread distribution	- Age uncertainty > $\pm 50$ years - Low-resolution proxy records (sub-decadal at best)	Sediment and foraminifera geochemistry	ENSO, PDO, NAO	Sub-decadal and above	Decadal and above	e.g., Dean and Kemp, 2004; Faust et al., 2016; Goslin et al., 2018; White et al., 2018
Lake sediments	Non-varved	- Continuous record > 1000 years in length - Widespread distribution	- Age uncertainty > $\pm 50$ years - Low-resolution proxy records (sub-decadal at best) - Human impact	Mn/Fe ratio; Grain size; Laminae colour scale	NAO, ENSO, PDO	Sub-decadal and above	Decadal and above	e.g., Kirby et al., 2010; Moy et al., 2002; Olsen et al., 2012
	Varved	- Independent varve chronologies - High-resolution proxy records (sub-annual)	- Human impact - Most varve chronologies are floating and need to be anchored to a calendar timescale			Annual	Annual/Multiannual and above	

14  
15  
16  
17  
18  
19  
20  
21  
22  
23  
24  
25  
26  
27  
28  
29  
30  
31  
32  
33  
34  
35  
36  
37  
38  
39  
40  
41  
42  
43  
44  
45  
46  
47  
48  
49  
50  
51  
52  
53  
54  
55  
56  
57  
58  
59  
60  
61  
62  
63  
64  
65

		<ul style="list-style-type: none"> <li>- Most continuous records &gt; 1000 years in length.</li> <li>- Widespread distribution</li> </ul>	<ul style="list-style-type: none"> <li>using other independent dating methods, e.g. <sup>14</sup>C dating and tephrochronology</li> </ul>					
Historical documents	<ul style="list-style-type: none"> <li>- High variety of resources</li> <li>- Good age control</li> <li>- High temporal resolution (sub-annual)</li> </ul>	<ul style="list-style-type: none"> <li>- Short continuous record length (the last few hundred years)</li> <li>- Most reporting on the North Atlantic and the Pacific</li> </ul>	<ul style="list-style-type: none"> <li>Ice-Snow observations;</li> <li>Phenological and biological observations, historical written evidence; Ships' logbooks</li> </ul>	NAO	Monthly to Seasonal	Seasonal and above	e.g., Küttel et al., 2010; Luterbacher et al., 2001, 1999; Mellado-Cano et al., 2019	

## 2.2.- Timescales and chronologies

Understanding the temporal and spatial expression of modes of variability over the Holocene requires precise chronological resolution covering a wide geographical range. This is a challenge for climate science that seeks to address the entire Holocene, as there are inherent dating uncertainties in most contexts and the most precise approaches are spatially and temporally constrained (Table 1).

There exists for the Holocene there exists a dendrochronological timescale that is considered to be accurate with virtually no uncertainties. This timescale underlies the  $^{14}\text{C}$  calibration curve (IntCal curve; Reimer et al., 2020), as tree rings record the atmospheric  $^{14}\text{C}$  concentrations during the period of their growth. Sampling of the Holocene IntCal curve is decadal, typically 10 rings per radiocarbon sample (Reimer et al., 2020, 2013), and the structure of the curve has implications for dating. Radiocarbon ages are commonly determined in the Holocene with 1 sigma counting errors of ca.  $\pm 20 - 50$  years; and the shape of the calibration curve, which can mean single age estimates will have 2 sigma calibrated ranges of 100 to, in some cases, 300 years. The sampling density of radiocarbon ages available at individual sites, as well as the shape of the radiocarbon calibration curve at different points, can influence the precision at which an event can be dated. This phenomenon can be overcome with the so-called wiggle match dating approach, i.e., the matching of a series of  $^{14}\text{C}$  determinations to the calibration curve (Pearson, 1986). However, this approach is expensive, and may pose potential issues of sample contamination and reworking that can influence the chronological accuracy (e.g., Blockley et al., 2007). Another approach to deal with the challenges of radiocarbon dating of individual sites is to calculate average dates by combining low-resolution radiocarbon dating in multiple records, which are correlated by biostratigraphy, to establish a robust regional chronology (e.g. Wanner et al., 2011). This approach has its own limitations. For example, Blaauw et al. (2007) tested proposed periods of regional wet conditions reported from biostratigraphically-correlated European raised bogs. Tests were based on improving the dating of the individual sites, using very high-resolution  $^{14}\text{C}$  sampling, and integrating formal Bayesian interrogation of the statistical likelihood synchronicity between sites. This study failed to reproduce many of the previously proposed synchronous wet shifts because of either the full chronological uncertainties of comparing climate events is not incorporated into the assessment of the timing of an event or, even if an event exists, that might not be synchronous between regions. Nevertheless, two periods of low solar activity, the Maunder and Spörer solar minima were statistically correlated with wetter conditions across multiple sites (Blaauw et al., 2007). In the marine realm, in addition, radiocarbon-based dating has an added source of uncertainty mostly deriving from regional differences in the radiocarbon ages of specific water masses that may have been isolated since they were in contact with the atmosphere (Stuiver et al., 1986; Stuiver and Braziunas, 1993). This is often referred as the marine reservoir effect and has been studied globally and regionally (Reimer and Reimer, 2001). There has been, however, notable success in improving the precision of radiocarbon-based chronologies using a high density of radiocarbon dates and Bayesian modelling techniques (e.g., Crann et al., 2015), although these have not as yet been applied to a sufficient number of Holocene sediment chronologies, in part

1  
2  
3 due to the number of dates required to achieve the best improvements in model precision  
4 (Blaauw et al., 2018).  
5  
6

7 Another important dating method relies on the radioactive decay of uranium and the ingrowth of  
8 thorium with age. The  $^{234}\text{U}/^{230}\text{Th}$  dating method has been particularly successful for speleothem  
9 records leading to absolute dating uncertainties on the order of 50-100 years for Holocene  
10 records (Wang et al., 2005). Such dating precision allows the linking of speleothem-based  
11 monsoon records to ice core-based climate records and/or comparisons to solar forcing records,  
12 although some timescale adjustments within uncertainties may still generate misleading results  
13 (Muscheler et al., 2004). When applied to dating fossil corals, U/Th dating uncertainties  
14 approach 0.1% for Holocene samples (Cobb et al., 2003b, 2013; Grothe et al., 2019) and near-  
15 absolute age (less than  $\pm 1$  year) for overlapping fossil coral ensembles during the last  
16 millennium (Dee et al., 2020) (Table 1).  
17  
18  
19  
20

21 Counting of annual layers of deposition in ice cores and lake sediments (varves) relies on the  
22 preservation of the annual layers. The Greenland ice core timescale, for example, accumulates  
23 approximately 100 years (2 sigma) of uncertainty years over the Holocene (Rasmussen et al.,  
24 2006), although this is of considerably greater precision than usual with  $^{14}\text{C}$  dating of single  
25 samples in the same period, and uncertainties are significantly smaller for the majority of the  
26 Holocene ice core (Table 1). One issue with comparing dating approaches is the different  
27 notations used in various chronologies, with the Greenland ice core record using “years b2k”  
28 (before 2000 CE), differing by 50 years from the commonly used “years BP” notation, where BP  
29 refers to before 1950 CE / AD 1950. This should, however, not be an issue if the reference used  
30 for a given chronology is clearly reported in the paper.  
31  
32  
33  
34

35 Varved lake sediments are more geographically dispersed than polar ice cores, with data  
36 reported from every continent and not necessarily at high-altitude sites. However, published  
37 records are dominantly from North America and Europe, with little coverage in the Southern  
38 Hemisphere (SH; Zolitschka et al., 2015). Varve chronologies accumulate a counting error  
39 ranging from approximately 1 - 10% (Ojala et al., 2015). The most common problem with varved  
40 sediments is that they are often not continuously layered across the whole of the Holocene and  
41 need to be anchored to calendar time by some other method (e.g., Snowball et al., 2010). For  
42 instance, radiocarbon dated records from parts of the NH suggest a short-lived climatic  
43 oscillation of ca. 2.8 ka BP, which may be correlated to a period of low solar activity (Wanner et  
44 al., 2011). This event has now been precisely constrained to a solar minimum at 2759 ( $\pm 39$ )  
45 years BP by combining sediment climate proxies and cosmogenic radionuclide tracers for solar  
46 activity from a varved lake record (Martin-Puertas et al., 2012).  
47  
48  
49  
50  
51

52 Variations in cosmic rays that are modulated by the solar and geomagnetic shielding leave a  
53 globally synchronous signal in cosmogenic radionuclide records as these particles are produced  
54 by the interaction of high-energy cosmic rays with the constituents of the atmosphere. This  
55 signal has been used to tie together ice core and absolutely dated tree ring records during the  
56 Holocene (Adolphi and Muscheler, 2016; Muscheler et al., 2014) and to U/Th-dated  
57 speleothems during the past 50 ka (Adolphi et al., 2018). This method also underlies the above-  
58 mentioned  $^{14}\text{C}$  wiggle-match dating technique and the synchronisation of  $^{10}\text{Be}$  records from  
59  
60  
61  
62  
63  
64  
65

1  
2  
3 Greenland ice cores and lake sediments (Czymzik et al., 2018; Martin-Puertas et al., 2012).  
4 Recently, the signature of solar storms has been found in tree rings and ice core records  
5 (Mekhaldi et al., 2015; Miyake et al., 2012). Synchronising these sharp radionuclide peaks  
6 allows the synchronisation of timescales with uncertainties of 1 year or less. These signatures  
7 have helped to resolve long-standing differences between tree ring and ice core timescales (Sigl  
8 et al., 2015).  
9

10  
11  
12 Finally, apart from absolute dating methods, there are correlation methods that have significant  
13 potential for aligning records on the same timescale. The most prominent method aims to  
14 recognise tephra horizons from the same eruption in different sites (Lane et al., 2013; Wulf et  
15 al., 2013). Especially promising for correlating records is the application of cryptotephra to lake,  
16 bog and ice core archives. For example, the event at ~2.8 ka BP highlighted above from a varve  
17 chronology is also recognised as a change in the precipitation signal in Irish bogs and is  
18 associated with several cryptotephra horizons in that region (e.g., Plunkett and Swindles, 2008).  
19 The technique has the greatest potential where multiple tephra horizons can anchor different  
20 varved lake sequences (e.g., Wulf et al., 2016), or where ice core and varved records can be  
21 anchored using widespread tephra (e.g., Lane et al., 2013).  
22  
23  
24  
25

### 26 **2.3.- Statistical approaches**

27  
28  
29 As mentioned in Section 2.1, the calibration of the proxy data is crucial for the reconstruction of  
30 modes of variability. From a statistical standpoint, the problem can be stated as follows: given a  
31 calibration set which contains both proxy data and climate variables, produce a reconstruction  
32 back in time that estimates the climate variables from ancient proxy data.  
33  
34

35  
36 To evaluate the robustness of the reconstruction approach, it is necessary to perform a  
37 calibration, or learning period, over only a fraction of the available time frame where both the  
38 proxy record and the mode of variability timeseries are overlapping, keeping part of it to test  
39 whether the proxy-based reconstruction is robust over this testing time period. Many issues can  
40 cause this idealised relationship to break down and yield incorrect reconstructions (see Section  
41 2.1).  
42  
43

44  
45 Given the above statistical definition there are two proposed approaches (Table 2) to estimate  
46 past changes in modes of variability:  
47

48  
49 a. A regression approach where the climate variables are treated as the response and the  
50 proxies as covariates in a regression model. These approaches may range from simple linear  
51 regression up to complex machine learning (see below). The fitted model is then used to predict  
52 the modes of variability for the ancient proxy data. We term this the 'forward regression'  
53 approach (though other names are sometimes used), which is very common in climate science  
54 (e.g., Cook et al., 2019; Juggins and Birks, 2012; Luterbacher et al., 2002; Mann et al., 1998;  
55 Michel et al., 2020; Xoplaki et al., 2005). Popular methods such as the Composite Plus Scale  
56 and Modern Analogue techniques fall under this banner.  
57  
58  
59  
60  
61  
62  
63  
64  
65

1  
2  
3  
4 b. An inverse approach by which a regression model is built that describes how the proxy reacts  
5 to changes in modes of variability. Inverse regression is then used to predict the climate variable  
6 from the proxy data via this fitted model. Sometimes this inverse regression is performed *ad hoc*  
7 (Huntley et al., 1993), though more recent approaches have used Bayes' theorem, which  
8 performs the inverse regression in a probabilistic manner (e.g., Cahill et al., 2015; Haslett et al.,  
9 2006; Luterbacher et al., 2016; Parnell et al., 2015; Tingley and Huybers, 2009). We term this  
10 the 'inverse regression' approach.  
11  
12

13  
14 The key difference between the two approaches is that in forward regression the climate  
15 variables are treated as the response variables, whereas in inverse regression the proxies are  
16 treated as response variables. In situations where normal distributions are assumed throughout,  
17 both can produce identical reconstructions. Some advantages and disadvantages of the  
18 approaches are shown in Table 2, although they have been discussed at length in other papers  
19 (Sweeney et al., 2018). In either case, the model should be thoroughly checked using the  
20 calibration period, and the use out-of-sample approaches is strongly recommended, such as  
21 cross-validation to check the fit of the model. Such an approach has been demonstrated by  
22 Cahill et al., (2016) . Once checked, estimates of climate variables must include uncertainties  
23 that are quantified via, e.g., 50% and 95% uncertainty intervals, at the very least. Both methods  
24 can be applied to the reconstruction of modes of variability. To our knowledge, regression  
25 methods have been mostly used until now, including principal component regression  
26 approaches (Cook et al., 2002; Ortega et al., 2015), partial least squares, elastic net and  
27 random forest (Breiman, 2001; Zou and Hastie, 2005). Michel et al. (2020) evaluated the  
28 strengths of these different methods to reconstruct the NAO over the last millennium using the  
29 PAGES 2K database. They showed that the random forest provides the best scores, which may  
30 be related to the capability of this method to account for non-linear linkages between the mode  
31 and proxy records, although we must be careful of overfitting with non-linear methods.  
32 Additionally, recent initiatives applying the inverse regression approach to reconstruct modes of  
33 variability are appearing (Hernández et al., In Review; Sánchez-López, 2016).  
34  
35  
36  
37  
38  
39  
40

41 The use of pseudo-proxy approaches within climate modelling can then further help to evaluate  
42 the capability of these approaches to appropriately reconstruct the variability modes. In such a  
43 pseudo-proxy experiment, simulated data are modified to mimic real-world proxies and  
44 instrumental observations (called pseudo-proxy and pseudo instrumental datasets). The  
45 reconstruction results are then compared with the available simulated target field, providing an  
46 estimation of the skill of the method in real-world applications (Lehner et al., 2012; Ortega et al.,  
47 2015; Smerdon, 2012).  
48  
49  
50

51 Table 2: Advantages and disadvantages of the forward and inverse regression approaches  
52

53 54 55 56 57 58 59 60 61 62 63 64 65	<b>Forward regression advantages</b>	<b>Forward regression disadvantages</b>
--	--------------------------------------	---



1  
2  
3  
4  
5  
6  
7  
8  
9  
10  
11  
12  
13  
14  
15  
16  
17  
18  
19  
20  
21  
22  
23  
24  
25  
26  
27  
28  
29  
30  
31  
32  
33  
34  
35  
36  
37  
38  
39  
40  
41  
42  
43  
44  
45  
46  
47  
48  
49  
50  
51  
52  
53  
54  
55  
56  
57  
58  
59  
60  
61  
62  
63  
64  
65

<ul style="list-style-type: none"> <li>·Fits into most standard regression modelling approaches so can be easily used with existing software packages (Ilvonen et al., 2016)</li> <li>·Simple regression models can be replaced with more complex models, e.g., machine learning approaches</li> </ul>	<ul style="list-style-type: none"> <li>·Does not model the causal link between the proxy and the climate variable</li> <li>·Can struggle to incorporate issues with the data such as measurement error (e.g., chronological error)</li> <li>·No simple way to include climate model information (e.g., to constrain the reconstructed climate variables)</li> </ul>
<p><b>Inverse regression advantages</b></p>	<p><b>Inverse regression disadvantages</b></p>
<ul style="list-style-type: none"> <li>·Directly models the causal relationship between the proxy and the climate variables</li> <li>·Allows for the easier inclusion of prior information (if the model is Bayesian) on climate changes over time</li> <li>·Easier to incorporate mechanistic models into the approach</li> </ul>	<ul style="list-style-type: none"> <li>·Very little software currently available (though see Parnell et al., 2016a)).</li> <li>·Requires considerable expertise to build suitable models; e.g. with high-dimensional proxy data</li> <li>·Model running is considerably slower and often requires high-dimensional numerical integration</li> </ul>

The recent rise in machine learning approaches may allow for far richer reconstructions, especially in situations where large data sets are available and where proxy data and/or climate variables are high dimensional (i.e., multiple measurements from each sample). Indeed, there is now a suite of probabilistic machine learning approaches (Chipman et al., 2010) that may fit more neatly into the current paradigm.

The introduction of mechanistic models is also a challenging target. These may occur in two different parts of the above-described approaches: the first part includes guiding the behaviour of the climate variables over time, and the second focuses on the inverse approach to create richer models of the proxy response to climate change, e.g., under non-stationary climate/proxy relationships. Whilst it has been possible for some time to use a few ensemble members of, e.g., a GCM to guide the climate reconstruction (Ilvonen et al., 2016), one can now attempt to calibrate such a mechanistic model via the proxy data. This possibility has been proposed in several recent papers under the (Bayesian) inverse regression approach (e.g., Carson et al., 2018; Parnell et al., 2015, 2016b). The introduction of such mechanistic models promises a superior understanding of climate dynamics.

Last but not least is the development of data assimilation techniques for proxy data over the last millennium (e.g., Hakim et al., 2016; Singh et al., 2018) within a climate model, some of which include modules that directly simulate the proxies to better reflect the observations - offering a new route for reconstructed modes of climate variability. Nevertheless, such methods are not dedicated to the reconstruction of the modes, which might hamper their results, since other aspects of the climate representation might interfere (model biases, absence of calibration over

1  
2  
3 present-day, proxy records that are poorly sensitive to a given mode) with the target of  
4 producing a robust reconstruction with a good confidence level.  
5  
6

### 7 **3.- Modes of climate variability**

8  
9

#### 10 **3.1.- El Niño-Southern Oscillation**

11

12 El Niño-Southern Oscillation (ENSO) is the largest source of interannual climate variability on a  
13 global scale, and arises from ocean-atmosphere interactions in the tropical Pacific (Fig. 1) (Diaz  
14 and Markgraf, 2000; McPhaden et al., 2006; Philander, 1989; Rasmusson and Wallace, 1983).  
15 During El Niño warm extremes, a weakening of the easterly trade winds leads to a reduction in  
16 upwelling of cooler subsurface waters, driving anomalous surface warming in the eastern and  
17 central equatorial Pacific Ocean and a slight cooling in the far western equatorial Pacific. The  
18 spatial pattern of El Niño events varies markedly, with some characterised by maximum  
19 warming in the eastern equatorial Pacific region – so-called “Eastern Pacific” events – while  
20 others exhibit maximum warming in the central Pacific region, often referred to as “Central  
21 Pacific” or El Niño Modoki events (Ashok et al., 2007; Capotondi et al., 2014). In both cases, the  
22 redistribution of surface ocean temperatures is associated with a large eastward shift in the  
23 Walker Cell, bringing enhanced atmospheric convection and increased precipitation to the  
24 central Pacific Ocean. This reorganization of large-scale atmospheric circulation further  
25 enhances central and eastern Pacific warming and leads to profound shifts in temperature and  
26 precipitation patterns across many regions of the world via atmospheric teleconnections  
27 (Halpert and Ropelewski, 1992; Ropelewski and Halpert, 1989). El Niño impacts include drought  
28 across the Maritime Continent and in parts of India, southwestern North America, and west  
29 Africa, while flooding occurs in Central and South America and East Africa (Ropelewski and  
30 Halpert, 1987). During a La Niña events, a strengthening of the Pacific trade winds drives  
31 increased upwelling resulting in cooler ocean surface temperatures, with a set of global climate  
32 impacts that are largely opposite to those of El Niño events (Horel and Wallace, 1981).  
33  
34  
35  
36  
37  
38  
39

40 Proxy-based reconstructions of ENSO rely on high-resolution archives (Fig. 2) such as corals,  
41 tree rings, ice cores, molluscs, speleothems and select lake and marine sediments collected  
42 from ENSO-sensitive regions (see review by Emile-Geay et al., (2020) and references therein).  
43 Individual ENSO reconstructions capture local changes in temperature and/or precipitation  
44 related to ENSO variability with varying fidelity, whereby calibration against instrumental climate  
45 records can reveal important information about proxy-specific and/or site-specific biases.  
46 Towards this goal, proxy system models, which link process models to observations to explain  
47 how archives are imprinted with environmental signals, leverage such calibration studies to  
48 inform the transformation of instrumental and/or model-derived variables of the physical climate  
49 system into plausible proxy-based records that can facilitate data-model intercomparison  
50 studies (Dee et al., 2015; Evans et al., 2013). Multiproxy syntheses of ENSO use networks of  
51 individual ENSO-sensitive records to increase signal-to-noise ratios (Braganza et al., 2009;  
52 Evans et al., 2002; Mann et al., 2000; Stahle et al., 1998; Wilson et al., 2010), with the most  
53 recent such reconstructions extending back several centuries (Dätwyler et al., 2019; Freund et  
54 al., 2019; McGregor et al., 2013).  
55  
56  
57  
58  
59  
60  
61  
62  
63  
64  
65

1  
2  
3  
4 Models and theory provide a compelling case for weakened ENSO variability during the mid-  
5 Holocene (commonly defined as 6-7 ka BP), but ENSO proxy-based reconstructions spanning  
6 the Holocene provide mixed support for this scenario (Fig. 2). Early proxy-based reconstructions  
7 from the far eastern (Moy et al., 2002; Rodbell et al., 1999) and western tropical Pacific  
8 (Tudhope et al., 2001) have lent support to this framework showing some decreased ENSO  
9 variability over the early and mid-Holocene. However, subsequent work from a diverse array of  
10 proxy-based records spanning the central to eastern tropical Pacific document a prolonged  
11 reduction in ENSO variability at some point during the 3-6 ka BP period (Carré et al., 2014;  
12 Chen et al., 2016; Cobb et al., 2013; Emile-Geay et al., 2016; Grothe et al., 2019; Koutavas and  
13 Joanides, 2012). In contrast, a newly available reconstruction based on single foraminifera  
14 chemistry analyses on a marine sediment core has revealed relatively low amplitude ENSO  
15 variability between 5.5-10 ka BP (White et al., 2018), in contrast to those derived from a coral-  
16 based reconstruction several hundred kilometres away (Cobb et al., 2013), which only show it  
17 for the mid-Holocene. This discrepancy between records (Table 3) has been suggested to result  
18 from the combination of centennial variability juxtaposed on the millennial scale changes over  
19 the Holocene (White et al., 2018), as also found in the modelled Holocene ENSO (Liu et al.,  
20 2014a). The proposed mechanism to explain the dampened ENSO in the early to mid-Holocene  
21 involves warming of the tropical Pacific thermocline due to insolation response of the south  
22 Pacific Sea Surface Temperature (SST) and/or changes in the strength of trade or westerly  
23 winds (see White et al., (2018) and references therein). As highlighted in these discrepancies,  
24 the high degree of internal variability in ENSO characteristics (amplitude, frequency, spatial  
25 footprint, and teleconnections) presents a significant barrier to the detection of forced responses  
26 in proxy-based records spanning the Holocene to present (see section 5).  
27  
28  
29  
30  
31  
32  
33

34 Existing proxy-based ENSO reconstructions spanning the last millennium rely largely on coral  
35 records that extend back several centuries (Fig. 2), in the case of coral records recovered from  
36 living coral colonies (Freund et al., 2019; Urban et al., 2000), and/or fossil coral records dated  
37 using  $^{234}\text{U}/^{230}\text{Th}$  (Chen et al., 2018; Cobb et al., 2003a). Other ENSO reconstructions include  
38 single foraminifera (Rustic et al., 2015) and tree ring-based records (Cook et al., 2008; D'Arrigo  
39 et al., 2005; Li et al., 2013, 2011; Liu et al., 2017). Against a backdrop of high variability in  
40 ENSO properties over the last millennium (Fig. 2), several studies have provided evidence for  
41 an intensification of ENSO during the Little Ice Age (LIA), approximately 400-500 years ago  
42 (Cobb et al., 2003a; Gergis and Fowler, 2009; Rustic et al., 2015). The larger availability of high-  
43 quality and resolution proxy-based ENSO records and the significant correlation between most  
44 of them during the last millennium (Table 3) provide a unique opportunity to constrain the  
45 relative roles of external forcing versus internal variability in shaping the decadal- to centennial-  
46 scale evolution of ENSO over recent centuries (see section 5).  
47  
48  
49  
50  
51

52 In recent years, a number of new proxy-based records of ENSO variability spanning the last  
53 centuries to millennia resolve a significant increase in the amplitude of ENSO in recent decades  
54 (Cobb et al., 2013; Grothe et al., 2019; Li et al., 2013; Liu et al., 2017; McGregor et al., 2013).  
55 This phenomenon is in agreement with analyses of 21st century projections of ENSO  
56 properties, which reveal evidence for an intensification of ENSO's hydrological response under  
57 anthropogenic forcing (Cai et al., 2015a, 2015b, 2014; Power et al., 2013), and/or an increase in  
58 the variability of ENSO SST anomalies (Cai et al., 2018). A new reconstruction of ENSO  
59  
60  
61  
62  
63  
64  
65

variations using a large network of published coral records reveals an intensification of central Pacific El Niño events in the last century (Freund et al., 2019), consistent with a shift towards stronger central Pacific El Niño events derived from an analysis of the instrumental record of climate (Wang et al., 2019a). Furthermore, the longest single high-resolution reconstruction of ENSO, derived from central Pacific corals, also supports an intensification of central Pacific ENSO impacts in the last 50 years relative to the previous millennia (Grothe et al., 2019). The addition of more multicentury proxy-based ENSO reconstructions would provide more context regarding the natural variability of ENSO, allowing a more robust assessment of the hypothesised anthropogenic shifts in ENSO's spatial footprint, which remains difficult to constrain with available records. At present, all available lines of evidence point to an intensification of ENSO's impacts in the coming decades, providing stakeholders with useful information to guide climate adaptation plans. With millions of people and many valuable ecosystems severely impacted by ENSO extremes, there is a pressing need to increase the number of centuries-long, high-resolution proxy-based reconstructions of ENSO variability from a gradient of sites spanning the tropical Pacific.

Table 3.- Summary of Spearman's rank correlation coefficients computed among the different reconstructions available for each mode of variability presented in this work. For each mode, the following information is included: the number of timeseries incorporated in the analysis, the total number of pairwise correlations computed, the amount (and percentage from the total in brackets) of pairwise correlations that are positive and significant at the 95 and 90% confidence levels, the lowest, highest and mean of all significant values at 90% correlation values. For each pairwise correlation the degrees of freedom were corrected to account for the timeseries autocorrelation. All pairwise correlations were performed between 1000 CE and 1850, or in the period of overlap between the two reconstructions if some of them were shorter. The industrial era (1850 onwards) was excluded to ensure that the calibration period of both timeseries was not included. All timeseries were interpolated to decadal resolution prior to the computation of the correlations. All Spearman's rank pairwise correlation coefficients for each mode and their associated p-values as well as links to original dataset sources are included in the supplementary material.

Mode	N° Timeseries	N° correlations	Significant at 95%	Significant at 90%	Lowest	Highest	Mean
<b>PDV</b>	8	28	3 (11%)	4 (14%)	-0.66	0.53	<b>0.08</b>
<b>ENSO</b>	11	55	19 (35%)	20 (36%)	-0.83	0.84	<b>0.20</b>
<b>AMV</b>	4	6	1 (17%)	1 (17%)	0.30	0.30	<b>0.30</b>
<b>NAO</b>	11	55	7 (13%)	10 (18%)	-0.27	0.52	<b>0.26</b>
<b>IOD</b>	-	-	-	-	-	-	-
<b>SAM</b>	3	3	2 (67%)	2 (67%)	0.18	0.47	<b>0.32</b>

### 3.2.- Pacific Decadal Variability

Pacific Decadal Variability (PDV), which characterises low-frequency variability in the Pacific Ocean (Fig. 1), is measured by a variety of statistical patterns in Pacific SSTs or sea surface heights, most commonly the Pacific Decadal Oscillation –PDO– (Mantua et al., 1997) and the Interdecadal Pacific Oscillation –IPO– (Power et al., 1999). The PDO is based on the leading component of SSTs in the Pacific Ocean north of 20°N; when PDO is negative, there are anomalously cool SSTs along the west coast of North America and warm SSTs in the central and western North Pacific (Mantua and Hare, 2002). The IPO is defined based on the second

1  
2  
3 principal component of low-frequency global SSTs (Henley et al., 2015), which allows a better  
4 definition of the IPO than using the tropical SST-based indices, since the latter includes  
5 many other variations, such as the global warming signal (Dai, 2013). During negative IPO  
6 phases, North Pacific SSTs are above average, while tropical Pacific SSTs are below average  
7 (Peng et al., 2015). Over the instrumental period, PDV has been marked by a combination of  
8 bidecadal and pentadecadal periodicities (i.e., 20 and 50 year cycles) thought to cause regime  
9 shifts when synchronised (Minobe, 1999). These shifts in PDV have been linked to global  
10 temperature trends (Kosaka and Xie, 2013; Meehl et al., 2016), as well as regional impacts on  
11 hydrology, ecological systems, and climate in North America (Dai, 2013; Kitzberger et al., 2007;  
12 Mantua et al., 1997; Trenberth et al., 2014), South America (Andreoli and Kayano, 2005; Boisier  
13 et al., 2016), East Asia (Hsu and Chen, 2011; Wang et al., 2008; Yao et al., 2018), and  
14 Australasia (Power et al., 1999; Rodriguez-Ramirez et al., 2014; Vance et al., 2015). The  
15 underlying dynamics of PDV, which may represent the superposition of multiple physical  
16 processes (Liu and Di Lorenzo, 2018; Newman et al., 2016; Schneider and Cornuelle, 2005),  
17 are not well understood. It is likely that at least some of the Pacific low-frequency variance  
18 originates from the ENSO system (Di Lorenzo et al., 2015; Newman et al., 2003) (see section  
19 5).

20  
21  
22 Reconstructions of PDV extending to the early- or mid-Holocene are derived from bidecadal or  
23 longer periodicities found in lacustrine and marine sediments. In a 13-ka lacustrine sediment  
24 record from Montana, USA (Stone and Fritz, 2006), it was suggested that the PDO may have  
25 experienced characteristic periodicities with fundamental state changes over time, with the  
26 strongest periodicity during the mid- Holocene and a complete breakdown of multidecadal  
27 frequencies from approximately 4.5 to 3.5 ka BP (Fig. 3). This shift in periodicity over the  
28 Holocene was also noted in a 10-ka reconstruction of PDV based on marine sediments near  
29 British Columbia, Canada, which revealed a change from bidecadal and pentadecadal variability  
30 in the early Holocene to only pentadecadal periodicities in the late Holocene (Ivanochko et al.,  
31 2008). Similarly, a 9.7 ka lacustrine record of PDO from California, USA, indicated the PDO  
32 regimes may have had variable length intervals over time, lasting from 150-550 years, with  
33 extended positive PDO phases recorded in the early-Holocene (9.7–8.85 cal ka BP), mid-to-late  
34 Holocene (4.8–3.2 cal ka BP), and late Holocene (1.5–0.15 cal ka BP) (Fig. 3; Kirby et al.,  
35 2010). Lacustrine and marine sediment records covering just the late Holocene also indicate  
36 that the prominent PDV periodicities may have varied over time (Beaufort and Grelaud, 2017;  
37 Lapointe et al., 2017).

38  
39  
40 Records of PDV covering the Medieval Climate Anomaly (MCA) are available from ice cores,  
41 tree rings, and speleothems (Fig. 3). A reconstruction based on an Antarctic ice core showed  
42 that the IPO was in a persistently positive state from 1000-1212 CE, and this period was  
43 associated with extended Australian megadrought conditions (Vance et al., 2015). A lack of  
44 variance in North Pacific SSTs was also detected in a speleothem-based reconstruction during  
45 the MCA from California, USA (850-1100 CE; (McCabe-Glynn et al., 2013)). A millennial-length  
46 North American tree ring reconstruction substantiated the breakdown of pentadecadal variability  
47 from 1000-1200 CE and likewise found that the MCA was characterised by an extremely  
48 persistent negative PDO state from 992-1300 CE, contemporaneous with severe drought in  
49 North America (MacDonald and Case, 2005). Unlike the persistent positive conditions identified  
50  
51  
52  
53  
54  
55  
56  
57  
58  
59  
60  
61  
62  
63  
64  
65

1  
2  
3 by Vance et al. (2015), MacDonald and Case, (2005) identified persistently negative PDO  
4 conditions during the MCA (Fig. 3).  
5  
6

7 Reconstructions of PDV from tree rings, coral, and historical records also extend through the  
8 LIA. By integrating a network of coral records from the South Pacific and tree rings from diverse  
9 locations around the Pacific Basin, Evans et al. (2001) showed that PDV was synchronised  
10 across the NH and SH over the past 200-years. A range of proxy-based records from both  
11 hemispheres indicate a muted PDV signal in the LIA and an increase in pentadecadal variability  
12 concurrent with the end of the LIA in the mid-1800s (Fig. 3). Shen et al. (2006), reconstructing  
13 PDO to the mid-1400s from Chinese historical documents, found inconsistent periodicities over  
14 the 530-year record: although the decadal and bidecadal signals were relatively consistent, the  
15 pentadecadal signal only existed after the end of the LIA around 1850. A lack of pentadecadal  
16 variability in the LIA was also reported in multiple NH tree ring-based PDO reconstructions  
17 (Biondi et al., 2001; MacDonald and Case, 2005); the bidecadal component may also have  
18 been weaker in the late-1700s and early-1800s (Biondi et al., 2001; Gedalof et al., 2002). This  
19 signal dampening extended to the SH, where a coral-based IPO reconstruction showed muted  
20 PDV in the 1700s (Linsley et al., 2008).  
21  
22  
23  
24  
25

26 Much of what we know about PDV is based on the 20th century, which was characterised by  
27 quasiregular regime shifts in the 1920s, 1940s, and 1970s (Mantua et al., 1997; Minobe, 2000).  
28 Proxy-based reconstructions of PDV often diverge on pre-instrumental regime phases and  
29 timing (McAfee, 2014; Wise, 2015), which is reflected in the low correlations shown in Table 3.  
30 However, these reconstructions consistently report that the 20th century is not characteristic of  
31 the pre-instrumental past. Reconstructions show that PDV, particularly the pentadecadal  
32 component, has been highly variable over time (Ivanochko et al., 2008; Kirby et al., 2010;  
33 MacDonald and Case, 2005), with a shift in the mid-1800s (D'Arrigo et al., 2001; Gedalof and  
34 Smith, 2001) leading to a notable increase in low-frequency (pentadecadal) variability over the  
35 past century (Biondi et al., 2001; Felis et al., 2010; McCabe-Glynn et al., 2013; Shen et al.,  
36 2006). These 20th century changes indicate that there may be different drivers of PDV in the  
37 instrumental period than in the palaeoclimate past. The increase in low-frequency variability  
38 after 1850 corresponds to an increase in greenhouse gas forcing (Shen et al., 2006), and in  
39 modelling simulations, PDV continues to show significant power at longer timescales while the  
40 bidecadal signal is overwhelmed by the warming forcing (d'Orgeville and Peltier, 2009). Other  
41 potential drivers of PDV change include an increasing influence of the tropical Pacific on PDV  
42 over the past century, as indicated by proxy records (D'Arrigo et al., 2015; Wise, 2015), and  
43 decadal warming trends in the Atlantic that may be affecting PDV through changes in Walker  
44 circulation (Cai et al., 2019).  
45  
46  
47  
48  
49  
50  
51

### 52 **3.3.- Atlantic Multidecadal Variability**

53  
54

55 The Atlantic Multidecadal Variability (AMV) - also referred to as the Atlantic Multidecadal  
56 Oscillation (AMO) - is a coherent pattern of multidecadal variability in the North Atlantic SSTs  
57 with an estimated period ranging from approximately 50-80 years (Schlesinger and  
58 Ramankutty, 1994). The AMV is defined as an area average of detrended low-pass filtered  
59 North Atlantic (0-65°N, 80-0°W; Fig. 1) SST anomalies (Enfield et al., 2001; Trenberth and  
60  
61  
62  
63  
64  
65

1  
2  
3 Shea, 2006). The AMV has wide-ranging climatic impacts on the circum-North Atlantic climate  
4 (Knight et al., 2006; Sutton and Hodson, 2005) and hurricane activity (Goldenberg et al., 2001)  
5 and farther afield including precipitation in Sahel, India and Brazil (Feng and Hu, 2008; Folland  
6 et al., 2001, 1986; Rowell et al., 1995).  
7  
8  
9

10 The origin of the AMV remains debated in the observational and modelling community. Several  
11 hypotheses include the response of the North Atlantic SSTs to external radiative forcing,  
12 specifically by either anthropogenic or volcanic aerosols (e.g., Booth et al., 2012; Otterå et al.,  
13 2010), atmospheric-induced surface heat flux (Clement et al., 2015) and changes in the Atlantic  
14 Meridional Overturning Circulation (see Zhang et al., (2019) for a comprehensive review on  
15 this). Uncertainty not only surrounds the origin of the AMV but also its long-term periodicity. This  
16 phenomenon is largely because the length of instrumental records (~150 years) is too short to  
17 study the multidecadal nature of this mode of climate variability, which is also complicated by  
18 the underlying anthropogenically forced warming. Similarly, reconstructing this mode in the past  
19 is also challenging as the temporal resolution of most marine proxy archives is often not  
20 sufficient to study this multidecadal timescale. Only a few long oceanic records from tropical  
21 Atlantic corals exist (Black et al., 2007; Haase- Schramm et al., 2003; Kilbourne et al., 2008;  
22 Vásquez- Bedoya et al., 2012), which were initially compiled together to study their  
23 multidecadal variability (Kilbourne et al., 2014) and further updated with shorter marine records  
24 by Svendsen et al. (2014). Past reconstructions of this mode of variability (Fig. 4) are heavily  
25 reliant on high-resolution terrestrial archives, including ice cores, lake varves, historical records  
26 and tree rings (Gray et al., 2004; Mann et al., 2009; Wang et al., 2017). These AMV  
27 reconstructions either exploit the hydro and temperature climate spatial patterns associated with  
28 this mode of climate variability in the modern and assume stationarity of these in the past or rely  
29 on the spectral properties in these archives. Other studies, however, have found similar AMV  
30 patterns (Mjell et al., 2016) and spectral peaks (50-80 years) (Moffa-Sanchez et al., 2015) in  
31 past flow reconstructions in deep components of the AMOC, hence hinting at past AMV-AMOC  
32 linkage over the recent millennia as suggested in the last millennium models (Lohmann et al.,  
33 2015). However, coeval changes in SST and in other reconstructions of deep flow strength in  
34 the North Atlantic are not always found (e.g. Mjell et al., 2015).  
35  
36  
37  
38  
39  
40  
41  
42

43 Continuous reconstructions of the AMV over the entire Holocene are sparse due to the limited  
44 availability of subdecadally resolved climate reconstructions to study a multidecadal mode (Fig.  
45 4). Spectral analysis of seven palaeoclimatic datasets from around the North Atlantic exhibit  
46 similar quasi-periodic oscillations to the AMV (55-70 year) with latitudinal variability in the timing  
47 of the stronger peaks across the last 8 ka (Knudsen et al., 2011). In contrast, the comparison  
48 between drought indices and SST suggested a stronger centennial AMV-like spatial pattern  
49 during the late Holocene compared with the early-Holocene (Feng et al., 2011).  
50  
51  
52

53 Studies focused on the Common Era suggest a fairly positive AMV over the first millennium (0-  
54 1000 CE; Fig. 4) (Mann et al., 2009; Singh et al., 2018). Over the last millennium (or part of),  
55 reconstructions predominantly show a negative AMV during the LIA and a positive AMV during  
56 the MCA (Gray et al., 2004; Mann et al., 2009; Singh et al., 2018; Wang et al., 2017) (Fig. 4).  
57 These findings are in line with the warmer surface temperatures from the tropical Atlantic  
58 records (Kilbourne et al., 2014). Analysis of the available reconstructions, however, present  
59  
60  
61  
62  
63  
64  
65

1  
2  
3 varied degrees of correlation amongst the available records (Table 3). Spectral analysis over  
4 the last millennia show varied results. Greenland ice cores reveal different periodicities between  
5 the LIA (~20 years) and the MCA (11 and 45 years), which are noticeably different from the  
6 modern (45-65 years) (Chylek et al., 2012), whereas SSTs from the Caribbean have revealed  
7 consistent multidecadal variability since 1350 CE. In contrast, data assimilation studies show a  
8 lack of distinct multidecadal/centennial variability over the last 2 ka with the strongest  
9 multidecadal peaks found after 1900 CE (Singh et al., 2018). From 1850 CE, AMV  
10 reconstructions consistently reveal multidecadal cycles underlain by the warming signal as seen  
11 in the observational timeseries (Alexander et al., 2014; Hetzinger et al., 2008; Singh et al.,  
12 2018).  
13  
14  
15  
16  
17

### 18 **3.4.- North Atlantic Oscillation**

19

20 The North Atlantic Oscillation (NAO), a mode of variability closely related to the Northern  
21 Annular Mode (NAM) / Arctic Oscillation (AO) (Thompson and Wallace, 2001, 2000), is the most  
22 prominent boreal winter (December to March) atmospheric mode of climate variability in the  
23 North Atlantic extra-tropics (Glueck and Stockton, 2001; Hurrell, 1995; Hurrell et al., 2003;  
24 Jones et al., 1997; Koder, 2002; Wanner et al., 2001). The pattern consists of two opposite-  
25 sign centres of action over the Icelandic low and Azores high (Fig. 1), with an equivalent  
26 barotropic structure explaining up to 50% of the winter variability of the troposphere pressure  
27 fields (Hurrell et al., 2003; Wanner et al., 2001). Changes in the mean circulation patterns over  
28 the North Atlantic associated with the NAO are accompanied by changes in the mean wind  
29 direction over the Atlantic, in the heat and moisture transport between the Atlantic and the  
30 surrounding areas, and in the intensity and number of storms and their paths (Hurrell, 1995).  
31 For a comprehensive review of the wide range of responses of marine, terrestrial and  
32 freshwater ecosystems to NAO variability, see Wanner et al., (2001).  
33  
34  
35  
36  
37

38 The NAO is typically defined through the leading Principal Component of gridded winter monthly  
39 Sea Level Pressure (SLP) (Portis et al., 2001; Stephenson et al., 2003), which leads to limits in  
40 its time extension since a sufficiently wide dataset on SLP mainly covers the last century. Over  
41 the past decades, there has been interest in documenting and understanding the NAO  
42 variability on annual to multidecadal timescales, by extending estimates of the NAO index as far  
43 back in time as possible (Fig. 5). The NAO variability within the instrumental period has been  
44 examined in the form of normalised pressure differences that reflect changes in the atmospheric  
45 pressure gradient between the so-called Icelandic Low and the subtropical northern Atlantic with  
46 suitably located instrumental SLP records (Stykkisholmur, Akureyri, Reykjavik; Gibraltar, Lisbon,  
47 Ponta Delgada). Recent efforts have also used other measures of the westerly strength  
48 including information from London and Paris (Cornes et al., 2013), ship logbook information  
49 from the Channel and the North Atlantic (Barriopedro et al., 2014; Mellado-Cano et al., 2019),  
50 and a combination of instrumental and ship log book data (Küttel et al., 2010). The timescales of  
51 the NAO range from days to centuries (Cook et al., 2019; Feldstein, 2000; Luterbacher et al.,  
52 2001, 1999; Ortega et al., 2015). Periods when the same state of the main NAO characteristics  
53 persist over several consecutive winters are observed within the instrumental record (e.g., the  
54 1960s were characterised by an unusually negative NAO index and the 1990s by unusually  
55 positive values (Osborn, 2004; Scaife et al., 2005).  
56  
57  
58  
59  
60  
61  
62  
63  
64  
65



1  
2  
3  
4  
5 The NAO accounts for 35 to 50% of the variance in the winter SLP field over the North Atlantic  
6 region (Cassou and Terray, 2001; Hurrell et al., 2003; Osborn et al., 1999), and other  
7 atmospheric circulation patterns are, therefore, important to fully characterise the winter climate  
8 in the region (Cassou and Terray, 2001; Trigo et al., 2008). In particular, studies suggest that  
9 non-linear relationships between atmospheric modes and winter precipitation in the Euro-  
10 Atlantic region, modulate the climatic imprint of the NAO (Álvarez-García et al., 2019; Comas-  
11 Bru et al., 2016; Moore et al., 2013; Pinto and Raible, 2012). This phenomenon may, in turn,  
12 affect the robustness of reconstructions of past NAO states if calibrated with a short period in  
13 the recent past. In particular, the East Atlantic (EA) pattern plays an important role in positioning  
14 the primary North Atlantic storm track (Moore et al., 2011; Woollings and Blackburn, 2011),  
15 likely affecting precipitation patterns over Europe and the Mediterranean (Comas-Bru and  
16 Hernández, 2018; Comas-Bru and McDermott, 2014; Trigo et al., 2008; Xoplaki et al., 2004).

21 A few NAO reconstructions for the last centuries have been published and/or compared with  
22 each other (Baker et al., 2015; Cook et al., 2019; Faust et al., 2016; Hernández et al., In Review;  
23 Luterbacher et al., 2001; Olsen et al., 2012; Ortega et al., 2015; Schmutz et al., 2000; Sjolte et  
24 al., 2018; Timm et al., 2004; Trouet et al., 2009). Taking into consideration the associated  
25 reconstruction uncertainties and disparate correlations between them (Table 3), they  
26 demonstrate with high confidence that the strong positive NAO phases of the 1990s and early  
27 20th century are not unusual in the context of the past centuries (Fig. 5). The NAO  
28 reconstruction by Trouet et al. (2009) yielded a persistent positive phase throughout most of the  
29 medieval era from the 11th to the 14th centuries, which is not, however, consistent with a strong  
30 NAO imprint in the Greenland ice core data (Sjolte et al., 2018; Vinther et al., 2010). Recent  
31 independent NAO reconstructions (Cook et al., 2019; Ortega et al., 2015) and transient model  
32 simulations neither support a persistent positive NAO during the MCA, nor a strong NAO phase  
33 shift during the LIA (Lehner et al., 2012; Masson-Delmotte et al., 2013; Moreno-Chamarro et al.,  
34 2017b; Yiou et al., 2012). Less is known about the NAO variability before medieval times  
35 (Hernández et al., In Review; Olsen et al., 2012).

41 A 5.2-ka lake sediment record from southwestern Greenland suggests that, approximately 4.5  
42 and 0.65 ka ago, variability associated with the NAO changed from generally positive to  
43 variable, with intermittently negative conditions (Olsen et al., 2012). Recently, a long marine  
44 reconstruction from the Irish Shelf suggested an easterly shift of the Icelandic Low at 4.2 ka,  
45 resulting in a transition from a zonal to more meridional flow of the westerly winds over the East  
46 North Atlantic (Curran et al., 2019). However, a negative NAO-type pattern is suggested for the  
47 early- and late-Holocene, proposed to be associated with periods of higher flux of ice rafting  
48 debris (IRD) recorded in North Atlantic sediments (Bond et al., 2001, 1997) as a result of an  
49 enhanced transport of sea ice (Blindheim and Østerhus, 2013; Brahim et al., 2019). A  
50 multiproxy lake record from the Middle Atlas in Morocco, also revealed that a multi-centennial-  
51 scale NAO-type pattern, potentially related to solar variability, modulates the Western  
52 Mediterranean climate (Zielhofer et al., 2017). Another study based on two speleothem records  
53 from NW Morocco and Germany suggested that during the early-Holocene, the NAO centres  
54 were shifted in response to the deglaciation of the Laurentide ice sheet, which affected the  
55 position of the southern rainfall correlation belt (Wassenburg et al., 2016). For the mid-  
56  
57  
58  
59  
60  
61  
62  
63  
64  
65

1  
2  
3  
4  
5  
6  
7  
8  
9  
10  
11  
12  
13  
14  
15  
16  
17  
18  
19  
20  
21  
22  
23  
24  
25  
26  
27  
28  
29  
30  
31  
32  
33  
34  
35  
36  
37  
38  
39  
40  
41  
42  
43  
44  
45  
46  
47  
48  
49  
50  
51  
52  
53  
54  
55  
56  
57  
58  
59  
60  
61  
62  
63  
64  
65

Holocene, Mauri et al. (2014), using a reconstruction of temperature over Europe mainly based on pollen data, suggested that the mean state atmospheric circulation may have been shifted into a positive NAO-like configuration, although this possibility remains debated due to model simulations do not reproduce such a signal (Găinușă-Bogdan et al., 2020).

#### 4.5.- Indian Ocean Dipole

The Indian Ocean Dipole (IOD) is an irregular oscillation of SSTs (Fig. 1) in which the western Indian Ocean becomes alternately warmer and colder than its eastern counterpart (Abram et al., 2015). By definition, the positive IOD phases correspond to a weakening in the zonal SST gradient, and vice versa. The IOD can be classified into different types (e.g., canonical IOD and IOD Modoki) according to the location and occurrence time (Endo and Tozuka, 2016; Guo et al., 2018). IOD affects precipitation and temperature across the regions around the Indian Ocean (Abram et al., 2015), such as Africa, Australia, southern China, and southern Asia. During positive IOD phases, abnormally warm SSTs in the western Indian Ocean cause a westward shift in the convection cell that is usually situated over the eastern Indian Ocean warm pool, bringing heavy rainfall over East Africa and severe droughts over the Indonesian region and southeastern Australia (Ummenhofer et al., 2016).

Direct instrumental SST records are the most reliable source of IOD variability, but they only extend back to 1958 CE. Longer estimates are derived via interpolation or assimilation of distant observations (e.g., HadSST4; Kennedy et al., (2019)). Long-term IOD reconstructions (Fig. 6) have been developed from proxy-base climate records, such as coral, marine sediments and tree rings (Abram et al., 2020, 2015, 2007; D'Arrigo et al., 2008; Kwiatkowski et al., 2015; Watanabe et al., 2019). For example, coral  $\delta^{18}\text{O}$  records are sensitive to the balance between evaporation and precipitation in the surface ocean, which is strongly related to SST, therefore allowing for monthly reconstructions that go back to 1846 CE (Abram et al., 2015). Coral Sr/Ca ratios also record SST variability and can reconstruct past IOD variations. Likewise, the Mg/Ca ratio and  $\delta^{18}\text{O}$  of foraminiferal records from sediments of the Indian Ocean reflect the thermocline and temperature variability and thus capture the IOD variability (D'Arrigo et al., 2008; Kuhnert et al., 2014; Kwiatkowski et al., 2015). Annual tree ring width measurements from Java (Indonesia) reflect local changes in the Palmer Drought Severity Index and thus describe IOD variability through one of its well-established climate impacts (D'Arrigo et al., 2008).

Coral-based IOD reconstructions show consistent variability on yearly scales (Fig. 6) and support that during the 20<sup>th</sup> century, the IOD experienced an increase in frequency and intensity of its positive phases (from every 20 years at the beginning to every 4 years at the end, with a mean every 17.3 years; Abram et al. (2020, 2008)). The increase in positive IOD phases may be caused by an enhanced warming of the western Indian Ocean and by strengthened IOD-monsoon interactions, as well as by increasing greenhouse gas concentrations (Cai et al., 2014; Nakamura et al., 2009). Extreme positive IOD values were rare before 1960 (Abram et al., 2020); however, three exceptionally strong positive IOD signals in 1961, 1994, and 1997 CE were detected in several coral records (Abram et al., 2015). Also noteworthy are the recorded low events in recent years, some of which have been linked to a strong sea-ice decline in Antarctica since 2016 (Meehl et al., 2019; Wang et al., 2019b). Comparisons of highly resolved

1  
2  
3  
4 last millennium IOD reconstructions with observations suggest that the latter tend to  
5 underestimate the recurrence interval of positive IOD events during the pre-industrial period  
6 (i.e., before 1850 CE), especially in smaller reconstruction windows (Abram et al., 2015). This  
7 phenomenon might explain why positive IOD events are less frequent during the pre-industrial  
8 period compared with the 20th century.  
9

10  
11 Early- and mid-Holocene IOD records are scarcer, especially for the western Indian Ocean, thus  
12 limiting the characterization of the west-east SST gradient. IOD Holocene reconstructions based  
13 on SST-sensitive records from the eastern Indian basin (Abram et al., 2009, 2007) and  
14 precipitation pattern changes between Sumatra and East Africa and Southeast India  
15 (Niedermeyer et al., 2014) suggest a tendency towards more negative phases (i.e., a  
16 strengthened zonal SST gradient) from the mid- to the late-Holocene. In particular, SST  
17 reconstructions from fossil corals covering approximately the past 6.5 ka revealed that IOD  
18 events were probably characterised by a more persistent and stronger positive IOD during  
19 the mid-Holocene, associated with a stronger Asian monsoon driving strengthened cross-  
20 equatorial winds that enhanced the cooling conditions in the East Indian ocean (Abram et al.,  
21 2007). This positive IOD condition was further confirmed by concomitant precipitation patterns  
22 between Sumatra and East Africa and Southeast India (Niedermeyer et al., 2014). However,  
23 opposite results have also been reported. In particular, planktic foraminifera records and Mg/Ca  
24 ratios from western Sumatra suggest that the thermocline was deeper, indicative of more  
25 negative IOD conditions, in the early- and mid-Holocene compared with the late-Holocene  
26 (Kwiatkowski et al., 2015). This disagreement with previous reconstructions can be partly  
27 attributed to the different temporal resolutions and sensitivity to different climate variables of the  
28 proxies used in each study (see section 2.1). Concretely, corals well reflect the seasonal  
29 variability of the IOD while the marine sediment proxies have a lower resolution and may be  
30 more reflective of long-term changes. The characteristics of certain species (i.e., warm-water  
31 planktic foraminifera) may less accurately represent the generally cold ocean upwelling  
32 conditions, causing an overestimation of its strength (Kwiatkowski et al., 2015). In addition, the  
33 mid-Holocene climate experienced global-scale anomalies and temperature patterns in the  
34 Indian Ocean that possibly reflected remote forcing rather than the IOD, which might hamper  
35 direct comparisons in SST reconstructions between the west and east Indian Ocean (Kuhnert et  
36 al., 2014). New reconstructions including accurate dating and multiple proxies are thereby  
37 needed to better constrain the IOD variability during the Holocene.  
38  
39  
40  
41  
42  
43  
44  
45  
46

### 47 **3.6.- Southern Annular Mode**

48

49  
50 The Southern Annular Mode (SAM) is the strongest mode of atmospheric circulation variability  
51 in the extratropical regions of the SH (Gong and Wang, 1999; Marshall, 2003; Thompson and  
52 Wallace, 2000). A positive phase is associated with stronger and poleward shifted westerly  
53 winds in midlatitudes, while the negative phase is characterised by weaker and more  
54 equatorward westerlies. The SAM can be defined either as the normalised difference in  
55 pressure between 40°S and 65°S (Fig. 1) (Gong and Wang, 1999), or as the first principal  
56 component of the geopotential height, generally southward of 20°S at 850 hPa (Thompson and  
57 Wallace, 2000). The two definitions lead to similar patterns and conclusions over the  
58 instrumental era.  
59  
60  
61  
62  
63  
64  
65

1  
2  
3  
4  
5 Changes in the SAM have been linked to widespread variations in the atmosphere, sea ice and  
6 the ocean (Gillett et al., 2006; Lefebvre et al., 2004; Sen Gupta and England, 2006; Thompson  
7 and Solomon, 2002; Thompson and Wallace, 2000). Corresponding shifts in westerlies induce  
8 anomalous temperature and precipitation patterns that include, for instance, dry conditions in  
9 Tasmania and warm anomalies over the Antarctic Peninsula during positive phases of the SAM  
10 (Gillett et al., 2006; Thompson and Solomon, 2002). The stronger winds enhance the transport  
11 of sea ice and surface oceanic waters that favour a decrease in sea-ice concentrations in the  
12 Weddell Sea and around the Antarctic Peninsula and an increase in the Ross Sea (Lefebvre et  
13 al., 2004; Oliva et al., 2017; Sen Gupta and England, 2006). Additionally, the stronger winds  
14 tend to increase upwelling in the Southern Ocean, causing a surface warming at high latitudes  
15 that may enhance the meridional overturning circulation in the Southern Ocean, although this  
16 effect could be partly counterbalanced by a concomitant increase in eddy activity (Gent, 2016;  
17 Meredith and Hogg, 2006; Sen Gupta and England, 2006). Furthermore, as the response of  
18 ocean surface currents, upwelling and eddies act at different timescales, the large-scale impacts  
19 of SAM variability may be different in interannual and longer periods (Ferreira et al., 2015).  
20  
21  
22  
23  
24

25 Instrumental data allow a direct estimate of the SAM index since 1957 CE (Marshall, (2003) and  
26 update <https://legacy.bas.ac.uk/met/gjma/sam.html>). To extend back beyond the 1960s, SAM  
27 reconstructions (Fig. 7) have to rely on a few weather stations and indirect (proxy-based)  
28 records, mainly derived from tree rings in the mid-latitudes of the SH continents and Antarctic  
29 ice cores (Abram et al., 2014; Dätwyler et al., 2018; Fogt et al., 2009; Hessel et al., 2017; Villalba  
30 et al., 2012; Zhang et al., 2010). Reconstructions using only tree ring records are for the  
31 summer only (Villalba et al., 2012), while the annual reconstructions using a wider range of  
32 proxies may be biased towards summer as their main source of information at midlatitudes is  
33 also the tree rings (Abram et al., 2014; Dätwyler et al., 2018).  
34  
35  
36  
37

38 Those reconstructions indicate that the increase in the SAM index in summer observed recently  
39 and attributed to a response to anthropogenic forcing (greenhouse gas and ozone forcing;  
40 Arblaster and Meehl, 2006; Thompson et al., 2011) is likely unprecedented in the context of the  
41 past centuries (Abram et al., 2014; Dätwyler et al., 2018). Despite some inconsistencies before  
42 the 19th century (Hessel et al., 2017), long term reconstructions suggest a minimum occurred in  
43 the 15th century (Fig. 7), with a weak positive trend after that period and a relatively stable index  
44 oscillating around neutral conditions for the first centuries of the last millennium (Abram et al.,  
45 2014; Dätwyler et al., 2018; Villalba et al., 2012). This phenomenon leads to a relatively high  
46 and significant correlation between the available reconstructions (Table 3).  
47  
48  
49  
50

51 There is currently no formal reconstruction of the SAM covering more than 1 ka (Fig. 7).  
52 However, as the changes in the position and strength of the SH westerly winds are a major  
53 characteristic of the climate of the mid-to high latitudes of the SH, several studies have  
54 attempted to reconstruct their evolution (Fletcher and Moreno, 2012; Kilian and Lamy, 2012;  
55 Reynhout et al., 2019; Saunders et al., 2018). Unfortunately, a clear common consensus on the  
56 behaviour of the westerlies cannot be reached from those studies because of some  
57 inconsistencies between their conclusions, partly due to the proxies selected, which are  
58 influenced by precipitation or temperature and thus only indirectly related to the winds. The  
59  
60  
61  
62  
63  
64  
65

proxies may also reflect regional changes that would prevent a general and simple conclusion that is valid for all regions and longitudes.

Many studies suggest that the westerlies were strong during the early- to mid-Holocene (Fletcher and Moreno, 2012; Kilian and Lamy, 2012; Reynhout et al., 2019; Saunders et al., 2018), although there is also evidence for long periods of reduced winds (Anderson et al., 2018; Reynhout et al., 2019; Saunders et al., 2018). The situation appears to be even more complex after 5 ka BP, with reconstructions showing significant centennial and millennial variability but no consistent trend among the available records, some of which suggest the development of a strong zonal regional asymmetry in the southern westerly winds (Anderson et al., 2018; Fletcher et al., 2018; Fletcher and Moreno, 2012; Reynhout et al., 2019; Saunders et al., 2018; Turney et al., 2017; Voigt et al., 2015).

#### **4.- Mode interactions**

This section summarises intra-basin and inter-basin interactions, interferences and interdependences between the modes previously described, starting with the modes in the Pacific basin (ENSO, PDV) followed by those in the Atlantic (AMV, NAO), the Indian basin (IOD) and Antarctica (SAM). For each case, we group such interactions over the observational period, the past two millennia, and the Holocene, and we summarise these in Figure 8. This Section also discusses climate signals, as recorded by proxies, that are simultaneously influenced by several modes, and that are thus sensitive to interplays between them, hampering their interpretation.

##### **4.1. Pacific basin**

Analysis based on observations suggests that atmospheric and oceanic teleconnections forced by ENSO can impact lower frequency variability, such as the PDV, through interactions of zonal and meridional modes in the Pacific (Di Lorenzo et al., 2015). However, this interaction might not be stationary in time, as found for the past millennium. While tree-ring records from California and Alberta consistently exhibit year-to-year ENSO variability across the past millennium, PDV-related multidecadal oscillations are not always present, in particular during the LIA (MacDonald and Case, 2005). In addition, two other independent multiproxy ENSO reconstructions based on precipitation- and temperature-sensitive records show no statistically significant correlation over the last millennium with PDV reconstructions based on North American and East Asian tree rings (Henke et al., 2017), yet this decoupling between ENSO/PDV is not supported by two other independent proxy-based records from Santa Barbara Basin laminated sediments covering the last 2.7 ka (Beaufort and Grelaud, 2017). In a longer context, the Santa Barbara Basin records suggest a dominant positive PDV and more intense warm ENSO events during the mid-Holocene (Friddell et al., 2003). Likewise, a record from Effingham Inlet shows evident bidecadal and pentadecadal variability in the early-Holocene but absent bidecadal variability during the late Holocene (Ivanochko et al., 2008). An opposite situation might have occurred for interannual ENSO variability, which banded corals from Papua New Guinea support, becoming stronger and more frequent over the course of the Holocene (Tudhope et al., 2001).

1  
2  
3  
4  
5 Regarding the link with other basins, both ENSO and NAO might have influenced the drought  
6 variability in Nicaragua over the past 1.4 ka (Stansell et al., 2013), and PDV variance has also  
7 been linked to the Atlantic Ocean (d'Orgeville and Peltier, 2007; Zhang and Delworth, 2006).  
8 The interplay between ENSO variability, Equatorial South Atlantic temperatures and the South  
9 American monsoon might have modulated mean moisture conditions in the high Ecuadorian  
10 Andes over the past a ka, with interdecadal Pacific and Atlantic variability providing the  
11 dominant forcing before and after 1500 CE, respectively (Ledru et al., 2013). ENSO may also  
12 have influenced Asian hydroclimate and monsoon variability in the MCA and LIA periods, with  
13 some possible contribution from the AMV and NAO as well (Chen et al., 2015). Medieval  
14 megadroughts over Europe have been connected with coinciding ENSO–NAO phases of the  
15 same sign during the MCA (Helama et al., 2009). A dynamic link is also suggested between the  
16 reconstructed ENSO variability and the NH climate in the past millennium, as a result of the  
17 interplay between ENSO, the Pacific Walker and monsoonal circulations, and NAO (Yan et al.,  
18 2011).  
19  
20  
21  
22  
23

24 The review by Cai et al. (2019) summarises the state of knowledge regarding tropical climate  
25 variability and interactions between modes such as ENSO, PDV, AMV, and IOD both in the  
26 instrumental period and in climate models. The review details the strong and complex  
27 connections between the Atlantic, Pacific, and Indian tropical climate on interannual to  
28 multidecadal timescales; it further highlights the need for extended proxy-based records of such  
29 modes of variability in the past to provide a longer perspective for such interactions.  
30  
31  
32

#### 33 **4.2. Atlantic, Arctic and Mediterranean basins**

34

35 Multidecadal interactions between the NAO and the AMV were reviewed for the instrumental  
36 period by Grossmann and Klotzbach, (2009), interactions that were mediated via changes in the  
37 salt and heat ocean transport and the Atlantic meridional temperature gradient. More recently,  
38 Zhang et al., (2019) reviewed the impacts and teleconnections of the AMV, both from  
39 observations and model simulations, and the mechanisms by which the AMV could drive PDO  
40 phase changes or modulate ENSO and NAO variability. The review also summarises recent  
41 advances in the palaeoclimate to reconstruct AMV variability and its associated impacts.  
42  
43  
44  
45

46 Proxy-based studies suggest that during the MCA, hydroclimate changes over the Sahel and  
47 Mediterranean regions were caused by phase modulations in both the NAO and AMV (Lüning et  
48 al., 2019, 2018): aridity in Morocco typically coincides with a positive NAO, while increased  
49 rainfall in western Sahel occurs with a positive AMV. Likewise, rainfall on the African eastern  
50 coast has been linked to IOD phase changes (Lüning et al., 2018). Decadal and multidecadal  
51 periodicities in both NAO reconstructions and NAO-sensitive climate proxies have been  
52 extensively linked to the AMV in studies covering the entire Holocene and shorter periods within  
53 it (Fig. 8; Ait Brahim et al., 2018; Knight et al., 2006, 2005; Knudsen et al., 2011; Ojala et al.,  
54 2015; Ólafsdóttir et al., 2013; Olsen et al., 2012; Wassenburg et al., 2016). Further interactions  
55 between the NAO and other modes of variability in the NH have been proposed for the past  
56 millennia. A varve record from Lake Kalliojärvi (Central Finland) suggests alternating influences  
57 from the NAO and Siberian High over the past four millennia (Saarni et al., 2016). A compilation  
58  
59  
60  
61  
62  
63  
64  
65

1  
2  
3 of Iberian marine and continental records suggests that local temperature and precipitation  
4 evolutions are explained by NAO interplays with the EA: the Roman Period (–200-500 CE) was  
5 dominated by persistent negative NAO and positive EA phases, the early Middle Ages (500-900  
6 CE) by positive NAO and negative EA phases, the MCA (900-1300 CE) by positive NAO and  
7 EA phases, and the LIA (1300-1850 CE) by negative phases in both indices (Sánchez-López et  
8 al., 2016). In a shorter-time perspective, reconstructions since 1675 CE NAO suggest that the  
9 NAO covaried intermittently with other Eurasian circulation indices and that these interactions  
10 modulate the impact of the NAO on the European climate (Luterbacher et al., 1999; Mellado-  
11 Cano et al., 2019).

12  
13  
14  
15  
16 Finally, potential links between the NAO and ENSO modes (Fig. 8) have been documented in a  
17 proxy-based record from Central America, with prevailing Niña-like conditions coinciding with  
18 positive NAO phases over most of the early Middle Ages and MCA periods, and opposite  
19 situations in the most recent centuries (Stansell et al., 2013). More intricate interactions arise  
20 when considering together NAO, ENSO and AMV mode variability (Zhang et al., 2019),  
21 emphasizing the need to enhance temporal and spatial resolutions in reconstruction coverages.  
22  
23

#### 24 25 **4.3. Indian basin**

26  
27 Interactions between the IOD, monsoon, and ENSO remain poorly understood (Fig. 8) due to  
28 the short span of observations, and the presence of different types of IOD with different  
29 influences on regional precipitation (Endo and Tozuka, 2016). Studies based on observations  
30 have related decadal and interannual variability in IOD to PDV and ENSO variability,  
31 respectively (Krishnamurthy and Krishnamurthy, 2016).  
32  
33

34  
35 A joint examination of IOD, ENSO and Asian monsoon reconstructions helps improve our  
36 understanding of precipitation and drought patterns in Africa, south-eastern Australia, and Asia  
37 (Abram et al., 2007; Endo and Tozuka, 2016; Fan et al., 2017). For example, the 1877 strong  
38 positive IOD event is widely revealed by coral-based SST reconstruction and tree ring PDSI  
39 records; this positive IOD event coincided with one of the strongest El Niño events in the last  
40 two centuries and with extreme Asian monsoon failure conditions (Abram et al., 2007; D'Arrigo  
41 et al., 2008), possibly leading to a major drought over Java (D'Arrigo et al., 2008). Other studies  
42 also support a relationship between IOD, ENSO and monsoon variability (Abram et al., 2008;  
43 D'Arrigo et al., 2008), a link that might also take place at decadal timescales between the PDV  
44 and the decadal modulations in the IOD (Krishnamurthy and Krishnamurthy, 2016). In the past  
45 millennium, a tight coupling has been detected between IOD and ENSO records, especially  
46 since 1590 CE (Abram et al., 2020). These interactions should be revisited with new proxy-  
47 based reconstructions incorporating state-of-the-art dating methods (e.g.,  $^{234}\text{U}/^{230}\text{Th}$  series) and  
48 archives (e.g., shells).  
49  
50

51  
52  
53  
54  
55 During the Holocene, interactions between IOD and ENSO might have modulated precipitation  
56 in Southeast Australia (Gouramanis et al., 2013) and Mauritian lowlands (de Boer et al., 2014),  
57 with quantifiable effects at Indian Ocean regional scales (Abram et al., 2008; Endo and Tozuka,  
58 2016). Since the early-Holocene, SST variability from northwest Sumatra have experienced two  
59 dominant modes, one Indian-wide associated with ENSO impacting the tropical Pacific and  
60  
61  
62  
63  
64  
65

1  
2  
3 Indian oceans, and the other associated with the IOD, independent from ENSO and controlled  
4 by the equatorial monsoon system (Li et al., 2018).  
5  
6

#### 7 **4.4. Antarctica**

8  
9

10 In the instrumental record, SAM and ENSO interactions are thought to be phase-dependent  
11 (Fogt and Bromwich, 2006; Gong et al., 2010; Lim et al., 2013), with La Niña (El Niño) events  
12 being more likely during positive (negative) SAM phases (Fogt et al., 2011).  
13  
14

15 Similar interactions have also been revealed in reconstructions of the last millennium,  
16 suggesting a shift from a dominant central Pacific La Niña-like pattern concurrent with a positive  
17 SAM to a dominant El Niño-like pattern and a negative SAM phase at the onset of the LIA, i.e.,  
18 approximately 1300 CE (Goodwin et al., 2014).  
19  
20

21 The linkage between the SAM and ENSO has likely fluctuated at millennial timescales over the  
22 Holocene due to its sensitivity to precession changes (Gomez et al., 2012). ENSO and SAM-like  
23 variability at centennial timescales were established after ~5.8 ka and reached peak  
24 development over the last 4600 years, according to a lake-sediment record from Chilean  
25 Patagonia (Moreno et al., 2018). Interestingly, multicentennial variability in the SAM might share  
26 a common structure and timing, within dating uncertainties, with palaeoclimate records from the  
27 NH over the last 3 ka, established through an interhemispheric coupling (Moreno et al., 2014).  
28  
29  
30  
31

### 32 **5.- External natural forcing and feedback mechanisms**

33

34 Climate variability during the Holocene was forced by a range of external natural forcings on  
35 different timescales. Orbital forcing varies on millennial timescales, solar forcing on decadal to  
36 centennial timescales and volcanic forcing on sub-decadal timescales (Figure 9). The  
37 timescales of the climate system response can, however, differ from the variability of the  
38 forcings, as the radiative imbalance imposed by changes in the forcings results in non-linear  
39 processes, i.e., feedbacks mechanisms, within the climate system (e.g., Hansen et al., 1997).  
40 For example, the climate system can respond fast when it is pushed past a threshold by a slow  
41 forcing (e.g., orbital forcing), or a response to a short term forcing (e.g. volcanic forcing) can be  
42 prolonged by ocean feedback. In the context of this review, variations in greenhouse gases prior  
43 to the industrial revolution are viewed as a feedback response of the climate system rather than  
44 a climate forcing itself, although some argue that the 20 ppm rise in CO<sub>2</sub> from -6000 CE to 1850  
45 CE was anthropogenic (Ruddiman et al., 2011), while others argue that the ocean acted as a  
46 CO<sub>2</sub> source until the late Holocene (Brovkin et al., 2019).  
47  
48  
49  
50  
51

#### 52 **5.1. Orbital forcing**

53  
54

55 The Earth's orbit is modulated by the gravitational pull of the major planets of the solar system.  
56 The eccentricity, obliquity and precession of the Earth's orbit vary with cycles of 100 ka, 41 ka  
57 and 25 ka, respectively, and have an effect on the distribution of seasonal insolation, and to a  
58 small extent, eccentricity affects total insolation. For example, at the end of the last ice age, the  
59 June insolation at 65°N was ~40 W/m<sup>2</sup> stronger than at present, while the autumn and winter  
60  
61  
62  
63  
64  
65



1  
2  
3 insolation was weaker (Fig. 9a). In itself, this phenomenon provides a stronger seasonality in  
4 temperature during the early- and mid-Holocene, which are most pronounced at high latitudes  
5 (Fig. 9a). However, this phenomenon is also thought to cause a number of dynamic changes in  
6 climatic patterns.  
7  
8

9  
10 Due to stronger modulation of insolation at high latitudes compared with low latitudes, the orbital  
11 forcing weakened the meridional temperature gradient during the early- to mid-Holocene. This  
12 phenomenon may, via different pathways, have weakened the AMOC (Fischer and Jungclaus,  
13 2010), in turn related to North Atlantic modes of variability (Brahim et al., 2019). Nevertheless,  
14 such a response remains model dependent, as other processes, such as the reduction of sea  
15 ice export from the Arctic towards the North Atlantic, can lead to salinification of the convection  
16 sites and an increase in the AMOC (Born et al., 2010). When analysing the PMIP3 database for  
17 6-ka BP, Găinușă-Bogdan et al. (2020) found that the ensemble mean of models does show an  
18 intensification of the AMOC for that period compared to preindustrial simulations. Such an  
19 increase is also corroborated by deep water reconstruction (Thornalley et al., 2013) and AMOC  
20 reconstruction (Ayache et al., 2018). This increase in AMOC can also be related to the potential  
21 impact of Sapropel event in the Mediterranean, which might have enhanced the AMOC in the  
22 early-Holocene (Swingedouw et al., 2019). The orbital warming of the Arctic temperatures could  
23 have been further amplified in the mid-Holocene by ice-albedo feedbacks on sea-ice (Park et  
24 al., 2018) and northward migration of high vegetation (Renssen et al., 2005). Modelled  
25 anomalies in atmospheric circulation during the mid-Holocene have, on the one hand, shown  
26 tendencies toward a more positive mean state of the NAO (e.g., Fischer and Jungclaus, 2010)  
27 and, on the other hand, a more negative AO (Park et al., 2018), with the latter result observed in  
28 multiple models as being connected to sea-ice loss. Nevertheless, the whole PMIP3 database  
29 exhibits a very model-dependent result (Găinușă-Bogdan et al., 2020), highlighting very poor  
30 agreement on this topic within models.  
31  
32  
33  
34  
35  
36  
37

38 Additionally, a recent review paper examining Holocene variability in the ENSO concluded that a  
39 range of proxy-based records and model simulations all point to a weaker mid-Holocene ENSO  
40 variability (Lu et al., 2018a) (see section 3.1). Although the reason for the weaker ENSO is  
41 thought to originate from orbital forcing, the exact governing mechanisms remain unclear.  
42  
43

44 The enhanced mid-Holocene NH summer insolation also increased the low-latitude land-ocean  
45 temperature contrast driving the summer monsoons (Sjolte et al., 2014). In models, this  
46 phenomenon leads to a stronger Indian monsoon (Liu et al., 2014b) and West African monsoon  
47 (Claussen et al., 1999). The changes in the African monsoon are associated with a widespread  
48 vegetation covering what is now the Sahara Desert, known as “Green Sahara” – which in itself  
49 further amplified the monsoon flow (Lu et al., 2018b). Model results indicate that the post Green  
50 Sahara decline in vegetation could have increased the Arctic sea-ice and contributed to the  
51 negative trend of the Holocene high latitude NH temperature (Muschitiello et al., 2015).  
52  
53  
54  
55

## 56 **5.2. Solar activity**

57

58 Solar variability is driven by magnetic fields generated by the solar dynamo and leads to  
59 different effects, including non-stationary active processes that are visible on the solar surface  
60  
61  
62  
63  
64  
65

1  
2  
3 such as sunspots and active regions. Solar activity can be quantified for the last 300 - 400 years  
4 using direct telescope-based solar observations, of which the most commonly used is the  
5 sunspot number (Clette et al., 2014; Svalgaard and Schatten, 2016) and, further back in time,  
6 indirect proxy data (Fig. 9b), i.e., cosmogenic radionuclides  $^{14}\text{C}$  and  $^{10}\text{Be}$  recorded in highly  
7 resolved natural archives such as tree rings and ice cores (Beer et al., 1990; Steinhilber et al.,  
8 2009; Stuiver and Braziunas, 1993). Cosmogenic radionuclides represent the incoming flux of  
9 galactic cosmic rays into the Earth's atmosphere, which is controlled by the heliomagnetic and  
10 geomagnetic field. Holocene solar activity reconstructions allow the identification of quasi-  
11 periodicities on different timescales such as the prominent 11-year sunspot cycle, Gleissberg  
12 (88 years), de-Vries (207 years) cycle and, more tentatively, 2400-year Hallstatt cycle, as well as  
13 occasional multidecadal episodes of low / high activity known as grand solar minima/maxima  
14 (Gray et al., 2010).  
15  
16  
17  
18  
19

20 Much of the evidence for solar-climate interactions relies on model simulations and statistical  
21 analyses showing 11-year sunspot cycle variations in atmospheric circulation patterns (Gray et  
22 al., 2010; Matthes et al., 2017). This evidence reveals that supposedly small solar variations (on  
23 the order of one per mil for total solar irradiance –TSI–) may cause significant climatic  
24 responses driven by feedback mechanisms and internal climate variability that are not yet fully  
25 understood (Gray et al., 2010; Haigh, 1996; Lean, 1997; Matthes et al., 2003; Swingedouw et  
26 al., 2011). Proposed sun-climate mechanisms include the following: i) changes in TSI affecting  
27 global mean surface temperature through direct heating and changes in Hadley and Walker  
28 circulation, which are sometimes expressed as the “bottom-up mechanisms” associated with  
29 ocean-atmosphere coupling (Gray et al., 2010; Haigh, 1996); ii) variations in the ultraviolet  
30 wavelength range, exceeding the range of relative TSI variability, triggering shifting  
31 stratospheric ozone concentrations and temperature gradients with an impact on the  
32 troposphere through effects on regional circulation patterns (Ineson et al., 2011; Thiéblemont et  
33 al., 2015), sometimes denoted the so-called “top-down mechanisms” (Haigh, 1994; Kodera,  
34 2002; Matthes et al., 2006); and iii) the possible effect of charged particles generated by galactic  
35 cosmic rays with proposed impacts on cloud formation and ozone abundance (Marsh and  
36 Svensmark, 2003; Seppälä et al., 2014; Svensmark et al., 2009). Regional modes of variability  
37 might act as feedback mechanisms that amplify the solar signal as the observed climatic  
38 response to the 11-year sunspot cycle seems to have a similar spatial distribution to the main  
39 regional circulation patterns with a maximum lag of 2-4 years, e.g., AO/NAO and ENSO  
40 (Andrews et al., 2015; Gray et al., 2013; Ineson et al., 2015; Scaife et al., 2013; Seppälä and  
41 Clilverd, 2014; Tourpali et al., 2005). For instance, there is evidence for solar-induced changes  
42 in ENSO over the early-Holocene (Hernández et al., 2010; Marchitto et al., 2010), although  
43 there is also sparse evidence for this relationship during the last millennium in proxy data and  
44 models (Otto-Bliesner et al., 2016). Moreover, these solar-induced changes are also observed  
45 in PDV evolution (Beaufort and Grelaud, 2017; McCabe-Glynn et al., 2013). In turn, the linkages  
46 with the NAO over the instrumental era has remained debated both due to the short time frame  
47 and large intrinsic variability in chemistry-climate models (Chiodo et al., 2019; Gillett and Fyfe,  
48 2013; Misios et al., 2016). On longer timescales, the number of studies reporting the interaction  
49 of solar forcing with modes of variability is still small. In the marine realm, episodes of low TSI  
50 over the last millennium could trigger persistent atmospheric blocking events associated with  
51 negative winter NAO conditions, affecting the strength of the North Atlantic subpolar gyre  
52  
53  
54  
55  
56  
57  
58  
59  
60  
61  
62  
63  
64  
65

1  
2  
3 (Moffa-Sánchez et al., 2014). Knudsen et al. (2014) and Menary and Scaife (2014) suggested  
4 that AMO variability might be paced by combined solar and volcanic forcings, but the impact of  
5 external forcings may have been modulated by the AMOC, resulting in a non-stationary  
6 relationship between AMO and these forcings. Reported evidence for the effects of solar forcing  
7 on atmospheric circulation is often focused on the NAO. Martin-Puertas et al. (2012) suggested  
8 the presence of a persistent reduced pressure gradient in the North Atlantic region resembling a  
9 negative NAO-like sea-level pressure pattern to explain a synchronous and in-phase response  
10 of early-spring wind strength to a grand solar minimum at 2.8 ka BP. A similar pattern could  
11 explain sun-climate linkages seen in Greenland ice cores for the last glacial maximum (Adolphi  
12 et al., 2014). Recent studies combining climate models with multiproxy reconstructions of  
13 atmospheric circulation for the North Atlantic region reveal a more complex picture as solar  
14 activity may have a major effect on the EA on decadal to centennial timescales, but no direct  
15 impact on the NAO over the last millennium (Michel et al., 2020; Sjolte et al., 2018).  
16  
17  
18  
19  
20

### 21 **5.3. Volcanism**

22  
23  
24 Large explosive volcanic eruptions impact the radiative forcing of the Earth system, as these  
25 events can emit a large amount of sulphur into the stratosphere, where it is transformed through  
26 chemical reactions and microphysical processes into sulphate aerosols (Robock, 2000; Stoffel  
27 et al., 2015). These aerosols have residence times of a few months to years in the stratosphere,  
28 where they are rapidly transported everywhere through Brewer-Dobson circulation. Their main  
29 radiative effect consists of reflecting shortwave radiation, the so-called parasol effect, leading to  
30 less shortwave radiation reaching the Earth's surface, thus tending to cool it. The direct radiative  
31 impact of a large tropical eruption, thus, lasts 2 to 3 years in total. If the eruption occurs at high  
32 latitudes, its transport within the stratosphere is not global, and the aerosols mainly remain at  
33 the high latitudes where the eruption occurs (Pausata et al., 2015; Toohey and Sigl, 2017).  
34 Nevertheless, a recent simulation of the relatively modest 1970 volcanic eruption that occurred  
35 in the Deception Volcano Island (Antarctica Peninsula) showed that ashes might have a larger  
36 distribution than previously thought (Geyer et al., 2017).  
37  
38  
39  
40  
41

42 Over the last millennium, volcanic eruptions have been reconstructed using the deposition of  
43 sulphate aerosols within the ice cores from Greenland and Antarctica (Fig. 9c). The impacts of  
44 these eruptions are believed to have a major influence on the variability of the last millennium  
45 (Schurer et al., 2013). The cumulative effects of all the volcanic eruptions can explain the  
46 negative trend observed in the recent reconstructions from the PAGES2K database (PAGES2k  
47 Consortium et al., 2017). Volcanic eruptions can activate dynamic feedbacks within the climate  
48 system, making their impact last longer or differing only due to their radiative forcing. For  
49 instance, large volcanic eruptions lead to a positive NAO during the first few winters following  
50 the eruption (Fischer et al., 2007; Michel et al., 2020; Ortega et al., 2015; Sigl et al., 2015; Sjolte  
51 et al., 2018). Nevertheless, such an effect remains difficult to be reproduced by climate models  
52 (Driscoll et al., 2012; Swingedouw et al., 2017; Toohey et al., 2014) and may mainly concern  
53 only the largest eruptions of the last millennium. The impact of volcanic eruptions on the chance  
54 of having an "El Niño" event within the following years has also been highlighted (Adams et al.,  
55 2003; Emile-Geay et al., 2008; Khodri et al., 2017; Maher et al., 2015; Mann et al., 2005;  
56 McGregor and Timmermann, 2010; Stevenson et al., 2017), but without a systematic response  
57  
58  
59  
60  
61  
62  
63  
64  
65

1  
2  
3 of ENSO to strong volcanic eruptions (Otto-Bliesner et al., 2016). Some caveats concerning the  
4 detection of such signals in proxy-based ENSO reconstructions also exist. Modelling studies  
5 also support a causal relationship between a spate of frequent tropical eruptions during the 17th  
6 century and the relatively strong ENSO variability documented during this time (Cobb et al.,  
7 2003a). In contrast, a new 317-year-long, monthly-resolved reconstruction of ENSO spans the  
8 Samalas eruption but finds no evidence for a consistent impact on ENSO variability (Dee et al.,  
9 2020). Thus, while there may be a dynamic link between volcanic eruptions and ENSO, it may  
10 be masked by strong internal variability in ENSO (e.g., Cobb et al., 2003a; Wittenberg, 2009).  
11 Volcanic eruptions may also trigger large-scale variations in the ocean heat content and Atlantic  
12 circulation on longer timescales (Mignot et al., 2011; Otterå et al., 2010; Swingedouw et al.,  
13 2015; Zanchettin et al., 2013). Such an effect leads to a far longer climate impact of up to a few  
14 decades (Swingedouw et al., 2015), but it remains controversial within climate models in terms  
15 of the exact response (Swingedouw et al., 2017). Finally, large volcanic eruptions, such as  
16 Samalas in 1257, the largest volcanic eruption of the last millennium, or a cluster of volcanic  
17 eruptions, have been suggested to have led to a long-lasting shift of the Atlantic subpolar  
18 circulation system (Moreno-Chamarro et al., 2017a; Schleussner et al., 2015; Xoplaki et al.,  
19 2018). This circulation system has indeed been identified as a tipping element of the climate  
20 system (Born et al., 2013), which means that for a sufficiently large forcing, it can shift from one  
21 mode to another. The associated decrease in northward heat transport may then help to explain  
22 the onset and long-term duration of the LIA (Miller et al., 2012).  
23  
24  
25  
26  
27  
28  
29

30 Volcanic activity could also have played a substantial role in climatic variability during the  
31 Holocene (Kobashi et al., 2017), but very little is known about this topic as well-dated and robust  
32 reconstructions of volcanic activity are scarce. Based on the GISP2 sulphate dataset, it has  
33 been suggested that there have been periods of more frequent explosive eruptions in the past  
34 (e.g. 9.5-11.5 ka cal BP; Zielinski et al., 1994), and based on ice core reconstruction from  
35 Antarctica, the last 2 ka may have been exceptional over the Holocene in terms of volcanic  
36 activity. Nevertheless, developments in volcanic activity reconstructions are starting to provide  
37 interesting benchmarks (e.g. Kobashi et al., (2017) for model simulations that merit further  
38 investigation to fully understand the potential role of volcanic eruptions over the Holocene.  
39  
40  
41  
42  
43

## 44 **6.- Summary and future perspectives**

45  
46  
47 Global instrumental records now extend over a century into the past and provide some coverage  
48 in parts of the 19th century (Folland et al., 2002). Improvement of these datasets is on-going as  
49 data recovery efforts uncover new and forgotten sources of direct climate observations and  
50 integrate them into existing datasets to improve global reanalyses (Compo et al., 2011; Slivinski  
51 et al., 2019). These efforts are crucial for our understanding of climate variability and for testing  
52 dynamical climate predictions against observations. Indeed, recent progress indicates that large  
53 fluctuations in ENSO (Luo et al., 2008), the NAO (Smith et al., 2019) and the AMV (Hermanson  
54 et al., 2014) can now be skilfully predicted at multiyear timescales. However, questions persist  
55 regarding the robustness of these results, especially given that our direct observational data and  
56 climate prediction tests are limited to the century timescale at best (O'Reilly et al., 2017) and  
57 sample only a few phases of low frequency climate variability.  
58  
59  
60  
61  
62  
63  
64  
65

1  
2  
3  
4  
5 Multidecadal variations occur in all the modes of climate variability discussed in this review, and  
6 the lack of long-term instrumental data for these fluctuations present important challenges to  
7 climate science. First, we still do not fully understand the mechanisms of low frequency climate  
8 variability. As presented in this review, many studies have indentified large changes in the  
9 strength of reconstructed modes of variability. The debate still rages concerning whether  
10 observed variations in climate modes are predominantly due to internal variability or external  
11 forcing (e.g., Mann et al., 2020), and it is often unknown whether proxy measures represent  
12 changes in the modes themselves, longer timescale changes in the climate background state,  
13 non-linear interactions amongst modes or genuine non-stationarity. Fluctuations in ENSO, PDV,  
14 AMV, NAO, IOD and the SAM are all known to occur and appear to be modulated by natural  
15 forcing from solar and volcanic effects as well as anthropogenic forcing (greenhouse-gas) for the  
16 industrial period (Fig. 9; e.g., (Booth et al., 2012; Smith et al., 2016b; Wu et al., 2019). However,  
17 there are also outstanding questions about the magnitude of the response to these forcing  
18 mechanisms and their accumulated and delayed effects on the climate system (Section 5 of this  
19 review). Second, modes of variability induce changes in regional rainfall, storms and temperature  
20 that are comparable in magnitude to the effects of anthropogenic climate change (e.g., Deser et  
21 al., 2012). For example, northern European winter warming and wetting in the 1990s due to low-  
22 frequency variability in the NAO exceeded the multidecadal rate of regional climate change  
23 (Scaife et al., 2005), and extreme events worldwide are as susceptible to modes of variability as  
24 they are to decades of climate change (Fereday et al., 2018; Kenyon and Hegerl, 2008).  
25 Moreover, known interactions exist between at least some modes of variability (IOD, SAM) and  
26 anthropogenic climate change (Fig. 9d; Cai et al., 2014; Thompson et al., 2011), but they are not  
27 fully understood and require further to better comprehend their current links and perform future  
28 projections (Shepherd, 2014; Wei et al., 2019). Regardless, profound changes in regional climate  
29 are driven by climate modes and need to be carefully considered if the future bounds on regional  
30 climate change are to be understood and anticipated. Finally, some observed variability still  
31 appear to be poorly simulated in current climate models. Large synthetic samples from dynamical  
32 climate models suggest that more extreme fluctuations than are contained in the recent  
33 observations are quite plausible (Kent et al., 2017; Thompson et al., 2017), but even state-of-the-  
34 art climate models still do not appear to properly represent the amplitude of observed multidecadal  
35 variability (Kravtsov et al., 2018; Ljungqvist et al., 2019). The multidecadal variability of the NAO  
36 is difficult to reproduce in climate models and even ensembles of simulations with multiple models  
37 rarely produce trends as large as the observed change in the NAO between the 1960s and 1990s  
38 (Bracegirdle et al., 2018). There is now growing evidence that the modelled signals in climate  
39 simulations of the atmospheric circulation over the North Atlantic are simply too weak regardless  
40 of their origin (Scaife and Smith, 2018). Similarly, the most extreme El Niño events and their  
41 asymmetry with La Niña events is not well reproduced in comprehensive models (Zhang and Sun,  
42 2014). These limitations challenge our ability to simulate the most severe and important  
43 fluctuations in regional climate and hence our ability to anticipate these climate impacts from  
44 modes of variability.  
45  
46  
47  
48  
49  
50  
51  
52  
53  
54  
55

56  
57 In addition to increasing information by obtaining new proxy-based reconstructions, a pressing  
58 issue is the lack of agreement between different proxy-based climate records, and continued  
59 efforts are needed to calibrate and combine multiple records to reduce reconstruction  
60  
61  
62  
63  
64  
65

1  
2  
3 uncertainties. Such a synthesis of proxy-based data would have great utility for testing climate  
4 models. New efforts in the generation of proxy-based climate data on long timescales, with  
5 quantified errors (e.g., Dee et al., 2015; Steiger et al., 2017) and the development of free software  
6 (e.g., ClimoRec by Michel et al., 2020) using well dated and verified proxy databases, or of  
7 palaeoclimate data reanalysis techniques could yield such datasets (Amrhein et al., 2018; Tardif  
8 et al., 2019).

11  
12 Hence, the presence of only a few cycles of low-frequency variability in our instrumental climate  
13 records, the importance of low-frequency variability for regional climate and the need for validation  
14 of climate models make modes of variability a high-priority topic for climate science. These points  
15 alone motivate the study of past variations in modes of climate variability using long climate-proxy  
16 records, and the extension of quantitative proxy-based records beyond the last millennium and  
17 their combination into improved reconstructions is needed to provide sufficiently long records with  
18 enough accuracy to understand low-frequency climate dynamics and draw robust conclusions  
19 from comparisons with climate models. This activity is all the more urgent given the current rapid  
20 rate of climate change.

## 24 25 26 **Acknowledgements**

27  
28  
29 A.H. is supported by a Beatriu de Pinós –Marie Curie Cofund programme fellowship (2016 BP  
30 00023) and HOLMODRIVE - North Atlantic Atmospheric Patterns influence on Western Iberia  
31 Climate: From the Lateglacial to the Present (PTDC/CTA-GEO/29029/2017) project funded by  
32 the Fundação para a Ciência e a Tecnologia, Portugal (FCT). A.H., S.G., and S.P-R. thank the  
33 Spanish research project PaleoModes (CGL2016-75281-C2-1-R) which provided some of their  
34 financial support. E.M.-C. contribution was funded by the project PARAMOUR (30454083) from  
35 the EOS program by the F.R.SFNRS. CM-P is supported by the Royal Society (ref: DH150185).  
36 P.O. contribution has been supported by the Ramon y Cajal senior tenure programme from the  
37 Spanish Ministry of Economy and Competitiveness. The Spanish PTI PolarCSIC  
38 (<https://www.polarcsic.es>) is also acknowledged for providing partial financial support to S.G. A.  
39 P.'s work was supported by a Science Foundation Ireland Career Development Award  
40 (17/CDA/4695), a research centre award (12/RC/2289\_P2), an investigator award (16/IA/4520),  
41 and a Marine Research Programme funded by the Irish Government, cofinanced by the  
42 European Regional Development Fund (Grant-Aid Agreement No. PBA/CC/18/01). J.S. is  
43 supported by the strategic research program of ModEling the Regional and Global Earth system  
44 (MERGE) hosted by the Faculty of Science at Lund University. D.S. is supported by Blue-Action  
45 (European Union's Horizon 2020 research and innovation program, Grant Number: 727852) and  
46 EUCP (European Union's Horizon 2020 research and innovation programme under grant  
47 agreement no 776613) projects as well as by the French national program LEFE/INSU with  
48 VADEMECUM project. G. X. thanks the funding from the Chinese Scholarship Council  
49 (201704910171). This study is partly based on discussions held during the joint workshop of the  
50 CLIMOVAR group and IBCC-lo2k project, Barcelona, 25–27 September 2013. PAGES and  
51 IBCC-lo2k are thanked for supporting this workshop.

## 52 53 54 55 56 57 58 59 60 **Figure Captions**

61  
62  
63  
64  
65

1  
2  
3  
4  
5 **Figure 1.** Modes of climate variability presented in this review. Squares indicate the area where  
6 the mode is usually defined. Blue and grey colours indicate oceanic and atmospheric modes,  
7 respectively.  
8  
9

10 **Figure 2.** ENSO reconstructions for the past 8000 years (links to original sources are included in  
11 the Supplementary Material). a-c. Reconstructions between -6000 and 1000 CE (left panels): a.  
12 Koutavas and Joanides (2012): Zonal SST gradient anomaly (in K; blue) relative to the Late  
13 Holocene (-2000–2000 CE), calculated as the difference between the averages of seven western  
14 and two eastern Pacific sediment cores. Meridional gradient in  $\delta^{18}\text{O}$  (in ‰ Vienna Pee-Dee  
15 Belemnite, VPDB; red) calculated as the difference between four northern and four southern  
16 sediment cores. Stronger gradients point to an increase in ENSO variability. Note the two series  
17 share the vertical axis. b. Chen et al. (2016). ENSO variability based on the standard deviation of  
18 the 2–7-year band in  $\delta^{18}\text{O}$  of a speleothem with sub-annual resolution. c. Grothe et al. (2019).  
19 Relative ENSO variance changes in high-pass filtered fossil coral  $\delta^{18}\text{O}$  relative to the 1987–2007  
20 CE. Coral data include those from Cobb et al. (2003a), Cobb et al. (2013), and McGregor et al.  
21 (2010). d-k. ENSO reconstructions covering the past millennium (right panels): d. Stahle et al.  
22 (1998; blue) and Mann et al. (2000; red). e. D’Arrigo et al. (2005; red) and Cook et al. (2008; blue).  
23 f. Braganza et al. (2009)’s R5 (red) and R8 (blue) indices. g. Gergis and Fowler, (2009)’s  
24 magnitude of El Niño (red) and La Niña events (blue) ranging from weak (1) to extreme (5). h.  
25 Wilson et al. (2010)’s Pacific ‘centre of action’ (blue) and ‘teleconnected’ (red) indices. i. Li et al.  
26 (2011; blue) and Li et al. (2013; red). j. McGregor et al. (2010; red) and Dätwyler et al., (2019;  
27 blue), with 95% confidence intervals (shading). k. Freund et al. (2019)’s annual El Niño Cold  
28 Tongue (red) and El Niño Warm Pool (blue) indices. Indices in d, e, f, h, i, and k are normalised  
29 with respect to the common period 1940–1970 to facilitate comparison. Yearly indices (thin lines)  
30 are smoothed with an 11-year running mean (thick lines), but in i the thick blue is the 21-year  
31 running ENSO variance provided by Li et al. (2011). Note the time axis has a different scale before  
32 and after 1000 CE (indicated by the vertical dashed line).  
33  
34  
35  
36  
37  
38  
39  
40

41 **Figure 3.** PDV reconstructions for the past 2500 years (links to original sources are included in  
42 the Supplementary Material). a. D’Arrigo et al. (2001; blue) and Gedalof and Smith (2001; red).  
43 b. Biondi et al. (2001; blue), and MacDonald and Case (2005; red). c. D’Arrigo and Wilson (2006;  
44 red), Shen et al. (2006; gray), and Felis et al. (2010; blue) and d. Mann et al. (2009; red) with 95%  
45 confidence intervals (shading), and Linsley et al. (2008; blue) with 1 sigma error (shading). All  
46 indices are smoothed with an 11-year running mean.  
47  
48  
49

50 **Figure 4.** AMV reconstructions for the past 1500 years (links to original sources are included in  
51 the Supplementary Material). a. Gray et al. (2004; blue), Mann et al. (2009; red), with 95%  
52 confidence intervals (shading); b. Kilbourne et al. (2014; red) with 1 sigma and 2 sigma (darker  
53 and lighter shading, respectively), and Wang et al. (2017; blue) with the root mean square error  
54 (shading). For clarity, the indices by Gray et al., (2004) and Kilbourne et al., (2014) are scaled,  
55 and the one by Wang et al. (2017) is smoothed with an 11-year running mean.  
56  
57  
58

59 **Figure 5.** NAO reconstructions for the past 5300 years (links to original sources are included in  
60 the Supplementary Material). a. Baker et al. (2015; red), and Faust et al. (2016; blue). b. Olsen et  
61  
62  
63  
64  
65

1  
2  
3 al. (2012; red) with estimated error (shading), and Timm et al. (2004; blue). c. Glueck and Stockton  
4 (2001; red) and December–February Luterbacher et al. (2001; blue). d. Trouet et al. (2009; blue)  
5 and Ortega et al. (2015; red), with the total ensemble spread and the regression uncertainty  
6 across the ensemble (lighter and darker shading respectively); e. Cook et al. (2019; red) with 90%  
7 quantile uncertainty (shading) and Mellado-Cano et al. (2019); f. Sjolte et al. (2018; red) and  
8 Michel et al. (2020; red). The indices with annual resolution from Glueck and Stockton (2001),  
9 Luterbacher et al. (2001), Timm et al. (2004), Ortega et al. (2015), Sjolte et al. (2018), Cook et al.  
10 (2019), Mellado-Cano et al. (2019), and Michel et al. (2020) are smoothed with an 11-year running  
11 mean. Note the time axis changes the scale before and after 1000 CE (indicated by the vertical  
12 dashed line).  
13  
14  
15  
16

17  
18 **Figure 6.** IOD proxy-based reconstruction and instrumental data (links to original sources are  
19 included in the Supplementary Material). Annual-mean Abram et al. (2008; blue), with the  
20 unfiltered and filtered Dipole Mode Index in lighter and darker colour, and Abram et al. (2020;  
21 red).  
22

23  
24 **Figure 7.** SAM index reconstructions and instrumental data for the past 1000 years (links to  
25 original sources are included in the Supplementary Material). a. Fogt et al., (2009; blue), and  
26 Villalba et al., (2012; red), with the associated uncertainty bands (shading). b. Abram et al. (2014;  
27 red) with 95% confidence intervals (shading), and Dätwyler et al. (2018; blue) with 90%  
28 confidence intervals (shading). All indices are smoothed with an 11-year running mean.  
29  
30

31  
32 **Figure 8.** Major modes of variability interactions. Arrows show connections between modes  
33 identified by the literature described in Section 7 for the instrumental (green), past millennium  
34 (blue) and Holocene (red) periods. Discontinuous lines indicate contradictory links or no link  
35 between PDV and ENSO according to different works (see Section 7 for details) and non-  
36 stationary links between the SAM and ENSO over time.  
37  
38

39  
40 **Figure 9.** External forcing for the past 8000 years. a. Insolation at 65°N (in W/m<sup>2</sup>). b. Total solar  
41 irradiance (in W/m<sup>2</sup>) from Steinhilber et al. (2009; blue) and Sjolte et al. (2018; red). c. Global  
42 volcanic forcing (in W/m<sup>2</sup>) from Sigl et al. (2015; green) and Kobashi et al. (2017; gray). d.  
43 Concentration of well-mixed greenhouse gases: CO<sub>2</sub> (in ppm, orange) from Bereiter et al. (2015;  
44 solid line) and Rubino et al. (2019; dashed lines); N<sub>2</sub>O (in ppb; gray) and CH<sub>4</sub> (in ppb; blue) from  
45 Spahni et al. (2005; solid lines) and Rubino et al. (2019; dashed lines). Note the different axis for  
46 CH<sub>4</sub>.  
47  
48

## 49 REFERENCES

- 50  
51  
52 Abram, N.J., Dixon, B.C., Rosevear, M.G., Plunkett, B., Gagan, M.K., Hantoro, W.S., Phipps, S.J., 2015. Optimized  
53 coral reconstructions of the Indian Ocean Dipole: An assessment of location and length considerations.  
54 *Paleoceanography* 30, 1391–1405. <https://doi.org/10.1002/2015PA002810>  
55 Abram, N.J., Gagan, M.K., Cole, J.E., Hantoro, W.S., Mudelsee, M., 2008. Recent intensification of tropical climate  
56 variability in the Indian Ocean. *Nat. Geosci.* 1, 849–853. <https://doi.org/10.1038/ngeo357>  
57 Abram, N.J., Gagan, M.K., Liu, Z., Hantoro, W.S., McCulloch, M.T., Suwargadi, B.W., 2007. Seasonal characteristics  
58 of the Indian Ocean Dipole during the Holocene epoch. *Nature* 445, 299–302.  
59 <https://doi.org/10.1038/nature05477>  
60  
61  
62  
63  
64  
65



- 1  
2  
3 Abram, N.J., McGregor, H.V., Gagan, M.K., Hantoro, W.S., Suwargadi, B.W., 2009. Oscillations in the southern  
4 extent of the Indo-Pacific Warm Pool during the mid-Holocene. *Quat. Sci. Rev.* 28, 2794–2803.  
5 <https://doi.org/10.1016/j.quascirev.2009.07.006>  
6  
7 Abram, N.J., Mulvaney, R., Vimeux, F., Phipps, S.J., Turner, J., England, M.H., 2014. Evolution of the Southern  
8 Annular Mode during the past millennium. *Nat. Clim. Change* 4, 564–569.  
9 <https://doi.org/10.1038/nclimate2235>  
10  
11 Abram, N.J., Wright, N.M., Ellis, B., Dixon, B.C., Wurtzel, J.B., England, M.H., Ummenhofer, C.C., Philibosian, B.,  
12 Cahyarini, S.Y., Yu, T.-L., Shen, C.-C., Cheng, H., Edwards, R.L., Heslop, D., 2020. Coupling of Indo-Pacific  
13 climate variability over the last millennium. *Nature* 579, 385–392. <https://doi.org/10.1038/s41586-020-2084-4>  
14  
15 Adams, J.B., Mann, M.E., Ammann, C.M., 2003. Proxy evidence for an El Niño-like response to volcanic forcing.  
16 *Nature* 426, 274–278. <https://doi.org/10.1038/nature02101>  
17  
18 Adolphi, F., Muscheler, R., 2016. Synchronizing the Greenland ice core and radiocarbon timescales over the  
19 Holocene &ndash; Bayesian wiggle-matching of cosmogenic radionuclide records. *Clim. Past* 12, 15–30.  
20 <https://doi.org/10.5194/cp-12-15-2016>  
21  
22 Adolphi, F., Muscheler, R., Svensson, A., Aldahan, A., Possnert, G., Beer, J., Sjolte, J., Björck, S., Matthes, K.,  
23 Thiéblemont, R., 2014. Persistent link between solar activity and Greenland climate during the Last Glacial  
24 Maximum. *Nat. Geosci.* 7, 662–666. <https://doi.org/10.1038/ngeo2225>  
25  
26 Ait Brahim, Y., Wassenburg, J.A., Cruz, F.W., Sifeddine, A., Scholz, D., Bouchaou, L., Dassié, E.P., Jochum, K.P.,  
27 Edwards, R.L., Cheng, H., 2018. Multi-decadal to centennial hydro-climate variability and linkage to solar  
28 forcing in the Western Mediterranean during the last 1000 years. *Sci. Rep.* 8, 1–8.  
29 <https://doi.org/10.1038/s41598-018-35498-x>  
30  
31 Alexander, M.A., Halimeda Kilbourne, K., Nye, J.A., 2014. Climate variability during warm and cold phases of the  
32 Atlantic Multidecadal Oscillation (AMO) 1871–2008. *J. Mar. Syst., Atlantic Multidecadal Oscillation-mechanism  
33 and impact on marine ecosystems* 133, 14–26. <https://doi.org/10.1016/j.jmarsys.2013.07.017>  
34  
35 Álvarez-García, F.J., OrtizBevia, M.J., Cabos, W., Tasambay-Salazar, M., RuizdeElvira, A., 2019. Linear and  
36 nonlinear links of winter European precipitation to Northern Hemisphere circulation patterns. *Clim. Dyn.* 52,  
37 6533–6555. <https://doi.org/10.1007/s00382-018-4531-6>  
38  
39 Amrhein, D.E., Wunsch, C., Marchal, O., Forget, G., 2018. A Global Glacial Ocean State Estimate Constrained by  
40 Upper-Ocean Temperature Proxies. *J. Clim.* 31, 8059–8079. <https://doi.org/10.1175/JCLI-D-17-0769.1>  
41  
42 Anderson, H.J., Moy, C.M., Vandergoes, M.J., Nichols, J.E., Riesselman, C.R., Hale, R.V., 2018. Southern  
43 Hemisphere westerly wind influence on southern New Zealand hydrology during the Lateglacial and Holocene.  
44 *J. Quat. Sci.* 33, 689–701. <https://doi.org/10.1002/jqs.3045>  
45  
46 Andreoli, R.V., Kayano, M.T., 2005. ENSO-related rainfall anomalies in South America and associated circulation  
47 features during warm and cold Pacific decadal oscillation regimes. *Int. J. Climatol.* 25, 2017–2030.  
48 <https://doi.org/10.1002/joc.1222>  
49  
50 Andrews, M.B., Knight, J.R., Gray, L.J., 2015. A simulated lagged response of the North Atlantic Oscillation to the  
51 solar cycle over the period 1960–2009. *Environ. Res. Lett.* 10, 054022. <https://doi.org/10.1088/1748-9326/10/5/054022>  
52  
53 Arblaster, J.M., Meehl, G.A., 2006. Contributions of External Forcings to Southern Annular Mode Trends. *J. Clim.* 19,  
54 2896–2905. <https://doi.org/10.1175/JCLI3774.1>  
55  
56 Ashok, K., Behera, S.K., Rao, S.A., Weng, H., Yamagata, T., 2007. El Niño Modoki and its possible teleconnection. *J.  
57 Geophys. Res. Oceans* 112. <https://doi.org/10.1029/2006JC003798>  
58  
59 Ayache, M., Swingedouw, D., Mary, Y., Eynaud, F., Colin, C., 2018. Multi-centennial variability of the AMOC over the  
60 Holocene: A new reconstruction based on multiple proxy-derived SST records. *Glob. Planet. Change* 170,  
61 172–189. <https://doi.org/10.1016/j.gloplacha.2018.08.016>  
62  
63 Baker, A., Hellstrom, J.C., Kelly, B.F.J., Mariethoz, G., Trouet, V., 2015. A composite annual-resolution stalagmite  
64 record of North Atlantic climate over the last three millennia. *Sci. Rep.* 5, 1–8.  
65 <https://doi.org/10.1038/srep10307>  
66  
67 Barnston, A.G., Livezey, R.E., 1987. Classification, Seasonality and Persistence of Low-Frequency Atmospheric  
68 Circulation Patterns. *Mon. Weather Rev.* 115, 1083–1126. [https://doi.org/10.1175/1520-0493\(1987\)115<1083:CSAPOL>2.0.CO;2](https://doi.org/10.1175/1520-0493(1987)115<1083:CSAPOL>2.0.CO;2)  
69  
70 Barriopedro, D., Gallego, D., Alvarez-Castro, M.C., García-Herrera, R., Wheeler, D., Peña-Ortiz, C., Barbosa, S.M.,  
71 2014. Witnessing North Atlantic westerlies variability from ships' logbooks (1685–2008). *Clim. Dyn.* 43, 939–  
72 955. <https://doi.org/10.1007/s00382-013-1957-8>

- 1  
2  
3 Bastos, A., Janssens, I.A., Gouveia, C.M., Trigo, R.M., Ciais, P., Chevallier, F., Peñuelas, J., Rödenbeck, C., Piao,  
4 S., Friedlingstein, P., Running, S.W., 2016. European land CO<sub>2</sub> sink influenced by NAO and East-Atlantic  
5 Pattern coupling. *Nat. Commun.* 7, 1–9. <https://doi.org/10.1038/ncomms10315>  
6  
7 Beaufort, L., Grelaud, M., 2017. A 2700-year record of ENSO and PDO variability from the Californian margin based  
8 on coccolithophore assemblages and calcification. *Prog. Earth Planet. Sci.* 4, 5.  
9 <https://doi.org/10.1186/s40645-017-0123-z>  
10  
11 Beer, J., Blinov, A., Bonani, G., Finkel, R.C., Hofmann, H.J., Lehmann, B., Oeschger, H., Sigg, A., Schwander, J.,  
12 Staffelbach, T., Stauffer, B., Suter, M., Wöflli, W., 1990. Use of <sup>10</sup>Be in polar ice to trace the 11-year cycle of  
13 solar activity. *Nature* 347, 164–166. <https://doi.org/10.1038/347164a0>  
14  
15 Beguería, S., Vicente-Serrano, S.M., Tomás-Burguera, M., Maneta, M., 2016. Bias in the variance of gridded data  
16 sets leads to misleading conclusions about changes in climate variability. *Int. J. Climatol.* 36, 3413–3422.  
17 <https://doi.org/10.1002/joc.4561>  
18  
19 Benito, G., Macklin, M.G., Panin, A., Rossato, S., Fontana, A., Jones, A.F., Machado, M.J., Matlakhova, E., Mozzi,  
20 P., Zielhofer, C., 2015. Recurring flood distribution patterns related to short-term Holocene climatic variability.  
21 *Sci. Rep.* 5, 16398. <https://doi.org/10.1038/srep16398>  
22  
23 Bereiter, B., Eggleston, S., Schmitt, J., Nehrbass-Ahles, C., Stocker, T.F., Fischer, H., Kipfstuhl, S., Chappellaz, J.,  
24 2015. Revision of the EPICA Dome C CO<sub>2</sub> record from 800 to 600 kyr before present. *Geophys. Res. Lett.* 42,  
25 542–549. <https://doi.org/10.1002/2014GL061957>  
26  
27 Biondi, F., Gershunov, A., Cayan, D.R., 2001. North Pacific Decadal Climate Variability since 1661. *J. Clim.* 14, 5–10.  
28 [https://doi.org/10.1175/1520-0442\(2001\)014<0005:NPDCVS>2.0.CO;2](https://doi.org/10.1175/1520-0442(2001)014<0005:NPDCVS>2.0.CO;2)  
29  
30 Blaauw, M., Christen, J.A., Bennett, K.D., Reimer, P.J., 2018. Double the dates and go for Bayes — Impacts of model  
31 choice, dating density and quality on chronologies. *Quat. Sci. Rev.* 188, 58–66.  
32 <https://doi.org/10.1016/j.quascirev.2018.03.032>  
33  
34 Blaauw, M., Christen, J.A., Mauquoy, D., van der Plicht, J., Bennett, K.D., 2007. Testing the timing of radiocarbon-  
35 dated events between proxy archives. *The Holocene* 17, 283–288. <https://doi.org/10.1177/0959683607075857>  
36  
37 Black, D.E., Abahazi, M.A., Thunell, R.C., Kaplan, A., Tappa, E.J., Peterson, L.C., 2007. An 8-century tropical Atlantic  
38 SST record from the Cariaco Basin: Baseline variability, twentieth-century warming, and Atlantic hurricane  
39 frequency. *Paleoceanography* 22. <https://doi.org/10.1029/2007PA001427>  
40  
41 Blindheim, J., Østerhus, S., 2013. The Nordic Seas, Main Oceanographic Features, in: *The Nordic Seas: An*  
42 *Integrated Perspective*. American Geophysical Union (AGU), pp. 11–37. <https://doi.org/10.1029/158GM03>  
43  
44 Blockley, S.P.E., Blaauw, M., Bronk Ramsey, C., van der Plicht, J., 2007. Building and testing age models for  
45 radiocarbon dates in Lateglacial and Early Holocene sediments. *Quat. Sci. Rev., Early Holocene climate*  
46 *oscillations - causes and consequences* 26, 1915–1926. <https://doi.org/10.1016/j.quascirev.2007.06.007>  
47  
48 Boisier, J.P., Rondanelli, R., Garreaud, R., Muñoz, F., 2016. Anthropogenic Contribution to the Southeast Pacific  
49 Precipitation Decline and Recent (2010–2015) Mega-Drought in Chile. *Am. Geophys. Union Fall Meet. 2015*  
50 *Abstr. Id H43E-1549* 43, 1–9. <https://doi.org/10.1002/2015GL067265.Abstract>  
51  
52 Bond, G., Kromer, B., Beer, J., Muscheler, R., Evans, M.N., Showers, W., Hoffmann, S., Lotti-Bond, R., Hajdas, I.,  
53 Bonani, G., 2001. Persistent Solar Influence on North Atlantic Climate During the Holocene. *Science* 294,  
54 2130–2136. <https://doi.org/10.1126/science.1065680>  
55  
56 Bond, G., Showers, W., Cheseby, M., Lotti, R., Almasi, P., deMenocal, P., Priore, P., Cullen, H., Hajdas, I., Bonani,  
57 G., 1997. A Pervasive Millennial-Scale Cycle in North Atlantic Holocene and Glacial Climates. *Science* 278,  
58 1257–1266. <https://doi.org/10.1126/science.278.5341.1257>  
59  
60 Booth, B.B.B., Dunstone, N.J., Halloran, P.R., Andrews, T., Bellouin, N., 2012. Aerosols implicated as a prime driver  
61 of twentieth-century North Atlantic climate variability. *Nature* 484, 228–232.  
62 <https://doi.org/10.1038/nature10946>  
63  
64 Born, A., Nisancioglu, K.H., Braconnot, P., 2010. Sea ice induced changes in ocean circulation during the Eemian.  
65 *Clim. Dyn.* 35, 1361–1371. <https://doi.org/10.1007/s00382-009-0709-2>  
66  
67 Born, A., Stocker, T.F., Raible, C.C., Levermann, A., 2013. Is the Atlantic subpolar gyre bistable in comprehensive  
68 coupled climate models? *Clim. Dyn.* 40, 2993–3007. <https://doi.org/10.1007/s00382-012-1525-7>  
69  
70 Bracegirdle, T.J., Lu, H., Eade, R., Woollings, T., 2018. Do CMIP5 Models Reproduce Observed Low-Frequency  
71 North Atlantic Jet Variability? *Geophys. Res. Lett.* 45, 7204–7212. <https://doi.org/10.1029/2018GL078965>  
72  
73 Bradley, R.S., 2015. Chapter 1 - Paleoclimatic Reconstruction, in: Bradley, R.S. (Ed.), *Paleoclimatology* (Third  
74 Edition). Academic Press, San Diego, pp. 1–11. <https://doi.org/10.1016/B978-0-12-386913-5.00001-6>  
75  
76 Braganza, K., Gergis, J.L., Power, S.B., Risbey, J.S., Fowler, A.M., 2009. A multiproxy index of the El Niño–Southern  
77 Oscillation, A.D. 1525–1982. *J. Geophys. Res. Atmospheres* 114. <https://doi.org/10.1029/2008JD010896>

- 1  
2  
3  
4 Brahim, Y.A., Wassenburg, J.A., Sha, L., Cruz, F.W., Deininger, M., Sifeddine, A., Bouchaou, L., Spötl, C., Edwards,  
5 R.L., Cheng, H., 2019. North Atlantic Ice-Rafting, Ocean and Atmospheric Circulation During the Holocene:  
6 Insights From Western Mediterranean Speleothems. *Geophys. Res. Lett.* 46, 7614–7623.  
7 <https://doi.org/10.1029/2019GL082405>
- 8 Breiman, L., 2001. Random Forests. *Mach. Learn.* 45, 5–32. <https://doi.org/10.1023/A:1010933404324>
- 9 Brovkin, V., Lorenz, S., Raddatz, T., Ilyina, T., Stemmler, I., Toohey, M., Claussen, M., 2019. What was the source of  
10 the atmospheric CO<sub>2</sub> increase during the Holocene? *Biogeosciences* 16, 2543–2555.  
11 <https://doi.org/10.5194/bg-16-2543-2019>
- 12 Cahill, N., Kemp, A.C., Horton, B.P., Parnell, A.C., 2016. A Bayesian hierarchical model for reconstructing relative  
13 sea level: from raw data to rates of change. *Clim. Past* 12, 525–542. <https://doi.org/10.5194/cp-12-525-2016>
- 14 Cahill, N., Kemp, A.C., Horton, B.P., Parnell, A.C., 2015. MODELING SEA-LEVEL CHANGE USING ERRORS-IN-  
15 VARIABLES INTEGRATED GAUSSIAN PROCESSES. *Ann. Appl. Stat.* 9, 547–571.
- 16 Cai, W., Borlace, S., Lengaigne, M., van Rensch, P., Collins, M., Vecchi, G., Timmermann, A., Santoso, A.,  
17 McPhaden, M.J., Wu, L., England, M.H., Wang, G., Guilyardi, E., Jin, F.-F., 2014. Increasing frequency of  
18 extreme El Niño events due to greenhouse warming. *Nat. Clim. Change* 4, 111–116.  
19 <https://doi.org/10.1038/nclimate2100>
- 20 Cai, W., Santoso, A., Wang, G., Yeh, S.-W., An, S.-I., Cobb, K.M., Collins, M., Guilyardi, E., Jin, F.-F., Kug, J.-S.,  
21 Lengaigne, M., McPhaden, M.J., Takahashi, K., Timmermann, A., Vecchi, G., Watanabe, M., Wu, L., 2015a.  
22 ENSO and greenhouse warming. *Nat. Clim. Change* 5, 849–859. <https://doi.org/10.1038/nclimate2743>
- 23 Cai, W., Wang, G., Dewitte, B., Wu, L., Santoso, A., Takahashi, K., Yang, Y., Carréric, A., McPhaden, M.J., 2018.  
24 Increased variability of eastern Pacific El Niño under greenhouse warming. *Nature* 564, 201–206.  
25 <https://doi.org/10.1038/s41586-018-0776-9>
- 26 Cai, W., Wang, G., Santoso, A., McPhaden, M.J., Wu, L., Jin, F.-F., Timmermann, A., Collins, M., Vecchi, G.,  
27 Lengaigne, M., England, M.H., Dommenges, D., Takahashi, K., Guilyardi, E., 2015b. Increased frequency of  
28 extreme La Niña events under greenhouse warming. *Nat. Clim. Change* 5, 132–137.  
29 <https://doi.org/10.1038/nclimate2492>
- 30 Cai, W., Wu, L., Lengaigne, M., Li, T., McGregor, S., Kug, J.-S., Yu, J.-Y., Stuecker, M.F., Santoso, A., Li, X., Ham,  
31 Y.-G., Chikamoto, Y., Ng, B., McPhaden, M.J., Du, Y., Dommenges, D., Jia, F., Kajtar, J.B., Keenlyside, N.,  
32 Lin, X., Luo, J.-J., Martín-Rey, M., Ruprich-Robert, Y., Wang, G., Xie, S.-P., Yang, Y., Kang, S.M., Choi, J.-Y.,  
33 Gan, B., Kim, G.-I., Kim, C.-E., Kim, S., Kim, J.-H., Chang, P., 2019. Pantropical climate interactions. *Science*  
34 363. <https://doi.org/10.1126/science.aav4236>
- 35 Capotondi, A., Wittenberg, A.T., Newman, M., Di Lorenzo, E., Yu, J.-Y., Braconnot, P., Cole, J., Dewitte, B., Giese,  
36 B., Guilyardi, E., Jin, F.-F., Karaukas, K., Kirtman, B., Lee, T., Schneider, N., Xue, Y., Yeh, S.-W., 2014.  
37 Understanding ENSO Diversity. *Bull. Am. Meteorol. Soc.* 96, 921–938. <https://doi.org/10.1175/BAMS-D-13-00117.1>
- 38 Carré, M., Sachs, J.P., Purca, S., Schauer, A.J., Braconnot, P., Falcón, R.A., Julien, M., Lavallée, D., 2014. Holocene  
39 history of ENSO variance and asymmetry in the eastern tropical Pacific. *Science* 345, 1045–1048.  
40 <https://doi.org/10.1126/science.1252220>
- 41 Carson, J., Crucifix, M., Preston, S., Wilkinson, R.D., 2018. Bayesian model selection for the glacial–interglacial  
42 cycle. *J. R. Stat. Soc. Ser. C Appl. Stat.* 67, 25–54. <https://doi.org/10.1111/rssc.12222>
- 43 Cassou, C., Terray, L., 2001. Dual influence of Atlantic and Pacific SST anomalies on the North Atlantic/Europe  
44 winter climate. *Geophys. Res. Lett.* 28, 3195–3198. <https://doi.org/10.1029/2000GL012510>
- 45 Chen, J., Chen, F., Feng, S., Huang, W., Liu, J., Zhou, A., 2015. Hydroclimatic changes in China and surroundings  
46 during the Medieval Climate Anomaly and Little Ice Age: spatial patterns and possible mechanisms. *Quat. Sci.*  
47 *Rev.* 107, 98–111. <https://doi.org/10.1016/j.quascirev.2014.10.012>
- 48 Chen, S., Hoffmann, S.S., Lund, D.C., Cobb, K.M., Emile-Geay, J., Adkins, J.F., 2016. A high-resolution speleothem  
49 record of western equatorial Pacific rainfall: Implications for Holocene ENSO evolution. *Earth Planet. Sci. Lett.*  
50 442, 61–71. <https://doi.org/10.1016/j.epsl.2016.02.050>
- 51 Chen, T., Cobb, K.M., Roff, G., Zhao, J., Yang, H., Hu, M., Zhao, K., 2018. Coral-Derived Western Pacific Tropical  
52 Sea Surface Temperatures During the Last Millennium. *Geophys. Res. Lett.* 45, 3542–3549.  
53 <https://doi.org/10.1002/2018GL077619>
- 54 Chiodo, G., Oehrlin, J., Polvani, L.M., Fyfe, J.C., Smith, A.K., 2019. Insignificant influence of the 11-year solar cycle  
55 on the North Atlantic Oscillation. *Nat. Geosci.* 12, 94–99. <https://doi.org/10.1038/s41561-018-0293-3>
- 56 Chipman, H.A., George, E.I., McCulloch, R.E., 2010. BART: Bayesian additive regression trees. *Ann. Appl. Stat.* 4,  
57 266–298. <https://doi.org/10.1214/09-AOAS285>
- 58  
59  
60  
61  
62  
63  
64  
65

- 1  
2  
3  
4 Christensen, J.H., Aldrian, E., Fonseca, I., Kanyanga, J., Kossin, J.P., Renwick, J., Stephenson, D.B., Zhou, T., 2013.  
5 Climate Phenomena and their Relevance for Future Regional Climate Change Supplementary Material.  
6 <https://doi.org/10.1017/cbo9781107415324.028>
- 7 Chylek, P., Folland, C., Frankcombe, L., Dijkstra, H., Lesins, G., Dubey, M., 2012. Greenland ice core evidence for  
8 spatial and temporal variability of the Atlantic Multidecadal Oscillation. *Geophys. Res. Lett.* 39.  
9 <https://doi.org/10.1029/2012GL051241>
- 10 Claussen, M., Kubatzki, C., Brovkin, V., Ganopolski, A., Hoelzmann, P., Pachur, H.-J., 1999. Simulation of an abrupt  
11 change in Saharan vegetation in the Mid-Holocene. *Geophys. Res. Lett.* 26, 2037–2040.  
12 <https://doi.org/10.1029/1999GL900494>
- 13 Clement, A., Bellomo, K., Murphy, L.N., Cane, M.A., Mauritsen, T., Rädel, G., Stevens, B., 2015. The Atlantic  
14 Multidecadal Oscillation without a role for ocean circulation. *Science* 350, 320–324.  
15 <https://doi.org/10.1126/science.aab3980>
- 16 Clette, F., Svalgaard, L., Vaquero, J.M., Cliver, E.W., 2014. Revisiting the Sunspot Number. *Space Sci. Rev.* 186,  
17 35–103. <https://doi.org/10.1007/s11214-014-0074-2>
- 18 Cobb, K.M., Charles, C.D., Cheng, H., Edwards, R.L., 2003a. El Niño/Southern Oscillation and tropical Pacific climate  
19 during the last millennium. *Nature* 424, 271–276. <https://doi.org/10.1038/nature01779>
- 20 Cobb, K.M., Charles, C.D., Cheng, H., Kastner, M., Edwards, R.L., 2003b. U/Th-dating living and young fossil corals  
21 from the central tropical Pacific. *Earth Planet. Sci. Lett.* 210, 91–103. [https://doi.org/10.1016/S0012-821X\(03\)00138-9](https://doi.org/10.1016/S0012-821X(03)00138-9)
- 22  
23 Cobb, K.M., Westphal, N., Sayani, H.R., Watson, J.T., Lorenzo, E.D., Cheng, H., Edwards, R.L., Charles, C.D., 2013.  
24 Highly Variable El Niño–Southern Oscillation Throughout the Holocene. *Science* 339, 67–70.  
25 <https://doi.org/10.1126/science.1228246>
- 26 Comas-Bru, L., Hernández, A., 2018. Reconciling North Atlantic climate modes: revised monthly indices for the East  
27 Atlantic and the Scandinavian patterns beyond the 20th century. *Earth Syst. Sci. Data* 10, 2329–2344.  
28 <https://doi.org/10.5194/essd-10-2329-2018>
- 29 Comas-Bru, L., McDermott, F., 2014. Impacts of the EA and SCA patterns on the European twentieth century NAO–  
30 winter climate relationship. *Q. J. R. Meteorol. Soc.* 140, 354–363. <https://doi.org/10.1002/qj.2158>
- 31 Comas-Bru, L., McDermott, F., Werner, M., 2016. The effect of the East Atlantic pattern on the precipitation  $\delta$  18 O-  
32 NAO relationship in Europe. *Clim. Dyn.* 47, 2059–2069.
- 33 Compo, G.P., Whitaker, J.S., Sardeshmukh, P.D., Matsui, N., Allan, R.J., Yin, X., Gleason, B.E., Vose, R.S.,  
34 Rutledge, G., Bessemoulin, P., Brönnimann, S., Brunet, M., Crouthamel, R.I., Grant, A.N., Groisman, P.Y.,  
35 Jones, P.D., Kruk, M.C., Kruger, A.C., Marshall, G.J., Maugeri, M., Mok, H.Y., Nordli, Ø., Ross, T.F., Trigo,  
36 R.M., Wang, X.L., Woodruff, S.D., Worley, S.J., 2011. The Twentieth Century Reanalysis Project. *Q. J. R.*  
37 *Meteorol. Soc.* 137, 1–28. <https://doi.org/10.1002/qj.776>
- 38 Cook, E.R., D'Arrigo, R.D., Anchukaitis, K.J., 2008. ENSO reconstructions from long tree-ring chronologies: Unifying  
39 the differences? Presented at the Reconciling ENSO Chronologies for the Past 500 Years, Moorea, French  
40 Polynesia.
- 41 Cook, E.R., D'Arrigo, R.D., Mann, M.E., 2002. A Well-Verified, Multiproxy Reconstruction of the Winter North Atlantic  
42 Oscillation Index since a.d. 1400. *J. Clim.* 15, 1754–1764. [https://doi.org/10.1175/1520-0442\(2002\)015<1754:AWVMRO>2.0.CO;2](https://doi.org/10.1175/1520-0442(2002)015<1754:AWVMRO>2.0.CO;2)
- 43  
44 Cook, E.R., Kushnir, Y., Smerdon, J.E., Williams, A.P., Anchukaitis, K.J., Wahl, E.R., 2019. A Euro-Mediterranean  
45 tree-ring reconstruction of the winter NAO index since 910 C.E. *Clim. Dyn.* 53, 1567–1580.  
46 <https://doi.org/10.1007/s00382-019-04696-2>
- 47  
48 Cook, E.R., Seager, R., Kushnir, Y., Briffa, K.R., Büntgen, U., Frank, D., Krusic, P.J., Tegel, W., Schrier, G. van der,  
49 Andreu-Hayles, L., Baillie, M., Baittinger, C., Bleicher, N., Bonde, N., Brown, D., Carrer, M., Cooper, R., Čufar,  
50 K., Dittmar, C., Esper, J., Griggs, C., Gunnarson, B., Günther, B., Gutierrez, E., Haneca, K., Helama, S.,  
51 Herzig, F., Heussner, K.-U., Hofmann, J., Janda, P., Kontic, R., Köse, N., Kyncl, T., Levanič, T., Linderholm,  
52 H., Manning, S., Melvin, T.M., Miles, D., Neuwirth, B., Nicolussi, K., Nola, P., Panayotov, M., Popa, I., Rothe,  
53 A., Seftigen, K., Seim, A., Svarva, H., Svoboda, M., Thun, T., Timonen, M., Touchan, R., Trotsiuk, V., Trouet,  
54 V., Walder, F., Ważny, T., Wilson, R., Zang, C., 2015. Old World megadroughts and pluvials during the  
55 Common Era. *Sci. Adv.* 1, e1500561. <https://doi.org/10.1126/sciadv.1500561>
- 56  
57 Cornes, R.C., Jones, P.D., Briffa, K.R., Osborn, T.J., 2013. Estimates of the North Atlantic Oscillation back to 1692  
58 using a Paris–London westerly index. *Int. J. Climatol.* 33, 228–248. <https://doi.org/10.1002/joc.3416>
- 59 Crann, C.A., Patterson, R.T., Macumber, A.L., Galloway, J.M., Roe, H.M., Blaauw, M., Swindles, G.T., Falck, H.,  
60 2015. Sediment accumulation rates in subarctic lakes: Insights into age-depth modeling from 22 dated lake  
61  
62  
63  
64  
65

- 1  
2  
3 records from the Northwest Territories, Canada. *Quat. Geochronol.* 27, 131–144.  
4 <https://doi.org/10.1016/j.quageo.2015.02.001>
- 5 Cropper, T., Hanna, E., Valente, M.A., Jónsson, T., 2015. A daily Azores-Iceland North Atlantic Oscillation index back  
6 to 1850. *Geosci. Data J.* 2, 12–24. <https://doi.org/10.1002/gdj3.23>
- 7 Curran, M.J., Rosenthal, Y., Wright, J.D., Morley, A., 2019. Atmospheric response to mid-Holocene warming in the  
8 northeastern Atlantic: Implications for future storminess in the Ireland/UK region. *Quat. Sci. Rev.* 225, 106004.  
9 <https://doi.org/10.1016/j.quascirev.2019.106004>
- 10 Czymzik, M., Muscheler, R., Adolphi, F., Mekhaldi, F., Dräger, N., Ott, F., Słowinski, M., Błaszczewicz, M., Aldahan,  
11 A., Possnert, G., Brauer, A., 2018. Synchronizing <sup>10</sup>Be in two varved lake sediment records to IntCal13 <sup>14</sup>C  
12 during three grand solar minima. *Clim. Past* 14, 687–696. <https://doi.org/10.5194/cp-14-687-2018>
- 13 d'Orgeville, M., Peltier, W.R., 2009. Implications of Both Statistical Equilibrium and Global Warming Simulations with  
14 CCSM3. Part I: On the Decadal Variability in the North Pacific Basin. *J. Clim.* 22, 5277–5297.  
15 <https://doi.org/10.1175/2009JCLI2428.1>
- 16 d'Orgeville, M., Peltier, W.R., 2007. On the Pacific Decadal Oscillation and the Atlantic Multidecadal Oscillation: Might  
17 they be related? *Geophys. Res. Lett.* 34. <https://doi.org/10.1029/2007GL031584>
- 18 Dai, A., 2013. The influence of the inter-decadal Pacific oscillation on US precipitation during 1923–2010. *Clim. Dyn.*  
19 41, 633–646. <https://doi.org/10.1007/s00382-012-1446-5>
- 20 D'Arrigo, R., Allan, R., Wilson, R., Palmer, J., Sakulich, J., Smerdon, J.E., Bijaksana, S., Ngkoimani, L.O., 2008.  
21 Pacific and Indian Ocean climate signals in a tree-ring record of Java monsoon drought. *Int. J. Climatol.* 28,  
22 1889–1901. <https://doi.org/10.1002/joc.1679>
- 23 D'Arrigo, R., Cook, E.R., Wilson, R.J., Allan, R., Mann, M.E., 2005. On the variability of ENSO over the past six  
24 centuries. *Geophys. Res. Lett.* 32. <https://doi.org/10.1029/2004GL022055>
- 25 D'Arrigo, R., Villalba, R., Wiles, G., 2001. Tree-ring estimates of Pacific decadal climate variability. *Clim. Dyn.* 18,  
26 219–224. <https://doi.org/10.1007/s003820100177>
- 27 D'Arrigo, R., Wilson, R., 2006. On the Asian expression of the PDO. *Int. J. Climatol.* 26, 1607–1617.  
28 <https://doi.org/10.1002/joc.1326>
- 29 D'Arrigo, R., Wilson, R., Wiles, G., Anchukaitis, K., Solomina, O., Davi, N., Deser, C., Dolgova, E., 2015. Tree-ring  
30 reconstructed temperature index for coastal northern Japan: implications for western North Pacific variability.  
31 *Int. J. Climatol.* 35, 3713–3720. <https://doi.org/10.1002/joc.4230>
- 32 Dätwyler, C., Abram, N.J., Grosjean, M., Wahl, E.R., Neukom, R., 2019. El Niño–Southern Oscillation variability,  
33 teleconnection changes and responses to large volcanic eruptions since AD 1000. *Int. J. Climatol.* 39, 2711–  
34 2724. <https://doi.org/10.1002/joc.5983>
- 35 Dätwyler, C., Neukom, R., Abram, N.J., Gallant, A.J.E., Grosjean, M., Jacques-Coper, M., Karoly, D.J., Villalba, R.,  
36 2018. Teleconnection stationarity, variability and trends of the Southern Annular Mode (SAM) during the last  
37 millennium. *Clim. Dyn.* 51, 2321–2339. <https://doi.org/10.1007/s00382-017-4015-0>
- 38 de Boer, E.J., Tjallingii, R., Vélez, M.I., Rijdsdijk, K.F., Vlug, A., Reichert, G.-J., Prendergast, A.L., de Louw, P.G.B.,  
39 Florens, F.B.V., Baider, C., Hooghiemstra, H., 2014. Climate variability in the SW Indian Ocean from an 8000-  
40 yr long multi-proxy record in the Mauritian lowlands shows a middle to late Holocene shift from negative IOD-  
41 state to ENSO-state. *Quat. Sci. Rev.* 86, 175–189. <https://doi.org/10.1016/j.quascirev.2013.12.026>
- 42 Dean, J.M., Kemp, A.E.S., 2004. A 2100 year BP record of the Pacific Decadal Oscillation, El Niño Southern  
43 Oscillation and Quasi-Biennial Oscillation in marine production and fluvial input from Saanich Inlet, British  
44 Columbia. *Palaeogeogr. Palaeoclimatol. Palaeoecol.* 213, 207–229.  
45 <https://doi.org/10.1016/j.palaeo.2004.05.001>
- 46 Dee, S., Emile-Geay, J., Evans, M.N., Allam, A., Steig, E.J., Thompson, D.M., 2015. PRYSM: An open-source  
47 framework for PProxY System Modeling, with applications to oxygen-isotope systems. *J. Adv. Model. Earth  
48 Syst.* 7, 1220–1247. <https://doi.org/10.1002/2015MS000447>
- 49 Dee, S.G., Cobb, K.M., Emile-Geay, J., Ault, T.R., Edwards, R.L., Cheng, H., Charles, C.D., 2020. No consistent  
50 ENSO response to volcanic forcing over the last millennium. *Science* 367, 1477–1481.  
51 <https://doi.org/10.1126/science.aax2000>
- 52 Dee, S.G., Parsons, L.A., Loope, G.R., Overpeck, J.T., Ault, T.R., Emile-Geay, J., 2017. Improved spectral  
53 comparisons of paleoclimate models and observations via proxy system modeling: Implications for multi-  
54 decadal variability. *Earth Planet. Sci. Lett.* 476, 34–46. <https://doi.org/10.1016/j.epsl.2017.07.036>
- 55 Deser, C., Phillips, A., Bourdette, V., Teng, H., 2012. Uncertainty in climate change projections: the role of internal  
56 variability. *Clim. Dyn.* 38, 527–546. <https://doi.org/10.1007/s00382-010-0977-x>
- 57  
58  
59  
60  
61  
62  
63  
64  
65

- 1  
2  
3 Di Lorenzo, E., Liguori, G., Schneider, N., Furtado, J.C., Anderson, B.T., Alexander, M.A., 2015. ENSO and  
4 meridional modes: A null hypothesis for Pacific climate variability. *Geophys. Res. Lett.* 42, 9440–9448.  
5 <https://doi.org/10.1002/2015GL066281>  
6  
7 Diaz, H.F., Markgraf, V. (Eds.), 2000. *El Niño and the Southern Oscillation: Multiscale Variability and Global and*  
8 *Regional Impacts*. Cambridge University Press, Cambridge. <https://doi.org/10.1017/CBO9780511573125>  
9  
10 Driscoll, S., Bozzo, A., Gray, L.J., Robock, A., Stenchikov, G., 2012. Coupled Model Intercomparison Project 5  
11 (CMIP5) simulations of climate following volcanic eruptions. *J. Geophys. Res. Atmospheres* 117.  
12 <https://doi.org/10.1029/2012JD017607>  
13  
14 Emile-Geay, J., Cobb, K.M., Carré, M., Braconnot, P., Leloup, J., Zhou, Y., Harrison, S.P., Corrège, T., McGregor,  
15 H.V., Collins, M., Driscoll, R., Elliot, M., Schneider, B., Tudhope, A., 2016. Links between tropical Pacific  
16 seasonal, interannual and orbital variability during the Holocene. *Nat. Geosci.* 9, 168–173.  
17 <https://doi.org/10.1038/ngeo2608>  
18  
19 Emile-Geay, J., Cobb, K.M., Cole, J.E., Elliot, M., 2020. Past ENSO variability: reconstructions, models, and  
20 implication, in: *El Niño Southern Oscillation in a Changing Climate*, AGU Monograph. AGU.  
21  
22 Emile-Geay, J., Seager, R., Cane, M.A., Cook, E.R., Haug, G.H., 2008. Volcanoes and ENSO over the Past  
23 Millennium. *J. Clim.* 21, 3134–3148. <https://doi.org/10.1175/2007JCLI1884.1>  
24  
25 Endo, S., Tozuka, T., 2016. Two flavors of the Indian Ocean Dipole. *Clim. Dyn.* 46, 3371–3385.  
26 <https://doi.org/10.1007/s00382-015-2773-0>  
27  
28 Enfield, D.B., Mestas-Núñez, A.M., Trimble, P.J., 2001. The Atlantic Multidecadal Oscillation and its relation to rainfall  
29 and river flows in the continental U.S. *Geophys. Res. Lett.* 28, 2077–2080.  
30 <https://doi.org/10.1029/2000GL012745>  
31  
32 Evans, M.N., Cane, M.A., Schrag, D.P., Kaplan, A., Linsley, B.K., Villalba, R., Wellington, G.M., 2001. Support for  
33 tropically-driven pacific decadal variability based on paleoproxy evidence. *Geophys. Res. Lett.* 28, 3689–3692.  
34 <https://doi.org/10.1029/2001GL013223>  
35  
36 Evans, M.N., Kaplan, A., Cane, M.A., 2002. Pacific sea surface temperature field reconstruction from coral  $\delta^{18}\text{O}$  data  
37 using reduced space objective analysis. *Paleoceanography* 17, 7-1-7–13.  
38 <https://doi.org/10.1029/2000PA000590>  
39  
40 Evans, M.N., Tolwinski-Ward, S.E., Thompson, D.M., Anchukaitis, K.J., 2013. Applications of proxy system modeling  
41 in high resolution paleoclimatology. *Quat. Sci. Rev.* 76, 16–28. <https://doi.org/10.1016/j.quascirev.2013.05.024>  
42  
43 Fan, F., Dong, X., Fang, X., Xue, F., Zheng, F., Zhu, J., 2017. Revisiting the relationship between the South Asian  
44 summer monsoon drought and El Niño warming pattern. *Atmospheric Sci. Lett.* 18, 175–182.  
45 <https://doi.org/10.1002/asl.740>  
46  
47 Faust, J.C., Fabian, K., Milzer, G., Giraudeau, J., Knies, J., 2016. Norwegian fjord sediments reveal NAO related  
48 winter temperature and precipitation changes of the past 2800 years. *Earth Planet. Sci. Lett.* 435, 84–93.  
49 <https://doi.org/10.1016/j.epsl.2015.12.003>  
50  
51 Feldstein, S.B., 2000. The Timescale, Power Spectra, and Climate Noise Properties of Teleconnection Patterns. *J.*  
52 *Clim.* 13, 4430–4440. [https://doi.org/10.1175/1520-0442\(2000\)013<4430:TTPSAC>2.0.CO;2](https://doi.org/10.1175/1520-0442(2000)013<4430:TTPSAC>2.0.CO;2)  
53  
54 Felis, T., Suzuki, A., Kuhnert, H., Rimbu, N., Kawahata, H., 2010. Pacific Decadal Oscillation documented in a coral  
55 record of North Pacific winter temperature since 1873. *Geophys. Res. Lett.* 37.  
56 <https://doi.org/10.1029/2010GL043572>  
57  
58 Feng, S., Hu, Q., 2008. How the North Atlantic Multidecadal Oscillation may have influenced the Indian summer  
59 monsoon during the past two millennia. *Geophys. Res. Lett.* 35. <https://doi.org/10.1029/2007GL032484>  
60  
61 Feng, S., Hu, Q., Oglesby, R.J., 2011. Influence of Atlantic sea surface temperatures on persistent drought in North  
62 America. *Clim. Dyn.* 37, 569–586. <https://doi.org/10.1007/s00382-010-0835-x>  
63  
64 Fereday, D., Chadwick, R., Knight, J., Scaife, A.A., 2018. Atmospheric Dynamics is the Largest Source of Uncertainty  
65 in Future Winter European Rainfall. *J. Clim.* 31, 963–977. <https://doi.org/10.1175/JCLI-D-17-0048.1>  
66  
67 Ferreira, D., Marshall, J., Bitz, C.M., Solomon, S., Plumb, A., 2015. Antarctic Ocean and Sea Ice Response to Ozone  
68 Depletion: A Two-Time-Scale Problem. *J. Clim.* 28, 1206–1226. <https://doi.org/10.1175/JCLI-D-14-00313.1>  
69  
70 Fischer, E.M., Luterbacher, J., Zorita, E., Tett, S.F.B., Casty, C., Wanner, H., 2007. European climate response to  
71 tropical volcanic eruptions over the last half millennium. *Geophys. Res. Lett.* 34.  
72 <https://doi.org/10.1029/2006GL027992>  
73  
74 Fischer, N., Jungclaus, J.H., 2010. Effects of orbital forcing on atmosphere and ocean heat transports in Holocene  
75 and Eemian climate simulations with a comprehensive Earth system model. *Clim. Past* 6, 155–168.  
76 <https://doi.org/10.5194/cp-6-155-2010>

- 1  
2  
3  
4 Fletcher, M.-S., Benson, A., Bowman, D.M.J.S., Gadd, P.S., Heijnis, H., Mariani, M., Saunders, K.M., Wolfe, B.B.,  
5 Zawadzki, A., 2018. Centennial-scale trends in the Southern Annular Mode revealed by hemisphere-wide fire  
6 and hydroclimatic trends over the past 2400 years. *Geology* 46, 363–366. <https://doi.org/10.1130/G39661.1>
- 7 Fletcher, M.-S., Moreno, P.I., 2012. Have the Southern Westerlies changed in a zonally symmetric manner over the  
8 last 14,000 years? A hemisphere-wide take on a controversial problem. *Quat. Int., PASH-2: Controversies in*  
9 *the late Quaternary of the Southern Hemisphere* 253, 32–46. <https://doi.org/10.1016/j.quaint.2011.04.042>
- 10 Fogt, R.L., Bromwich, D.H., 2006. Decadal Variability of the ENSO Teleconnection to the High-Latitude South Pacific  
11 Governed by Coupling with the Southern Annular Mode. *J. Clim.* 19, 979–997.  
12 <https://doi.org/10.1175/JCLI3671.1>
- 13 Fogt, R.L., Bromwich, D.H., Hines, K.M., 2011. Understanding the SAM influence on the South Pacific ENSO  
14 teleconnection. *Clim. Dyn.* 36, 1555–1576. <https://doi.org/10.1007/s00382-010-0905-0>
- 15 Fogt, R.L., Perlwitz, J., Monaghan, A.J., Bromwich, D.H., Jones, J.M., Marshall, G.J., 2009. Historical SAM  
16 Variability. Part II: Twentieth-Century Variability and Trends from Reconstructions, Observations, and the  
17 IPCC AR4 Models. *J. Clim.* 22, 5346–5365. <https://doi.org/10.1175/2009JCLI2786.1>
- 18 Folland, C.K., Colman, A.W., Rowell, D.P., Davey, M.K., 2001. Predictability of Northeast Brazil Rainfall and Real-  
19 Time Forecast Skill, 1987–98. *J. Clim.* 14, 1937–1958. [https://doi.org/10.1175/1520-0442\(2001\)014<1937:PONBRA>2.0.CO;2](https://doi.org/10.1175/1520-0442(2001)014<1937:PONBRA>2.0.CO;2)
- 20 Folland, C.K., Karl, T.R., Salinger, M.J., 2002. Observed climate variability and change. *Weather* 57, 269–278.  
21 <https://doi.org/10.1256/004316502320517353>
- 22 Folland, C.K., Knight, J., Linderholm, H.W., Fereday, D., Ineson, S., Hurrell, J.W., 2009. The Summer North Atlantic  
23 Oscillation: Past, Present, and Future. *J. Clim.* 22, 1082–1103. <https://doi.org/10.1175/2008JCLI2459.1>
- 24 Folland, C.K., Palmer, T.N., Parker, D.E., 1986. Sahel rainfall and worldwide sea temperatures, 1901–85. *Nature*  
25 320, 602–607. <https://doi.org/10.1038/320602a0>
- 26 Frappier, A., Sahagian, D., González, L.A., Carpenter, S.J., 2002. El Niño Events Recorded by Stalagmite Carbon  
27 Isotopes. *Science* 298, 565–565. <https://doi.org/10.1126/science.1076446>
- 28 Freund, M.B., Henley, B.J., Karoly, D.J., McGregor, H.V., Abram, N.J., Dommenges, D., 2019. Higher frequency of  
29 Central Pacific El Niño events in recent decades relative to past centuries. *Nat. Geosci.* 12, 450–455.  
30 <https://doi.org/10.1038/s41561-019-0353-3>
- 31 Friddell, J.E., Thunell, R.C., Guilderson, T.P., Kashgarian, M., 2003. Increased northeast Pacific climatic variability  
32 during the warm middle Holocene. *Geophys. Res. Lett.* 30. <https://doi.org/10.1029/2002GL016834>
- 33 Gagan, M.K., Dunbar, G.B., Suzuki, A., 2012. The effect of skeletal mass accumulation in *Porites* on coral Sr/Ca and  
34  $\delta^{18}\text{O}$  paleothermometry. *Paleoceanography* 27. <https://doi.org/10.1029/2011PA002215>
- 35 Găinușă-Bogdan, A., Swingedouw, D., Yiou, P., Cattiaux, J., Codron, F., Michel, S., 2020. AMOC and summer sea  
36 ice as key drivers of the spread in mid-holocene winter temperature patterns over Europe in PMIP3 models.  
37 *Glob. Planet. Change* 184, 103055. <https://doi.org/10.1016/j.gloplacha.2019.103055>
- 38 Gedalof, Z., Mantua, N.J., Peterson, D.L., 2002. A multi-century perspective of variability in the Pacific Decadal  
39 Oscillation: new insights from tree rings and coral. *Geophys. Res. Lett.* 29, 2204–2204.  
40 <https://doi.org/10.1029/2002GL015824>
- 41 Gedalof, Z., Smith, D.J., 2001. Interdecadal climate variability and regime-scale shifts in Pacific North America.  
42 *Geophys. Res. Lett.* 28, 1515–1518.
- 43 Gent, P.R., 2016. Effects of Southern Hemisphere Wind Changes on the Meridional Overturning Circulation in Ocean  
44 Models. *Annu. Rev. Mar. Sci.* 8, 79–94. <https://doi.org/10.1146/annurev-marine-122414-033929>
- 45 Gergis, J.L., Fowler, A.M., 2009. A history of ENSO events since A.D. 1525: implications for future climate change.  
46 *Clim. Change* 92, 343–387. <https://doi.org/10.1007/s10584-008-9476-z>
- 47 Geyer, A., Marti, A., Giralt, S., Folch, A., 2017. Potential ash impact from Antarctic volcanoes: Insights from  
48 Deception Island's most recent eruption. *Sci. Rep.* 7, 1–10. <https://doi.org/10.1038/s41598-017-16630-9>
- 49 Gillett, N.P., Fyfe, J.C., 2013. Annular mode changes in the CMIP5 simulations. *Geophys. Res. Lett.* 40, 1189–1193.  
50 <https://doi.org/10.1002/grl.50249>
- 51 Gillett, N.P., Kell, T.D., Jones, P.D., 2006. Regional climate impacts of the Southern Annular Mode. *Geophys. Res.*  
52 *Lett.* 33. <https://doi.org/10.1029/2006GL027721>
- 53 Glueck, M.F., Stockton, C.W., 2001. Reconstruction of the North Atlantic Oscillation, 1429–1983. *Int. J. Climatol.* 21,  
54 1453–1465. <https://doi.org/10.1002/joc.684>
- 55 Goldenberg, S.B., Landsea, C.W., Mestas-Núñez, A.M., Gray, W.M., 2001. The Recent Increase in Atlantic Hurricane  
56 Activity: Causes and Implications. *Science* 293, 474–479. <https://doi.org/10.1126/science.1060040>
- 57  
58  
59  
60  
61  
62  
63  
64  
65

- 1  
2  
3 Gomez, B., Carter, L., Orpin, A.R., Cobb, K.M., Page, M.J., Trustrum, N.A., Palmer, A.S., 2012. ENSO/SAM  
4 interactions during the middle and late Holocene. *The Holocene* 22, 23–30.  
5 <https://doi.org/10.1177/0959683611405241>  
6  
7 Gong, D., Wang, S., 1999. Definition of Antarctic Oscillation index. *Geophys. Res. Lett.* 26, 459–462.  
8 <https://doi.org/10.1029/1999GL900003>  
9  
10 Gong, D.-Y., Luterbacher, J., 2008. Variability of the low-level cross-equatorial jet of the western Indian Ocean since  
11 1660 as derived from coral proxies. *Geophys. Res. Lett.* 35. <https://doi.org/10.1029/2007GL032409>  
12  
13 Gong, T., Feldstein, S.B., Luo, D., 2010. The Impact of ENSO on Wave Breaking and Southern Annular Mode  
14 Events. *J. Atmospheric Sci.* 67, 2854–2870. <https://doi.org/10.1175/2010JAS3311.1>  
15  
16 Goodwin, I.D., Browning, S., Lorrey, A.M., Mayewski, P.A., Phipps, S.J., Bertler, N.A.N., Edwards, R.P., Cohen, T.J.,  
17 van Ommen, T., Curran, M., Barr, C., Stager, J.C., 2014. A reconstruction of extratropical Indo-Pacific sea-  
18 level pressure patterns during the Medieval Climate Anomaly. *Clim. Dyn.* 43, 1197–1219.  
19 <https://doi.org/10.1007/s00382-013-1899-1>  
20  
21 Gornitz, V., 2009. Paleoclimate Proxies, An Introduction, in: Gornitz, V. (Ed.), *Encyclopedia of Paleoclimatology and*  
22 *Ancient Environments*. Springer Netherlands, Dordrecht, pp. 716–721. [https://doi.org/10.1007/978-1-4020-](https://doi.org/10.1007/978-1-4020-4411-3_171)  
23 [4411-3\\_171](https://doi.org/10.1007/978-1-4020-4411-3_171)  
24  
25 Goslin, J., Fruergaard, M., Sander, L., Gałka, M., Menviel, L., Monkenbusch, J., Thibault, N., Clemmensen, L.B.,  
26 2018. Holocene centennial to millennial shifts in North-Atlantic storminess and ocean dynamics. *Sci. Rep.* 8,  
27 1–12. <https://doi.org/10.1038/s41598-018-29949-8>  
28  
29 Gouramanis, C., De Deckker, P., Switzer, A.D., Wilkins, D., 2013. Cross-continent comparison of high-resolution  
30 Holocene climate records from southern Australia — Deciphering the impacts of far-field teleconnections.  
31 *Earth-Sci. Rev.* 121, 55–72. <https://doi.org/10.1016/j.earscirev.2013.02.006>  
32  
33 Gray, L.J., Beer, J., Geller, M., Haigh, J.D., Lockwood, M., Matthes, K., Cubasch, U., Fleitmann, D., Harrison, G.,  
34 Hood, L., Luterbacher, J., Meehl, G.A., Shindell, D., Geel, B. van, White, W., 2010. Solar Influences on  
35 Climate. *Rev. Geophys.* 48. <https://doi.org/10.1029/2009RG000282>  
36  
37 Gray, L.J., Scaife, A.A., Mitchell, D.M., Osprey, S., Ineson, S., Hardiman, S., Butchart, N., Knight, J., Sutton, R.,  
38 Kodera, K., 2013. A lagged response to the 11 year solar cycle in observed winter Atlantic/European weather  
39 patterns. *J. Geophys. Res. Atmospheres* 118, 13,405–13,420. <https://doi.org/10.1002/2013JD020062>  
40  
41 Gray, S.T., Graumlich, L.J., Betancourt, J.L., Pederson, G.T., 2004. A tree-ring based reconstruction of the Atlantic  
42 Multidecadal Oscillation since 1567 A.D. *Geophys. Res. Lett.* 31. <https://doi.org/10.1029/2004GL019932>  
43  
44 Grossmann, I., Klotzbach, P.J., 2009. A review of North Atlantic modes of natural variability and their driving  
45 mechanisms. *J. Geophys. Res. Atmospheres* 114. <https://doi.org/10.1029/2009JD012728>  
46  
47 Grothe, P.R., Cobb, K.M., Liguori, G., Lorenzo, E.D., Capotondi, A., Lu, Y., Cheng, H., Edwards, R.L., Southon, J.R.,  
48 Santos, G.M., Deocampo, D.M., Lynch-Stieglitz, J., Chen, T., Sayani, H.R., Thompson, D.M., Conroy, J.L.,  
49 Moore, A.L., Townsend, K., Hagos, M., O'Connor, G., Toth, L.T., 2019. Enhanced El Niño-Southern  
50 Oscillation variability in recent decades. *Geophys. Res. Lett.* n/a. <https://doi.org/10.1029/2019GL083906>  
51  
52 Guo, F., Liu, Q., Yang, J., Fan, L., 2018. Three types of Indian Ocean Basin modes. *Clim. Dyn.* 51, 4357–4370.  
53 <https://doi.org/10.1007/s00382-017-3676-z>  
54  
55 Haase-Schramm, A., Böhm, F., Eisenhauer, A., Dullo, W.-C., Joachimski, M.M., Hansen, B., Reitner, J., 2003. Sr/Ca  
56 ratios and oxygen isotopes from sclerosponges: Temperature history of the Caribbean mixed layer and  
57 thermocline during the Little Ice Age. *Paleoceanography* 18. <https://doi.org/10.1029/2002PA000830>  
58  
59 Haigh, J.D., 1996. The Impact of Solar Variability on Climate. *Science* 272, 981–984.  
60 <https://doi.org/10.1126/science.272.5264.981>  
61  
62 Haigh, J.D., 1994. The role of stratospheric ozone in modulating the solar radiative forcing of climate. *Nature* 370,  
63 544–546. <https://doi.org/10.1038/370544a0>  
64  
65 Hakim, G.J., Emile-Geay, J., Steig, E.J., Noone, D., Anderson, D.M., Tardif, R., Steiger, N., Perkins, W.A., 2016. The  
66 last millennium climate reanalysis project: Framework and first results. *J. Geophys. Res. Atmospheres* 121,  
67 6745–6764. <https://doi.org/10.1002/2016JD024751>  
68  
69 Halpert, M.S., Ropelewski, C.F., 1992. Surface Temperature Patterns Associated with the Southern Oscillation. *J.*  
70 *Clim.* 5, 577–593. [https://doi.org/10.1175/1520-0442\(1992\)005<0577:STPAWT>2.0.CO;2](https://doi.org/10.1175/1520-0442(1992)005<0577:STPAWT>2.0.CO;2)  
71  
72 Hannachi, A., Jolliffe, I.T., Stephenson, D.B., 2007. Empirical orthogonal functions and related techniques in  
73 atmospheric science: A review. *Int. J. Climatol.* 27, 1119–1152. <https://doi.org/10.1002/joc.1499>  
74  
75 Hansen, J., Sato, M., Ruedy, R., 1997. Radiative forcing and climate response. *J. Geophys. Res. Atmospheres* 102,  
76 6831–6864. <https://doi.org/10.1029/96JD03436>



- 1  
2  
3  
4 Haslett, J., Whitley, M., Bhattacharya, S., Salter-Townshend, M., Wilson, S.P., Allen, J.R.M., Huntley, B., Mitchell,  
5 F.J.G., 2006. Bayesian palaeoclimate reconstruction. *J. R. Stat. Soc. Ser. A Stat. Soc.* 169, 395–438.  
6 <https://doi.org/10.1111/j.1467-985X.2006.00429.x>
- 7 Haywood, A.M., Valdes, P.J., Aze, T., Barlow, N., Burke, A., Dolan, A.M., von der Heydt, A.S., Hill, D.J., Jamieson,  
8 S.S.R., Otto-Bliesner, B.L., Salzmann, U., Saupe, E., Voss, J., 2019. What can Palaeoclimate Modelling do for  
9 you? *Earth Syst. Environ.* 3, 1–18. <https://doi.org/10.1007/s41748-019-00093-1>
- 10 Helama, S., Meriläinen, J., Tuomenvirta, H., 2009. Multicentennial megadrought in northern Europe coincided with a  
11 global El Niño–Southern Oscillation drought pattern during the Medieval Climate Anomaly. *Geology* 37, 175–  
12 178. <https://doi.org/10.1130/G25329A.1>
- 13 Henke, L.M.K., Lambert, F.H., Charman, D.J., 2017. Was the Little Ice Age more or less El Niño-like than the  
14 Medieval Climate Anomaly? Evidence from hydrological and temperature proxy data. *Clim. Past* 13, 267–301.  
15 <https://doi.org/10.5194/cp-13-267-2017>
- 16 Henley, B.J., Gergis, J., Karoly, D.J., Power, S., Kennedy, J., Folland, C.K., 2015. A Tripole Index for the Interdecadal  
17 Pacific Oscillation. *Clim. Dyn.* 45, 3077–3090. <https://doi.org/10.1007/s00382-015-2525-1>
- 18 Hermanson, L., Eade, R., Robinson, N.H., Dunstone, N.J., Andrews, M.B., Knight, J.R., Scaife, A.A., Smith, D.M.,  
19 2014. Forecast cooling of the Atlantic subpolar gyre and associated impacts. *Geophys. Res. Lett.* 41, 5167–  
20 5174. <https://doi.org/10.1002/2014GL060420>
- 21 Hernández, A., Giralt, S., Bao, R., Sáez, A., Leng, M.J., Barker, P.A., 2010. ENSO and solar activity signals from  
22 oxygen isotopes in diatom silica during late glacial-Holocene transition in Central Andes (18°S). *J.*  
23 *Paleolimnol.* 44, 413–429. <https://doi.org/10.1007/s10933-010-9412-x>
- 24 Hernández, A., Sánchez-López, G., Pla-Rabes, S., Comas-Bru, L., Parnell, A., Cahill, N., Geyer, A., Trigo, R.M.,  
25 Giralt, S., In Review. Evaluating the decadal-to-centennial evolution of a new proxy-based NAO reconstruction  
26 during the Common Era. *Sci. Rep.* <https://doi.org/10.31223/osf.io/p7ft6>
- 27 Hessl, A., Allen, K.J., Vance, T., Abram, N.J., Saunders, K.M., 2017. Reconstructions of the southern annular mode  
28 (SAM) during the last millennium. *Prog. Phys. Geogr. Earth Environ.* 41, 834–849.  
29 <https://doi.org/10.1177/0309133317743165>
- 30 Hetzinger, S., Pfeiffer, M., Dullo, W.-C., Keenlyside, N., Latif, M., Zinke, J., 2008. Caribbean coral tracks Atlantic  
31 Multidecadal Oscillation and past hurricane activity. *Geology* 36, 11–14. <https://doi.org/10.1130/G24321A.1>
- 32 Horel, J.D., Wallace, J.M., 1981. Planetary-Scale Atmospheric Phenomena Associated with the Southern Oscillation.  
33 *Mon. Weather Rev.* 109, 813–829. [https://doi.org/10.1175/1520-0493\(1981\)109<0813:PSAPAW>2.0.CO;2](https://doi.org/10.1175/1520-0493(1981)109<0813:PSAPAW>2.0.CO;2)
- 34 Hsu, H.-H., Chen, Y.-L., 2011. Decadal to bi-decadal rainfall variation in the western Pacific: A footprint of South  
35 Pacific decadal variability? *Geophys. Res. Lett.* 38. <https://doi.org/10.1029/2010GL046278>
- 36 Huntley, B., Spicer, R.A., Chaloner, W.G., Jarzembowski, E.A., 1993. The Use of Climate Response Surfaces to  
37 Reconstruct Palaeoclimate from Quaternary Pollen and Plant Macrofossil Data [and Discussion]. *Philos.*  
38 *Trans. Biol. Sci.* 341, 215–224.
- 39 Hurrell, J.W., 1995. Decadal Trends in the North Atlantic Oscillation: Regional Temperatures and Precipitation.  
40 *Science* 269, 676–679. <https://doi.org/10.1126/science.269.5224.676>
- 41 Hurrell, J.W., Kushnir, Y., Ottersen, G., Visbeck, M., 2003. An Overview of the North Atlantic Oscillation, in: W, H.J.,  
42 Y, K., G, O., M, V. (Eds.), *The North Atlantic Oscillation: Climatic Significance and Environmental Impact.*  
43 American Geophysical Union (AGU), Washington, US, pp. 1–35.
- 44 Ilvonen, L., Holmström, L., Seppä, H., Veski, S., 2016. A Bayesian multinomial regression model for palaeoclimate  
45 reconstruction with time uncertainty. *Environmetrics* 27, 409–422. <https://doi.org/10.1002/env.2393>
- 46 Ineson, S., Maycock, A.C., Gray, L.J., Scaife, A.A., Dunstone, N.J., Harder, J.W., Knight, J.R., Lockwood, M.,  
47 Manners, J.C., Wood, R.A., 2015. Regional climate impacts of a possible future grand solar minimum. *Nat.*  
48 *Commun.* 6, 1–8. <https://doi.org/10.1038/ncomms8535>
- 49 Ineson, S., Scaife, A.A., Knight, J.R., Manners, J.C., Dunstone, N.J., Gray, L.J., Haigh, J.D., 2011. Solar forcing of  
50 winter climate variability in the Northern Hemisphere. *Nat. Geosci.* 4, 753–757.  
51 <https://doi.org/10.1038/ngeo1282>
- 52 Ionita, M., Lohmann, G., Rimbu, N., Chelcea, S., Dima, M., 2012. Interannual to decadal summer drought variability  
53 over Europe and its relationship to global sea surface temperature. *Clim. Dyn.* 38, 363–377.  
54 <https://doi.org/10.1007/s00382-011-1028-y>
- 55 Ivanochko, T.S., Calvert, S.E., Thomson, R.E., Pedersen, T.F., 2008. Geochemical reconstruction of Pacific decadal  
56 variability from the eastern North Pacific during the Holocene This article is one of a series of papers published  
57 in this Special Issue on the theme Polar Climate Stability Network. *Can. J. Earth Sci.* 45, 1317–1329.  
58 <https://doi.org/10.1139/E08-037>
- 59  
60  
61  
62  
63  
64  
65

- 1  
2  
3  
4 Jerez, S., Trigo, R.M., Vicente-Serrano, S.M., Pozo-Vázquez, D., Lorente-Plazas, R., Lorenzo-Lacruz, J., Santos-  
5 Alamillos, F., Montávez, J.P., 2013. The Impact of the North Atlantic Oscillation on Renewable Energy  
6 Resources in Southwestern Europe. *J. Appl. Meteorol. Climatol.* 52, 2204–2225.  
7 <https://doi.org/10.1175/JAMC-D-12-0257.1>
- 8 Jones, P.D., Briffa, K.R., Osborn, T.J., Lough, J.M., van Ommen, T.D., Vinther, B.M., Luterbacher, J., Wahl, E.R.,  
9 Zwiers, F.W., Mann, M.E., Schmidt, G.A., Ammann, C.M., Buckley, B.M., Cobb, K.M., Esper, J., Goosse, H.,  
10 Graham, N., Jansen, E., Kiefer, T., Kull, C., Küttel, M., Mosley-Thompson, E., Overpeck, J.T., Riedwyl, N.,  
11 Schulz, M., Tudhope, A.W., Villalba, R., Wanner, H., Wolff, E., Xoplaki, E., 2009. High-resolution  
12 palaeoclimatology of the last millennium: a review of current status and future prospects. *The Holocene* 19, 3–  
13 49. <https://doi.org/10.1177/0959683608098952>
- 14 Jones, P.D., Jonsson, T., Wheeler, D., 1997. Extension to the North Atlantic oscillation using early instrumental  
15 pressure observations from Gibraltar and south-west Iceland. *Int. J. Climatol.* 17, 1433–1450.  
16 [https://doi.org/10.1002/\(SICI\)1097-0088\(19971115\)17:13<1433::AID-JOC203>3.0.CO;2-P](https://doi.org/10.1002/(SICI)1097-0088(19971115)17:13<1433::AID-JOC203>3.0.CO;2-P)
- 17 Jones, P.D., Mann, M.E., 2004. Climate over past millennia. *Rev. Geophys.* 42.  
18 <https://doi.org/10.1029/2003RG000143>
- 19 Jones, Philip D., 2001. Early European Instrumental Records, in: Jones, P. D., Ogilvie, A.E.J., Davies, T.D., Briffa,  
20 K.R. (Eds.), *History and Climate: Memories of the Future?* Springer US, Boston, MA, pp. 55–77.  
21 [https://doi.org/10.1007/978-1-4757-3365-5\\_4](https://doi.org/10.1007/978-1-4757-3365-5_4)
- 22 Juggins, S., Birks, H.J.B., 2012. Quantitative Environmental Reconstructions from Biological Data, in: Birks, H.J.B.,  
23 Lotter, A.F., Juggins, S., Smol, J.P. (Eds.), *Tracking Environmental Change Using Lake Sediments: Data*  
24 *Handling and Numerical Techniques, Developments in Paleoenvironmental Research.* Springer Netherlands,  
25 Dordrecht, pp. 431–494. [https://doi.org/10.1007/978-94-007-2745-8\\_14](https://doi.org/10.1007/978-94-007-2745-8_14)
- 26 Kennedy, J.J., Rayner, N.A., Atkinson, C.P., Killick, R.E., 2019. An Ensemble Data Set of Sea Surface Temperature  
27 Change From 1850: The Met Office Hadley Centre HadSST.4.0.0.0 Data Set. *J. Geophys. Res. Atmospheres*  
28 124, 7719–7763. <https://doi.org/10.1029/2018JD029867>
- 29 Kent, C., Pope, E., Thompson, V., Lewis, K., Scaife, A.A., Dunstone, N., 2017. Using climate model simulations to  
30 assess the current climate risk to maize production. *Environ. Res. Lett.* 12, 054012.  
31 <https://doi.org/10.1088/1748-9326/aa6cb9>
- 32 Kenyon, J., Hegerl, G.C., 2008. Influence of Modes of Climate Variability on Global Temperature Extremes. *J. Clim.*  
33 21, 3872–3889. <https://doi.org/10.1175/2008JCLI2125.1>
- 34 Khodri, M., Izumo, T., Vialard, J., Janicot, S., Cassou, C., Lengaigne, M., Mignot, J., Gastineau, G., Guilyardi, E.,  
35 Lebas, N., Robock, A., McPhaden, M.J., 2017. Tropical explosive volcanic eruptions can trigger El Niño by  
36 cooling tropical Africa. *Nat. Commun.* 8, 1–13. <https://doi.org/10.1038/s41467-017-00755-6>
- 37 Kilbourne, K.H., Alexander, M.A., Nye, J.A., 2014. A low latitude paleoclimate perspective on Atlantic multidecadal  
38 variability. *J. Mar. Syst., Atlantic Multidecadal Oscillation-mechanism and impact on marine ecosystems* 133,  
39 4–13. <https://doi.org/10.1016/j.jmarsys.2013.09.004>
- 40 Kilbourne, K.H., Quinn, T.M., Webb, R., Guilderson, T., Nyberg, J., Winter, A., 2008. Paleoclimate proxy perspective  
41 on Caribbean climate since the year 1751: Evidence of cooler temperatures and multidecadal variability.  
42 *Paleoceanography* 23. <https://doi.org/10.1029/2008PA001598>
- 43 Kilian, R., Lamy, F., 2012. A review of Glacial and Holocene paleoclimate records from southernmost Patagonia (49–  
44 55°S). *Quat. Sci. Rev.* 53, 1–23. <https://doi.org/10.1016/j.quascirev.2012.07.017>
- 45 Kirby, M.E., Lund, S.P., Patterson, W.P., Anderson, M.A., Bird, B.W., Ivanovici, L., Monarrez, P., Nielsen, S., 2010. A  
46 Holocene record of Pacific Decadal Oscillation (PDO)-related hydrologic variability in Southern California  
47 (Lake Elsinore, CA). *J. Paleolimnol.* 44, 819–839. <https://doi.org/10.1007/s10933-010-9454-0>
- 48 Kitzberger, T., Brown, P.M., Heyerdahl, E.K., Swetnam, T.W., Veblen, T.T., 2007. Contingent Pacific-Atlantic Ocean  
49 influence on multicentury wildfire synchrony over western North America. *Proc. Natl. Acad. Sci. U. S. A.* 104,  
50 543–548. <https://doi.org/10.1073/pnas.0606078104>
- 51 Knight, J.R., Allan, R.J., Folland, C.K., Vellinga, M., Mann, M.E., 2005. A signature of persistent natural thermohaline  
52 circulation cycles in observed climate. *Geophys. Res. Lett.* 32, 1–4. <https://doi.org/10.1029/2005GL024233>
- 53 Knight, J.R., Folland, C.K., Scaife, A.A., 2006. Climate impacts of the Atlantic Multidecadal Oscillation. *Geophys.*  
54 *Res. Lett.* 33. <https://doi.org/10.1029/2006GL026242>
- 55 Knudsen, M.F., Jacobsen, B.H., Seidenkrantz, M.-S., Olsen, J., 2014. Evidence for external forcing of the Atlantic  
56 Multidecadal Oscillation since termination of the Little Ice Age. *Nat. Commun.* 5, 3323.  
57 <https://doi.org/10.1038/ncomms4323>  
58  
59  
60  
61  
62  
63  
64  
65

- 1  
2  
3 Knudsen, M.F., Seidenkrantz, M.-S., Jacobsen, B.H., Kuijpers, A., 2011. Tracking the Atlantic Multidecadal  
4 Oscillation through the last 8,000 years. *Nat. Commun.* 2, 1–8. <https://doi.org/10.1038/ncomms1186>
- 5 Kobashi, T., Menviel, L., Jeltsch-Thömmes, A., Vinther, B.M., Box, J.E., Muscheler, R., Nakaegawa, T., Pfister, P.L.,  
6 Döring, M., Leuenberger, M., Wanner, H., Ohmura, A., 2017. Volcanic influence on centennial to millennial  
7 Holocene Greenland temperature change. *Sci. Rep.* 7, 1–10. <https://doi.org/10.1038/s41598-017-01451-7>
- 8 Kodera, K., 2002. Solar cycle modulation of the North Atlantic Oscillation: Implication in the spatial structure of the  
9 NAO. *Geophys. Res. Lett.* 29, 59-1-59–4. <https://doi.org/10.1029/2001GL014557>
- 10 Kosaka, Y., Xie, S.-P., 2013. Recent global-warming hiatus tied to equatorial Pacific surface cooling. *Nature* 501,  
11 403–407. <https://doi.org/10.1038/nature12534>
- 12 Koutavas, A., Joanides, S., 2012. El Niño–Southern Oscillation extrema in the Holocene and Last Glacial Maximum.  
13 *Paleoceanography* 27. <https://doi.org/10.1029/2012PA002378>
- 14 Kravtsov, S., Grimm, C., Gu, S., 2018. Global-scale multidecadal variability missing in state-of-the-art climate models.  
15 *Npj Clim. Atmospheric Sci.* 1, 1–10. <https://doi.org/10.1038/s41612-018-0044-6>
- 16 Krishnamurthy, L., Krishnamurthy, V., 2016. Decadal and interannual variability of the Indian Ocean SST. *Clim. Dyn.*  
17 46, 57–70. <https://doi.org/10.1007/s00382-015-2568-3>
- 18 Kuhnert, H., Kuhlmann, H., Mohtadi, M., Meggers, H., Baumann, K.-H., Pätzold, J., 2014. Holocene tropical western  
19 Indian Ocean sea surface temperatures in covariation with climatic changes in the Indonesian region.  
20 *Paleoceanography* 29, 423–437. <https://doi.org/10.1002/2013PA002555>
- 21 Küttel, M., Xoplaki, E., Gallego, D., Luterbacher, J., García-Herrera, R., Allan, R., Barriendos, M., Jones, P.D.,  
22 Wheeler, D., Wanner, H., 2010. The importance of ship log data: reconstructing North Atlantic, European and  
23 Mediterranean sea level pressure fields back to 1750. *Clim. Dyn.* 34, 1115–1128.  
24 <https://doi.org/10.1007/s00382-009-0577-9>
- 25 Kwiatkowski, C., Prange, M., Varma, V., Steinke, S., Hebbeln, D., Mohtadi, M., 2015. Holocene variations of  
26 thermocline conditions in the eastern tropical Indian Ocean. *Quat. Sci. Rev.* 114, 33–42.  
27 <https://doi.org/10.1016/j.quascirev.2015.01.028>
- 28 Lachniet, M.S., Burns, S.J., Piperno, D.R., Asmerom, Y., Polyak, V.J., Moy, C.M., Christenson, K., 2004. A 1500-year  
29 El Niño/Southern Oscillation and rainfall history for the Isthmus of Panama from speleothem calcite. *J.*  
30 *Geophys. Res. Atmospheres* 109. <https://doi.org/10.1029/2004JD004694>
- 31 Lane, C.S., Brauer, A., Blockley, S.P.E., Dulski, P., 2013. Volcanic ash reveals time-transgressive abrupt climate  
32 change during the Younger Dryas. *Geology* 41, 1251–1254. <https://doi.org/10.1130/G34867.1>
- 33 Lapointe, F., Francus, P., Lamoureux, S.F., Vuille, M., Jenny, J.-P., Bradley, R.S., Massa, C., 2017. Influence of  
34 North Pacific decadal variability on the western Canadian Arctic over the past 700 years. *Clim. Past* 13, 411–  
35 420. <https://doi.org/10.5194/cp-13-411-2017>
- 36 Lean, J., 1997. The Sun's Variable Radiation and Its Relevance for Earth. *Annu. Rev. Astron. Astrophys.* 35, 33–67.  
37 <https://doi.org/10.1146/annurev.astro.35.1.33>
- 38 Ledru, M.-P., Jomelli, V., Samaniego, P., Vuille, M., Hidalgo, S., Herrera, M., Ceron, C., 2013. The Medieval Climate  
39 Anomaly and the Little Ice Age in the eastern Ecuadorian Andes. *Clim. Past* 9, 307–321.  
40 <https://doi.org/10.5194/cp-9-307-2013>
- 41 Lee, J., Sperber, K.R., Gleckler, P.J., Bonfils, C.J.W., Taylor, K.E., 2019. Quantifying the agreement between  
42 observed and simulated extratropical modes of interannual variability. *Clim. Dyn.* 52, 4057–4089.  
43 <https://doi.org/10.1007/s00382-018-4355-4>
- 44 Lefebvre, W., Goosse, H., Timmermann, R., Fichefet, T., 2004. Influence of the Southern Annular Mode on the sea  
45 ice–ocean system. *J. Geophys. Res. Oceans* 109. <https://doi.org/10.1029/2004JC002403>
- 46 Lehner, F., Raible, C.C., Stocker, T.F., 2012. Testing the robustness of a precipitation proxy-based North Atlantic  
47 Oscillation reconstruction. *Quat. Sci. Rev.* 45, 85–94. <https://doi.org/10.1016/j.quascirev.2012.04.025>
- 48 Li, J., Xie, S.-P., Cook, E.R., Huang, G., D'Arrigo, R., Liu, F., Ma, J., Zheng, X.-T., 2011. Interdecadal modulation of  
49 El Niño amplitude during the past millennium. *Nat. Clim. Change* 1, 114–118.  
50 <https://doi.org/10.1038/nclimate1086>
- 51 Li, J., Xie, S.-P., Cook, E.R., Morales, M.S., Christie, D.A., Johnson, N.C., Chen, F., D'Arrigo, R., Fowler, A.M., Gou,  
52 X., Fang, K., 2013. El Niño modulations over the past seven centuries. *Nat. Clim. Change* 3, 822–826.  
53 <https://doi.org/10.1038/nclimate1936>
- 54 Li, Z., Chen, M.-T., Lin, D.-C., Shi, X., Liu, S., Wang, H., Yokoyama, Y., Shen, C.-C., Mii, H.-S., Troa, R.A., Zuraida,  
55 R., Triarso, E., Hendrigan, M., 2018. Evidence of solar insolation and internal forcing of sea surface  
56 temperature changes in the eastern tropical Indian Ocean during the Holocene. *Quat. Int.* 490, 1–9.  
57 <https://doi.org/10.1016/j.quaint.2018.04.001>
- 58  
59  
60  
61  
62  
63  
64  
65

- 1  
2  
3  
4 Lim, E.-P., Hendon, H.H., Rashid, H., 2013. Seasonal Predictability of the Southern Annular Mode due to Its  
5 Association with ENSO. *J. Clim.* 26, 8037–8054. <https://doi.org/10.1175/JCLI-D-13-00006.1>
- 6 Linsley, B.K., Zhang, P., Kaplan, A., Howe, S.S., Wellington, G.M., 2008. Interdecadal-decadal climate variability from  
7 multicoral oxygen isotope records in the South Pacific Convergence Zone region since 1650 A.D.  
8 *Paleoceanography* 23. <https://doi.org/10.1029/2007PA001539>
- 9 Liu, Y., Cobb, K.M., Song, H., Li, Q., Li, C.-Y., Nakatsuka, T., An, Z., Zhou, W., Cai, Q., Li, J., Leavitt, S.W., Sun, C.,  
10 Mei, R., Shen, C.-C., Chan, M.-H., Sun, J., Yan, L., Lei, Y., Ma, Y., Li, X., Chen, D., Linderholm, H.W., 2017.  
11 Recent enhancement of central Pacific El Niño variability relative to last eight centuries. *Nat. Commun.* 8, 1–8.  
12 <https://doi.org/10.1038/ncomms15386>
- 13 Liu, Z., Di Lorenzo, E., 2018. Mechanisms and Predictability of Pacific Decadal Variability. *Curr. Clim. Change Rep.*  
14 4, 128–144. <https://doi.org/10.1007/s40641-018-0090-5>
- 15 Liu, Z., Lu, Z., Wen, X., Otto-Bliesner, B.L., Timmermann, A., Cobb, K.M., 2014a. Evolution and forcing mechanisms  
16 of El Niño over the past 21,000 years. *Nature* 515, 550–553. <https://doi.org/10.1038/nature13963>
- 17 Liu, Z., Wen, X., Brady, E.C., Otto-Bliesner, B., Yu, G., Lu, H., Cheng, H., Wang, Y., Zheng, W., Ding, Y., Edwards,  
18 R.L., Cheng, J., Liu, W., Yang, H., 2014b. Chinese cave records and the East Asia Summer Monsoon. *Quat.*  
19 *Sci. Rev.* 83, 115–128. <https://doi.org/10.1016/j.quascirev.2013.10.021>
- 20 Ljungqvist, F.C., Zhang, Qiong, Brattström, G., Krusic, P.J., Seim, A., Li, Q., Zhang, Qiang, Moberg, A., 2019.  
21 Centennial-Scale Temperature Change in Last Millennium Simulations and Proxy-Based Reconstructions. *J.*  
22 *Clim.* 32, 2441–2482. <https://doi.org/10.1175/JCLI-D-18-0525.1>
- 23 Lohmann, K., Mignot, J., Langehaug, H.R., Jungclauss, J.H., Matei, D., Otterå, O.H., Gao, Y.Q., Mjell, T.L.,  
24 Ninnemann, U.S., Kleiven, H.F., 2015. Using simulations of the last millennium to understand climate  
25 variability seen in palaeo-observations: similar variation of Iceland–Scotland overflow strength and Atlantic  
26 Multidecadal Oscillation. *Clim. Past* 11, 203–216. <https://doi.org/10.5194/cp-11-203-2015>
- 27 Lu, Z., Liu, Z., Zhu, J., Cobb, K.M., 2018a. A Review of Paleo El Niño–Southern Oscillation. *Atmosphere* 9, 130.  
28 <https://doi.org/10.3390/atmos9040130>
- 29 Lu, Z., Miller, P.A., Zhang, Qiong, Zhang, Qiang, Wårlind, D., Nieradzick, L., Sjolte, J., Smith, B., 2018b. Dynamic  
30 Vegetation Simulations of the Mid-Holocene Green Sahara. *Geophys. Res. Lett.* 45, 8294–8303.  
31 <https://doi.org/10.1029/2018GL079195>
- 32 Lüning, S., Gałka, M., Danladi, I.B., Adagunodo, T.A., Vahrenholt, F., 2018. Hydroclimate in Africa during the  
33 Medieval Climate Anomaly. *Palaeogeogr. Palaeoclimatol. Palaeoecol.* 495, 309–322.  
34 <https://doi.org/10.1016/j.palaeo.2018.01.025>
- 35 Lüning, S., Schulte, L., Garcés-Pastor, S., Danladi, I.B., Gałka, M., 2019. The Medieval Climate Anomaly in the  
36 Mediterranean Region. *Paleoceanogr. Paleoclimatology* 34, 1625–1649.  
37 <https://doi.org/10.1029/2019PA003734>
- 38 Luo, J.-J., Masson, S., Behera, S.K., Yamagata, T., 2008. Extended ENSO Predictions Using a Fully Coupled  
39 Ocean–Atmosphere Model. *J. Clim.* 21, 84–93. <https://doi.org/10.1175/2007JCLI1412.1>
- 40 Luterbacher, J., Schmutz, C., Gyalistras, D., Xoplaki, E., Wanner, H., 1999. Reconstruction of monthly NAO and EU  
41 indices back to AD 1675. *Geophys. Res. Lett.* 26, 2745–2748. <https://doi.org/10.1029/1999GL900576>
- 42 Luterbacher, J., Werner, J.P., Smerdon, J.E., Fernández-Donado, L., González-Rouco, F.J., Barriopedro, D.,  
43 Ljungqvist, F.C., Büntgen, U., Zorita, E., Wagner, S., Esper, J., McCarroll, D., Toreti, A., Frank, D., Jungclauss,  
44 J.H., Barriendos, M., Bertolin, C., Bothe, O., Brázdil, R., Camuffo, D., Dobrovolný, P., Gagen, M., García-  
45 Bustamante, E., Ge, Q., Gómez-Navarro, J.J., Guiot, J., Hao, Z., Hegerl, G.C., Holmgren, K., Klimenko, V.V.,  
46 Martín-Chivelet, J., Pfister, C., Roberts, N., Schindler, A., Schurer, A., Solomina, O., Gunten, L. von, Wahl, E.,  
47 Wanner, H., Wetter, O., Xoplaki, E., Yuan, N., Zanchettin, D., Zhang, H., Zerefos, C., 2016. European summer  
48 temperatures since Roman times. *Environ. Res. Lett.* 11, 024001. <https://doi.org/10.1088/1748-9326/11/2/024001>
- 49 Luterbacher, J., Xoplaki, E., Dietrich, D., Jones, P.D., Davies, T.D., Portis, D., Gonzalez-Rouco, J.F., Storch, H. von,  
50 Gyalistras, D., Casty, C., Wanner, H., 2001. Extending North Atlantic oscillation reconstructions back to 1500.  
51 *Atmospheric Sci. Lett.* 2, 114–124. <https://doi.org/10.1006/asle.2002.0047>
- 52 Luterbacher, J., Xoplaki, E., Dietrich, D., Rickli, R., Jacobeit, J., Beck, C., Gyalistras, D., Schmutz, C., Wanner, H.,  
53 2002. Reconstruction of sea level pressure fields over the Eastern North Atlantic and Europe back to 1500.  
54 *Clim. Dyn.* 18, 545–561. <https://doi.org/10.1007/s00382-001-0196-6>
- 55 MacDonald, G.M., Case, R.A., 2005. Variations in the Pacific Decadal Oscillation over the past millennium. *Geophys.*  
56 *Res. Lett.* 32. <https://doi.org/10.1029/2005GL022478>
- 57  
58  
59  
60  
61  
62  
63  
64  
65

- 1  
2  
3  
4 Maher, N., McGregor, S., England, M.H., Gupta, A.S., 2015. Effects of volcanism on tropical variability. *Geophys. Res. Lett.* 42, 6024–6033. <https://doi.org/10.1002/2015GL064751>
- 5  
6 Mann, M.E., Bradley, R.S., Hughes, M.K., 1998. Global-scale temperature patterns and climate forcing over the past six centuries. *Nature* 392, 779–787. <https://doi.org/10.1038/33859>
- 7  
8 Mann, M.E., Cane, M.A., Zebiak, S.E., Clement, A., 2005. Volcanic and Solar Forcing of the Tropical Pacific over the Past 1000 Years. *J. Clim.* 18, 447–456. <https://doi.org/10.1175/JCLI-3276.1>
- 9  
10 Mann, M.E., Gille, E., Overpeck, J., Gross, W., Bradley, R.S., Keimig, F.T., Hughes, M.K., 2000. Global Temperature Patterns in Past Centuries: An Interactive Presentation. *Earth Interact.* 4, 1–1. [https://doi.org/10.1175/1087-3562\(2000\)004<0001:GTPIPC>2.3.CO;2](https://doi.org/10.1175/1087-3562(2000)004<0001:GTPIPC>2.3.CO;2)
- 11  
12 Mann, M.E., Steinman, B.A., Miller, S.K., 2020. Absence of internal multidecadal and interdecadal oscillations in climate model simulations. *Nat. Commun.* 11, 49. <https://doi.org/10.1038/s41467-019-13823-w>
- 13  
14 Mann, M.E., Zhang, Z., Rutherford, S., Bradley, R.S., Hughes, M.K., Shindell, D., Ammann, C., Faluvegi, G., Ni, F., 2009. Global signatures and dynamical origins of the Little Ice Age and Medieval Climate Anomaly. *Science* 326, 1256–1260. <https://doi.org/10.1126/science.1177303>
- 15  
16  
17 Mantua, N.J., Hare, S.R., 2002. The Pacific Decadal Oscillation. *J. Oceanogr.* 58, 35–44. <https://doi.org/10.1023/A:1015820616384>
- 18  
19 Mantua, N.J., Hare, S.R., Zhang, Y., Wallace, J.M., Francis, R.C., 1997. A Pacific Interdecadal Climate Oscillation with Impacts on Salmon Production\*. *Bull. Am. Meteorol. Soc.* 78, 1069–1080. [https://doi.org/10.1175/1520-0477\(1997\)078<1069:APICOW>2.0.CO;2](https://doi.org/10.1175/1520-0477(1997)078<1069:APICOW>2.0.CO;2)
- 20  
21 Marchitto, T.M., Muscheler, R., Ortiz, J.D., Carriquiry, J.D., Geen, A. van, 2010. Dynamical Response of the Tropical Pacific Ocean to Solar Forcing During the Early Holocene. *Science* 330, 1378–1381. <https://doi.org/10.1126/science.1194887>
- 22  
23 Marcott, S.A., Shakun, J.D., Clark, P.U., Mix, A.C., 2013. A Reconstruction of Regional and Global Temperature for the Past 11,300 Years. *Science* 339, 1198–1201. <https://doi.org/10.1126/science.1228026>
- 24  
25 Marsh, N., Svensmark, H., 2003. Galactic cosmic ray and El Niño–Southern Oscillation trends in International Satellite Cloud Climatology Project D2 low-cloud properties. *J. Geophys. Res. Atmospheres* 108. <https://doi.org/10.1029/2001JD001264>
- 26  
27 Marshall, G.J., 2003. Trends in the Southern Annular Mode from Observations and Reanalyses. *J. Clim.* 16, 4134–4143. [https://doi.org/10.1175/1520-0442\(2003\)016<4134:TITSAM>2.0.CO;2](https://doi.org/10.1175/1520-0442(2003)016<4134:TITSAM>2.0.CO;2)
- 28  
29 Martin-Puertas, C., Matthes, K., Brauer, A., Muscheler, R., Hansen, F., Petrick, C., Aldahan, A., Possnert, G., Geel, B. van, 2012. Regional atmospheric circulation shifts induced by a grand solar minimum. *Nat. Geosci.* 5, 397–401. <https://doi.org/10.1038/ngeo1460>
- 30  
31 Masson-Delmotte, V., Schulz, M., Abe-Ouchi, A., Beer, J., Ganopolski, A., Gonzalez Rouco, J.F., Jansen, E., Lambeck, K., Luterbacher, J., Naish, T., Osborn, T., Otto-Bliesner, B., Quinn, T., Ramesh, R., Rojas, M., Shao, X., Timmermann, A., 2013. Information from paleoclimate archives, in: Stocker, T.F., Qin, D., Plattner, G.-K., Tignor, M.M.B., Allen, S.K., Boschung, J., Nauels, A., Xia, Y., Bex, V., Midgley, P.M. (Eds.), *Climate Change 2013: The Physical Science Basis*. Cambridge University Press, pp. 383–464. <https://doi.org/10.1017/CBO9781107415324.013>
- 32  
33 Matthes, K., Funke, B., Andersson, M.E., Barnard, L., Beer, J., Charbonneau, P., Clilverd, M.A., Dudok de Wit, T., Haberreiter, M., Hendry, A., Jackman, C.H., Kretzschmar, M., Kruschke, T., Kunze, M., Langematz, U., Marsh, D.R., Maycock, A.C., Misios, S., Rodger, C.J., Scaife, A.A., Seppälä, A., Shangguan, M., Sinnhuber, M., Tourpali, K., Usoskin, I., Kamp, M. van de, Verronen, P.T., Versick, S., 2017. Solar forcing for CMIP6 (v3.2). *Geosci. Model Dev.* 10, 2247–2302. <https://doi.org/10.5194/gmd-10-2247-2017>
- 34  
35 Matthes, K., Kodera, K., Haigh, J.D., Shindell, D.T., Shibata, K., Langematz, U., Rozanov, E., Kuroda, Y., 2003. GRIPS Solar Experiments Intercomparison Project: Initial Results. *Pap. Meteorol. Geophys.* 54, 71–90. <https://doi.org/10.2467/mripapers.54.71>
- 36  
37 Matthes, K., Kuroda, Y., Kodera, K., Langematz, U., 2006. Transfer of the solar signal from the stratosphere to the troposphere: Northern winter. *J. Geophys. Res. Atmospheres* 111. <https://doi.org/10.1029/2005JD006283>
- 38  
39 Mauri, A., Davis, B. a. S., Collins, P.M., Kaplan, J.O., 2014. The influence of atmospheric circulation on the mid-Holocene climate of Europe: a data–model comparison. *Clim. Past* 10, 1925–1938. <https://doi.org/10.5194/cp-10-1925-2014>
- 40  
41 McAfee, S.A., 2014. Consistency and the Lack Thereof in Pacific Decadal Oscillation Impacts on North American Winter Climate. *J. Clim.* 27, 7410–7431. <https://doi.org/10.1175/JCLI-D-14-00143.1>
- 42  
43  
44  
45  
46  
47  
48  
49  
50  
51  
52  
53  
54  
55  
56  
57  
58  
59  
60  
61  
62  
63  
64  
65

- 1  
2  
3  
4 McCabe-Glynn, S., Johnson, K.R., Strong, C., Berkelhammer, M., Sinha, A., Cheng, H., Edwards, R.L., 2013.  
5 Variable North Pacific influence on drought in southwestern North America since AD 854. *Nat. Geosci.* 6, 617–  
6 621. <https://doi.org/10.1038/ngeo1862>
- 7 McGregor, S., Timmermann, A., 2010. The Effect of Explosive Tropical Volcanism on ENSO. *J. Clim.* 24, 2178–2191.  
8 <https://doi.org/10.1175/2010JCLI3990.1>
- 9 McGregor, S., Timmermann, A., England, M.H., Elison Timm, O., Wittenberg, A.T., 2013. Inferred changes in El  
10 Niño–Southern Oscillation variance over the past six centuries. *Clim. Past* 9, 2269–2284.  
11 <https://doi.org/10.5194/cp-9-2269-2013>
- 12 McGregor, S., Timmermann, A., Timm, O., 2010. A unified proxy for ENSO and PDO variability since 1650. *Clim.*  
13 *Past* 6, 1–17. <https://doi.org/10.5194/cp-6-1-2010>
- 14 McPhaden, M.J., Zebiak, S.E., Glantz, M.H., 2006. ENSO as an Integrating Concept in Earth Science. *Science* 314,  
15 1740–1745. <https://doi.org/10.1126/science.1132588>
- 16 Meehl, G.A., Arblaster, J.M., Chung, C.T.Y., Holland, M.M., DuVivier, A., Thompson, L., Yang, D., Bitz, C.M., 2019.  
17 Sustained ocean changes contributed to sudden Antarctic sea ice retreat in late 2016. *Nat. Commun.* 10, 1–9.  
18 <https://doi.org/10.1038/s41467-018-07865-9>
- 19 Meehl, G.A., Hu, A., Santer, B.D., Xie, S.P., 2016. Contribution of the Interdecadal Pacific Oscillation to twentieth-  
20 century global surface temperature trends. *Nat. Clim. Change* 6, 1005–1008.  
21 <https://doi.org/10.1038/nclimate3107>
- 22 Mekhaldi, F., Muscheler, R., Adolphi, F., Aldahan, A., Beer, J., McConnell, J.R., Possnert, G., Sigl, M., Svensson, A.,  
23 Synal, H.-A., Welten, K.C., Woodruff, T.E., 2015. Multiradionuclide evidence for the solar origin of the cosmic-  
24 ray events of AD 774/5 and 993/4. *Nat. Commun.* 6, 1–8. <https://doi.org/10.1038/ncomms9611>
- 25 Mellado-Cano, J., Barriopedro, D., García-Herrera, R., Trigo, R.M., Hernández, A., 2019. Examining the North  
26 Atlantic Oscillation, East Atlantic Pattern, and Jet Variability since 1685. *J. Clim.* 32, 6285–6298.  
27 <https://doi.org/10.1175/JCLI-D-19-0135.1>
- 28 Menary, M.B., Scaife, A.A., 2014. Naturally forced multidecadal variability of the Atlantic meridional overturning  
29 circulation. *Clim. Dyn.* 42, 1347–1362. <https://doi.org/10.1007/s00382-013-2028-x>
- 30 Meredith, M.P., Hogg, A.M., 2006. Circumpolar response of Southern Ocean eddy activity to a change in the  
31 Southern Annular Mode. *Geophys. Res. Lett.* 33. <https://doi.org/10.1029/2006GL026499>
- 32 Michel, S., Swingedouw, D., Chavent, M., Ortega, P., Mignot, J., Khodri, M., 2020. Reconstructing climatic modes of  
33 variability from proxy records using ClimIndRec version 1.0. *Geosci. Model Dev.* 13, 841–858.  
34 <https://doi.org/10.5194/gmd-13-841-2020>
- 35 Mignot, J., Khodri, M., Frankignoul, C., Servonnat, J., 2011. Volcanic impact on the Atlantic Ocean over the last  
36 millennium. *Clim. Past* 7, 1439–1455. <https://doi.org/10.5194/cp-7-1439-2011>
- 37 Miller, G.H., Geirsdóttir, Á., Zhong, Y., Larsen, D.J., Otto-Bliesner, B.L., Holland, M.M., Bailey, D.A., Refsnider, K.A.,  
38 Lehman, S.J., Southon, J.R., Anderson, C., Björnsson, H., Thordarson, T., 2012. Abrupt onset of the Little Ice  
39 Age triggered by volcanism and sustained by sea-ice/ocean feedbacks. *Geophys. Res. Lett.* 39.  
40 <https://doi.org/10.1029/2011GL050168>
- 41 Minobe, S., 2000. Spatio-temporal structure of the pentadecadal variability over the North Pacific. *Prog. Oceanogr.*  
42 47, 381–408. [https://doi.org/10.1016/S0079-6611\(00\)00042-2](https://doi.org/10.1016/S0079-6611(00)00042-2)
- 43 Minobe, S., 1999. Resonance in bidecadal and pentadecadal climate oscillations over the North Pacific: Role in  
44 climatic regime shifts. *Geophys. Res. Lett.* 26, 855–858. <https://doi.org/10.1029/1999GL900119>
- 45 Misios, S., Mitchell, D.M., Gray, L.J., Tourpali, K., Matthes, K., Hood, L., Schmidt, H., Chiodo, G., Thiéblemont, R.,  
46 Rozanov, E., Krivolutsky, A., 2016. Solar signals in CMIP-5 simulations: effects of atmosphere–ocean  
47 coupling. *Q. J. R. Meteorol. Soc.* 142, 928–941. <https://doi.org/10.1002/qj.2695>
- 48 Mitchell, J.M., 1976. An overview of climatic variability and its causal mechanisms. *Quat. Res.* 6, 481–493.  
49 [https://doi.org/10.1016/0033-5894\(76\)90021-1](https://doi.org/10.1016/0033-5894(76)90021-1)
- 50 Miyake, F., Nagaya, K., Masuda, K., Nakamura, T., 2012. A signature of cosmic-ray increase in ad 774–775 from tree  
51 rings in Japan. *Nature* 486, 240–242. <https://doi.org/10.1038/nature11123>
- 52 Mjell, T.L., Ninnemann, U.S., Eldevik, T., Kleiven, H.K.F., 2015. Holocene multidecadal- to millennial-scale variations  
53 in Iceland-Scotland overflow and their relationship to climate. *Paleoceanography* 30, 558–569.  
54 <https://doi.org/10.1002/2014PA002737>
- 55 Mjell, T.L., Ninnemann, U.S., Kleiven, H.F., Hall, I.R., 2016. Multidecadal changes in Iceland Scotland Overflow  
56 Water vigor over the last 600 years and its relationship to climate. *Geophys. Res. Lett.* 43, 2111–2117.  
57 <https://doi.org/10.1002/2016GL068227>
- 58  
59  
60  
61  
62  
63  
64  
65

- 1  
2  
3  
4 Moffa-Sánchez, P., Born, A., Hall, I.R., Thornalley, D.J.R., Barker, S., 2014. Solar forcing of North Atlantic surface  
5 temperature and salinity over the past millennium. *Nat. Geosci.* 7, 275–278. <https://doi.org/10.1038/ngeo2094>  
6  
7 Moffa-Sánchez, P., Hall, I.R., Thornalley, D.J.R., Barker, S., Stewart, C., 2015. Changes in the strength of the Nordic  
8 Seas Overflows over the past 3000 years. *Quat. Sci. Rev.* 123, 134–143.  
9 <https://doi.org/10.1016/j.quascirev.2015.06.007>  
10  
11 Moore, G.W.K., Pickart, R.S., Renfrew, I.A., 2011. Complexities in the climate of the subpolar North Atlantic: a case  
12 study from the winter of 2007. *Q. J. R. Meteorol. Soc.* 137, 757–767. <https://doi.org/10.1002/qj.778>  
13  
14 Moore, G.W.K., Renfrew, I.A., Pickart, R.S., 2013. Multidecadal Mobility of the North Atlantic Oscillation. *J. Clim.* 26,  
15 2453–2466. <https://doi.org/10.1175/JCLI-D-12-00023.1>  
16  
17 Moreno, P.I., Vilanova, I., Villa-Martínez, R., Dunbar, R.B., Mucciarone, D.A., Kaplan, M.R., Garreaud, R.D., Rojas,  
18 M., Moy, C.M., Pol-Holz, R.D., Lambert, F., 2018. Onset and Evolution of Southern Annular Mode-Like  
19 Changes at Centennial Timescale. *Sci. Rep.* 8, 1–9. <https://doi.org/10.1038/s41598-018-21836-6>  
20  
21 Moreno, P.I., Vilanova, I., Villa-Martínez, R., Garreaud, R.D., Rojas, M., Pol-Holz, R.D., 2014. Southern Annular  
22 Mode-like changes in southwestern Patagonia at centennial timescales over the last three millennia. *Nat.*  
23 *Commun.* 5, 1–7. <https://doi.org/10.1038/ncomms5375>  
24  
25 Moreno-Chamarro, E., Zanchettin, D., Lohmann, K., Jungclaus, J.H., 2017a. An abrupt weakening of the subpolar  
26 gyre as trigger of Little Ice Age-type episodes. *Clim. Dyn.* 48, 727–744. <https://doi.org/10.1007/s00382-016-3106-7>  
27  
28 Moreno-Chamarro, E., Zanchettin, D., Lohmann, K., Luterbacher, J., Jungclaus, J.H., 2017b. Winter amplification of  
29 the European Little Ice Age cooling by the subpolar gyre. *Sci. Rep.* 7, 1–8. <https://doi.org/10.1038/s41598-017-07969-0>  
30  
31 Moy, C.M., Seltzer, G.O., Rodbell, D.T., Anderson, D.M., 2002. Variability of El Niño/Southern Oscillation activity at  
32 millennial timescales during the Holocene epoch. *Nature* 420, 162–165. <https://doi.org/10.1038/nature01194>  
33  
34 Muscheler, R., Adolphi, F., Knudsen, M.F., 2014. Assessing the differences between the IntCal and Greenland ice-  
35 core time scales for the last 14,000 years via the common cosmogenic radionuclide variations. *Quat. Sci.*  
36 *Rev., Dating, Synthesis, and Interpretation of Palaeoclimatic Records and Model-data Integration: Advances*  
37 *of the INTIMATE project (INTEgration of Ice core, Marine and TErrestrial records, COST Action ES0907)* 106,  
38 81–87. <https://doi.org/10.1016/j.quascirev.2014.08.017>  
39  
40 Muscheler, R., Beer, J., Vonmoos, M., 2004. Causes and timing of the 8200yr BP event inferred from the comparison  
41 of the GRIP 10Be and the tree ring  $\Delta^{14}C$  record. *Quat. Sci. Rev., Holocene climate variability - a marine*  
42 *perspective* 23, 2101–2111. <https://doi.org/10.1016/j.quascirev.2004.08.007>  
43  
44 Muschitiello, F., Zhang, Q., Sundqvist, H.S., Davies, F.J., Renssen, H., 2015. Arctic climate response to the  
45 termination of the African Humid Period. *Quat. Sci. Rev.* 125, 91–97.  
46 <https://doi.org/10.1016/j.quascirev.2015.08.012>  
47  
48 Nakamura, N., Kayanne, H., Iijima, H., McClanahan, T.R., Behera, S.K., Yamagata, T., 2009. Mode shift in the Indian  
49 Ocean climate under global warming stress. *Geophys. Res. Lett.* 36. <https://doi.org/10.1029/2009GL040590>  
50  
51 Neukom, R., Barboza, L.A., Erb, M.P., Shi, F., Emile-Geay, J., Evans, M.N., Franke, J., Kaufman, D.S., Lücke, L.,  
52 Rehfeld, K., Schurer, A., Zhu, F., Brönnimann, S., Hakim, G.J., Henley, B.J., Ljungqvist, F.C., McKay, N.,  
53 Valler, V., von Gunten, L., PAGES 2k Consortium, 2019. Consistent multidecadal variability in global  
54 temperature reconstructions and simulations over the Common Era. *Nat. Geosci.* 12, 643–649.  
55 <https://doi.org/10.1038/s41561-019-0400-0>  
56  
57 Newman, M., Alexander, M.A., Ault, T.R., Cobb, K.M., Deser, C., Di Lorenzo, E., Mantua, N.J., Miller, A.J., Minobe,  
58 S., Nakamura, H., Schneider, N., Vimont, D.J., Phillips, A.S., Scott, J.D., Smith, C.A., 2016. The Pacific  
59 decadal oscillation, revisited. *J. Clim.* 29, 4399–4427. <https://doi.org/10.1175/JCLI-D-15-0508.1>  
60  
61 Newman, M., Compo, G.P., Alexander, M.A., 2003. ENSO-Forced Variability of the Pacific Decadal Oscillation. *J.*  
62 *Clim.* 16, 3853–3857. [https://doi.org/10.1175/1520-0442\(2003\)016<3853:EVOTPD>2.0.CO;2](https://doi.org/10.1175/1520-0442(2003)016<3853:EVOTPD>2.0.CO;2)  
63  
64 Niedermeyer, E.M., Sessions, A.L., Feakins, S.J., Mohtadi, M., 2014. Hydroclimate of the western Indo-Pacific Warm  
65 Pool during the past 24,000 years. *Proc. Natl. Acad. Sci.* 111, 9402–9406.  
<https://doi.org/10.1073/pnas.1323585111>  
66  
67 Ojala, A.E.K., Launonen, I., Holmström, L., Tiljander, M., 2015. Effects of solar forcing and North Atlantic oscillation  
68 on the climate of continental Scandinavia during the Holocene. *Quat. Sci. Rev.* 112, 153–171.  
69 <https://doi.org/10.1016/j.quascirev.2015.01.021>  
70  
71 Ólafsdóttir, K.B., Geirsdóttir, Á., Miller, G.H., Larsen, D.J., 2013. Evolution of NAO and AMO strength and cyclicity  
72 derived from a 3-ka varve-thickness record from Iceland. *Quat. Sci. Rev.* 69, 142–154.  
73 <https://doi.org/10.1016/j.quascirev.2013.03.009>  
74  
75

- 1  
2  
3  
4 Oliva, M., Navarro, F., Hrbáček, F., Hernández, A., Nývlt, D., Pereira, P., Ruiz-Fernández, J., Trigo, R., 2017. Recent  
5 regional climate cooling on the Antarctic Peninsula and associated impacts on the cryosphere. *Sci. Total*  
6 *Environ.* 580, 210–223. <https://doi.org/10.1016/j.scitotenv.2016.12.030>
- 7 Olsen, J., Anderson, N.J., Knudsen, M.F., 2012. Variability of the North Atlantic Oscillation over the past 5,200 years.  
8 *Nat. Geosci.* 5, 808–812. <https://doi.org/10.1038/ngeo1589>
- 9 O'Reilly, C.H., Woollings, T., Zanna, L., 2017. The Dynamical Influence of the Atlantic Multidecadal Oscillation on  
10 Continental Climate. *J. Clim.* 30, 7213–7230. <https://doi.org/10.1175/JCLI-D-16-0345.1>
- 11 Ortega, P., Lehner, F., Swingedouw, D., Masson-Delmotte, V., Raible, C.C., Casado, M., Yiou, P., 2015. A model-  
12 tested North Atlantic Oscillation reconstruction for the past millennium. *Nature* 523, 71–74.  
13 <https://doi.org/10.1038/nature14518>
- 14 Ortega, P., Swingedouw, D., Masson-Delmotte, V., Risi, C., Vinther, B., Yiou, P., Vautard, R., Yoshimura, K., 2014.  
15 Characterizing atmospheric circulation signals in Greenland ice cores: insights from a weather regime  
16 approach. *Clim. Dyn.* 43, 2585–2605. <https://doi.org/10.1007/s00382-014-2074-z>
- 17 Osborn, T.J., 2004. Simulating the winter North Atlantic Oscillation: the roles of internal variability and greenhouse  
18 gas forcing. *Clim. Dyn.* 22, 605–623. <https://doi.org/10.1007/s00382-004-0405-1>
- 19 Osborn, T.J., Briffa, K.R., Tett, S.F.B., Jones, P.D., Trigo, R.M., 1999. Evaluation of the North Atlantic Oscillation as  
20 simulated by a coupled climate model. *Clim. Dyn.* 15, 685–702. <https://doi.org/10.1007/s003820050310>
- 21 Otterå, O.H., Bentsen, M., Drange, H., Suo, L., 2010. External forcing as a metronome for Atlantic multidecadal  
22 variability. *Nat. Geosci.* 3, 688–694. <https://doi.org/10.1038/ngeo955>
- 23 Otto-Bliesner, B.L., Brady, E.C., Fasullo, J., Jahn, A., Landrum, L., Stevenson, S., Rosenbloom, N., Mai, A., Strand,  
24 G., 2016. Climate Variability and Change since 850 CE: An Ensemble Approach with the Community Earth  
25 System Model. *Bull. Am. Meteorol. Soc.* 97, 735–754. <https://doi.org/10.1175/BAMS-D-14-00233.1>
- 26 PAGES2k Consortium, Emile-Geay, J., McKay, N.P., Kaufman, D.S., von Gunten, L., Wang, J., Anchukaitis, K.J.,  
27 Abram, N.J., Addison, J.A., Curran, M.A.J., Evans, M.N., Henley, B.J., Hao, Z., Martrat, B., McGregor, H.V.,  
28 Neukom, R., Pederson, G.T., Stenni, B., Thirumalai, K., Werner, J.P., Xu, C., Divine, D.V., Dixon, B.C.,  
29 Gergis, J., Mundo, I.A., Nakatsuka, T., Phipps, S.J., Routson, C.C., Steig, E.J., Tierney, J.E., Tyler, J.J., Allen,  
30 K.J., Bertler, N.A.N., Björklund, J., Chase, B.M., Chen, M.-T., Cook, E., de Jong, R., DeLong, K.L., Dixon,  
31 D.A., Ekaykin, A.A., Ersek, V., Filipsson, H.L., Francus, P., Freund, M.B., Frezzotti, M., Gaire, N.P., Gajewski,  
32 K., Ge, Q., Goosse, H., Gornostaeva, A., Grosjean, M., Horiuchi, K., Hormes, A., Husum, K., Isaksson, E.,  
33 Kandasamy, S., Kawamura, K., Kilbourne, K.H., Koç, N., Leduc, G., Linderholm, H.W., Lorrey, A.M.,  
34 Mikhalenko, V., Mortyn, P.G., Motoyama, H., Moy, A.D., Mulvaney, R., Munz, P.M., Nash, D.J., Oerter, H.,  
35 Opel, T., Orsi, A.J., Ovchinnikov, D.V., Porter, T.J., Roop, H.A., Saenger, C., Sano, M., Sauchyn, D.,  
36 Saunders, K.M., Seidenkrantz, M.-S., Severi, M., Shao, X., Sicre, M.-A., Sigl, M., Sinclair, K., George, S.S.,  
37 Jacques, J.-M.S., Thamban, M., Kuwar Thapa, U., Thomas, E.R., Turney, C., Uemura, R., Viau, A.E.,  
38 Vladimirova, D.O., Wahl, E.R., White, J.W.C., Yu, Z., Zinke, J., 2017. A global multiproxy database for  
39 temperature reconstructions of the Common Era. *Sci. Data* 4, 170088. <https://doi.org/10.1038/sdata.2017.88>
- 40 Park, H.-S., Kim, S.-J., Seo, K.-H., Stewart, A.L., Kim, S.-Y., Son, S.-W., 2018. The impact of Arctic sea ice loss on  
41 mid-Holocene climate. *Nat. Commun.* 9, 1–9. <https://doi.org/10.1038/s41467-018-07068-2>
- 42 Parker, D., Folland, C., Scaife, A., Knight, J., Colman, A., Baines, P., Dong, B., 2007. Decadal to multidecadal  
43 variability and the climate change background. *J. Geophys. Res. Atmospheres* 112.  
44 <https://doi.org/10.1029/2007JD008411>
- 45 Parker, D.E., Legg, T.P., Folland, C.K., 1992. A new daily central England temperature series, 1772–1991. *Int. J.*  
46 *Climatol.* 12, 317–342. <https://doi.org/10.1002/joc.3370120402>
- 47 Parnell, A., Sweeney, J., Doan, T., 2016. *Bclim: Bayesian Palaeoclimate Reconstruction from Pollen Data.*
- 48 Parnell, A.C., Haslett, J., Sweeney, J., Doan, T.K., Allen, J.R.M., Huntley, B., 2016. Joint palaeoclimate  
49 reconstruction from pollen data via forward models and climate histories. *Quat. Sci. Rev.* 151, 111–126.  
50 <https://doi.org/10.1016/j.quascirev.2016.09.007>
- 51 Parnell, A.C., Sweeney, J., Doan, T.K., Salter-Townshend, M., Allen, J.R.M., Huntley, B., Haslett, J., 2015. Bayesian  
52 inference for palaeoclimate with time uncertainty and stochastic volatility. *J. R. Stat. Soc. Ser. C Appl. Stat.* 64,  
53 115–138. <https://doi.org/10.1111/rssc.12065>
- 54 Pausata, F.S.R., Chafik, L., Caballero, R., Battisti, D.S., 2015. Impacts of high-latitude volcanic eruptions on ENSO  
55 and AMOC. *Proc. Natl. Acad. Sci.* 112, 13784–13788. <https://doi.org/10.1073/pnas.1509153112>
- 56 Pearson, G.W., 1986. Precise Calendrical Dating of Known Growth-Period Samples Using a 'Curve Fitting'  
57 Technique. *Radiocarbon* 28, 292–299. <https://doi.org/10.1017/S0033822200007396>
- 58  
59  
60  
61  
62  
63  
64  
65



- 1  
2  
3 Peng, Y., Shen, C., Cheng, H., Xu, Y., 2015. Simulation of the Interdecadal Pacific Oscillation and its impacts on the  
4 climate over eastern China during the last millennium. *J. Geophys. Res. Atmospheres* 120, 7573–7585.  
5 <https://doi.org/10.1002/2015JD023104>  
6  
7 Philander, G., 1989. *El Niño, La Niña, and the Southern Oscillation*, International Geophysics Series. Academic  
8 Press, San Diego.  
9  
10 Phillips, A.S., Deser, C., Fasullo, J., 2014. Evaluating Modes of Variability in Climate Models. *Eos Trans. Am.*  
11 *Geophys. Union* 95, 453–455. <https://doi.org/10.1002/2014EO490002>  
12  
13 Pinto, J.G., Raible, C.C., 2012. Past and recent changes in the North Atlantic oscillation. *Wiley Interdiscip. Rev. Clim.*  
14 *Change* 3, 79–90. <https://doi.org/10.1002/wcc.150>  
15  
16 Plunkett, G., Swindles, G.T., 2008. Determining the Sun's influence on Lateglacial and Holocene climates: a focus on  
17 climate response to centennial-scale solar forcing at 2800cal.BP. *Quat. Sci. Rev., INTEgration of Ice-core,*  
18 *Marine and Terrestrial records (INTIMATE): Refining the record of the Last Glacial-Interglacial Transition* 27,  
19 175–184. <https://doi.org/10.1016/j.quascirev.2007.01.015>  
20  
21 Portis, D.H., Walsh, J.E., El Hamly, M., Lamb, P.J., 2001. Seasonality of the North Atlantic Oscillation. *J. Clim.* 14,  
22 2069–2078. [https://doi.org/10.1175/1520-0442\(2001\)014<2069:SOTNAO>2.0.CO;2](https://doi.org/10.1175/1520-0442(2001)014<2069:SOTNAO>2.0.CO;2)  
23  
24 Power, S., Casey, T., Folland, C., Colman, A., Mehta, V., 1999. Inter-decadal modulation of the impact of ENSO on  
25 Australia. *Clim. Dyn.* 15, 319–324. <https://doi.org/10.1007/s003820050284>  
26  
27 Power, S., Delage, F., Chung, C., Kociuba, G., Keay, K., 2013. Robust twenty-first-century projections of El Niño and  
28 related precipitation variability. *Nature* 502, 541–545. <https://doi.org/10.1038/nature12580>  
29  
30 Prohom, M., Barriendos, M., Sanchez-Lorenzo, A., 2016. Reconstruction and homogenization of the longest  
31 instrumental precipitation series in the Iberian Peninsula (Barcelona, 1786–2014). *Int. J. Climatol.* 36, 3072–  
32 3087. <https://doi.org/10.1002/joc.4537>  
33  
34 Raible, C.C., Lehner, F., González-Rouco, J.F., Fernández-Donado, L., 2014. Changing correlation structures of the  
35 Northern Hemisphere atmospheric circulation from 1000 to 2100 AD. *Clim. Past* 10, 537–550.  
36 <https://doi.org/10.5194/cp-10-537-2014>  
37  
38 Rasmussen, S.O., Andersen, K.K., Svensson, A.M., Steffensen, J.P., Vinther, B.M., Clausen, H.B., Siggaard-  
39 Andersen, M.-L., Johnsen, S.J., Larsen, L.B., Dahl-Jensen, D., Bigler, M., Röthlisberger, R., Fischer, H., Goto-  
40 Azuma, K., Hansson, M.E., Ruth, U., 2006. A new Greenland ice core chronology for the last glacial  
41 termination. *J. Geophys. Res. Atmospheres* 111. <https://doi.org/10.1029/2005JD006079>  
42  
43 Rasmusson, E.M., Wallace, J.M., 1983. Meteorological Aspects of the El Niño/Southern Oscillation. *Science* 222,  
44 1195–1202. <https://doi.org/10.1126/science.222.4629.1195>  
45  
46 Reimer, P., Austin, W.E.N., Bard, E., Bayliss, A., Blackwell, P.G., Bronk Ramsey, C., Butzin, M., Cheng, H., Edwards,  
47 R.L., Friedrich, M., Grootes, P.M., Guilderson, T.P., Hajdas, I., Heaton, T.J., Hogg, A.G., 2020. The IntCal20  
48 Northern Hemisphere radiocarbon age calibration curve (0-55 kcal BP). *Radiocarbon*.  
49  
50 Reimer, P.J., Bard, E., Bayliss, A., Beck, J.W., Blackwell, P.G., Ramsey, C.B., Buck, C.E., Cheng, H., Edwards, R.L.,  
51 Friedrich, M., Grootes, P.M., Guilderson, T.P., Hafliðason, H., Hajdas, I., Hatté, C., Heaton, T.J., Hoffmann,  
52 D.L., Hogg, A.G., Hughen, K.A., Kaiser, K.F., Kromer, B., Manning, S.W., Niu, M., Reimer, R.W., Richards,  
53 D.A., Scott, E.M., Southon, J.R., Staff, R.A., Turney, C.S.M., Plicht, J. van der, 2013. IntCal13 and Marine13  
54 Radiocarbon Age Calibration Curves 0–50,000 Years cal BP. *Radiocarbon* 55, 1869–1887.  
55  
56 Reimer, P.J., Reimer, R.W., 2001. A Marine Reservoir Correction Database and On-Line Interface. *Radiocarbon* 43,  
57 461–463. <https://doi.org/10.1017/S003822200038339>  
58  
59 Renssen, H., Goosse, H., Fichefet, T., Brovkin, V., Driesschaert, E., Wolk, F., 2005. Simulating the Holocene climate  
60 evolution at northern high latitudes using a coupled atmosphere-sea ice-ocean-vegetation model. *Clim. Dyn.*  
61 24, 23–43. <https://doi.org/10.1007/s00382-004-0485-y>  
62  
63 Reynhout, S.A., Sagredo, E.A., Kaplan, M.R., Aravena, J.C., Martini, M.A., Moreno, P.I., Rojas, M., Schwartz, R.,  
64 Schaefer, J.M., 2019. Holocene glacier fluctuations in Patagonia are modulated by summer insolation intensity  
65 and paced by Southern Annular Mode-like variability. *Quat. Sci. Rev.* 220, 178–187.  
<https://doi.org/10.1016/j.quascirev.2019.05.029>  
66  
67 Robock, A., 2000. Volcanic eruptions and climate. *Rev. Geophys.* 38, 191–219.  
<https://doi.org/10.1029/1998RG000054>  
68  
69 Rodbell, D.T., Seltzer, G.O., Anderson, D.M., Abbott, M.B., Enfield, D.B., Newman, J.H., 1999. An ~15,000-Year  
70 Record of El Niño-Driven Alluviation in Southwestern Ecuador. *Science* 283, 516–520.  
<https://doi.org/10.1126/science.283.5401.516>

- 1  
2  
3 Rodriguez-Ramirez, A., Grove, C.A., Zinke, J., Pandolfi, J.M., Zhao, J., 2014. Coral Luminescence Identifies the  
4 Pacific Decadal Oscillation as a Primary Driver of River Runoff Variability Impacting the Southern Great  
5 Barrier Reef. *PLOS ONE* 9, e84305. <https://doi.org/10.1371/journal.pone.0084305>  
6  
7 Ropelewski, C.F., Halpert, M.S., 1989. Precipitation Patterns Associated with the High Index Phase of the Southern  
8 Oscillation. *J. Clim.* 2, 268–284. [https://doi.org/10.1175/1520-0442\(1989\)002<0268:PPAWTH>2.0.CO;2](https://doi.org/10.1175/1520-0442(1989)002<0268:PPAWTH>2.0.CO;2)  
9  
10 Ropelewski, C.F., Halpert, M.S., 1987. Global and Regional Scale Precipitation Patterns Associated with the El  
11 Niño/Southern Oscillation. *Mon. Weather Rev.* 115, 1606–1626. [https://doi.org/10.1175/1520-0493\(1987\)115<1606:GARSPP>2.0.CO;2](https://doi.org/10.1175/1520-0493(1987)115<1606:GARSPP>2.0.CO;2)  
12  
13 Roundy, P.E., 2014. On the Interpretation of EOF Analysis of ENSO, Atmospheric Kelvin Waves, and the MJO. *J.*  
14 *Clim.* 28, 1148–1165. <https://doi.org/10.1175/JCLI-D-14-00398.1>  
15  
16 Rowell, D.P., Folland, C.K., Maskell, K., Ward, M.N., 1995. Variability of summer rainfall over tropical north Africa  
17 (1906–92): Observations and modelling. *Q. J. R. Meteorol. Soc.* 121, 669–704.  
18 <https://doi.org/10.1002/qj.49712152311>  
19  
20 Rubino, M., Etheridge, D.M., Thornton, D.P., Howden, R., Allison, C.E., Francey, R.J., Langenfelds, R.L., Steele,  
21 L.P., Trudinger, C.M., Spencer, D.A., Curran, M.A.J., Ommen, T.D. van, Smith, A.M., 2019. Revised records  
22 of atmospheric trace gases CO<sub>2</sub>, CH<sub>4</sub>, N<sub>2</sub>O, and δ<sup>13</sup>C-CO<sub>2</sub> over the last 2000 years from Law Dome,  
23 Antarctica. *Earth Syst. Sci. Data* 11, 473–492. <https://doi.org/10.5194/essd-11-473-2019>  
24  
25 Ruddiman, W.F., Kutzbach, J.E., Vavrus, S.J., 2011. Can natural or anthropogenic explanations of late-Holocene  
26 CO<sub>2</sub> and CH<sub>4</sub> increases be falsified?: The Holocene. <https://doi.org/10.1177/0959683610387172>  
27  
28 Rustic, G.T., Koutavas, A., Marchitto, T.M., Linsley, B.K., 2015. Dynamical excitation of the tropical Pacific Ocean  
29 and ENSO variability by Little Ice Age cooling. *Science* 350, 1537–1541.  
30 <https://doi.org/10.1126/science.aac9937>  
31  
32 Saarni, S., Saarinen, T., Dulski, P., 2016. Between the North Atlantic Oscillation and the Siberian High: A 4000-year  
33 snow accumulation history inferred from varved lake sediments in Finland. *The Holocene* 26, 423–431.  
34 <https://doi.org/10.1177/0959683615609747>  
35  
36 Sánchez-López, G., 2016. North Atlantic Oscillation imprints in the Central Iberian Peninsula for the last two  
37 millennia: from ordination analyses to the Bayesian approach. University of Barcelona, Barcelona.  
38  
39 Sánchez-López, G., Hernández, A., Pla-Rabes, S., Trigo, R.M., Toro, M., Granados, I., Sáez, A., Masqué, P., Pueyo,  
40 J.J., Rubio-Inglés, M.J., Giralt, S., 2016. Climate reconstruction for the last two millennia in central Iberia: The  
41 role of East Atlantic (EA), North Atlantic Oscillation (NAO) and their interplay over the Iberian Peninsula. *Quat.*  
42 *Sci. Rev.* 149, 135–150. <https://doi.org/10.1016/j.quascirev.2016.07.021>  
43  
44 Saunders, K.M., Roberts, S.J., Perren, B., Butz, C., Sime, L., Davies, S., Nieuwenhuyze, W.V., Grosjean, M.,  
45 Hodgson, D.A., 2018. Holocene dynamics of the Southern Hemisphere westerly winds and possible links to  
46 CO<sub>2</sub> outgassing. *Nat. Geosci.* 11, 650–655. <https://doi.org/10.1038/s41561-018-0186-5>  
47  
48 Scaife, A.A., Ineson, S., Knight, J.R., Gray, L., Kodera, K., Smith, D.M., 2013. A mechanism for lagged North Atlantic  
49 climate response to solar variability. *Geophys. Res. Lett.* 40, 434–439. <https://doi.org/10.1002/grl.50099>  
50  
51 Scaife, A.A., Knight, J.R., Vallis, G.K., Folland, C.K., 2005. A stratospheric influence on the winter NAO and North  
52 Atlantic surface climate. *Geophys. Res. Lett.* 32. <https://doi.org/10.1029/2005GL023226>  
53  
54 Scaife, A.A., Smith, D., 2018. A signal-to-noise paradox in climate science. *Npj Clim. Atmospheric Sci.* 1, 1–8.  
55 <https://doi.org/10.1038/s41612-018-0038-4>  
56  
57 Schlesinger, M.E., Ramankutty, N., 1994. An oscillation in the global climate system of period 65–70 years. *Nature*  
58 367, 723–726. <https://doi.org/10.1038/367723a0>  
59  
60 Schleussner, C.-F., Divine, D.V., Donges, J.F., Miettinen, A., Donner, R.V., 2015. Indications for a North Atlantic  
61 ocean circulation regime shift at the onset of the Little Ice Age. *Clim. Dyn.* 45, 3623–3633.  
62 <https://doi.org/10.1007/s00382-015-2561-x>  
63  
64 Schmutz, C., Luterbacher, J., Gyalistras, D., Xoplaki, E., Wanner, H., 2000. Can we trust proxy-based NAO index  
65 reconstructions? *Geophys. Res. Lett.* 27, 1135–1138. <https://doi.org/10.1029/1999GL011045>  
66  
67 Schneider, N., Cornuelle, B.D., 2005. The Forcing of the Pacific Decadal Oscillation. *J. Clim.* 18, 4355–4373.  
68 <https://doi.org/10.1175/JCLI3527.1>  
69  
70 Schurer, A.P., Hegerl, G.C., Mann, M.E., Tett, S.F.B., Phipps, S.J., 2013. Separating Forced from Chaotic Climate  
71 Variability over the Past Millennium. *J. Clim.* 26, 6954–6973. <https://doi.org/10.1175/JCLI-D-12-00826.1>  
72  
73 Sen Gupta, A., England, M.H., 2006. Coupled Ocean–Atmosphere–Ice Response to Variations in the Southern  
74 Annular Mode. *J. Clim.* 19, 4457–4486. <https://doi.org/10.1175/JCLI3843.1>  
75  
76 Seppälä, A., Cillverd, M.A., 2014. Energetic particle forcing of the Northern Hemisphere winter stratosphere:  
77 comparison to solar irradiance forcing. *Front. Phys.* 2. <https://doi.org/10.3389/fphy.2014.00025>

- 1  
2  
3  
4 Seppälä, A., Matthes, K., Randall, C.E., Mironova, I.A., 2014. What is the solar influence on climate? Overview of  
5 activities during CAWSES-II. *Prog. Earth Planet. Sci.* 1, 24. <https://doi.org/10.1186/s40645-014-0024-3>  
6  
7 Shaman, J., 2014. The Seasonal Effects of ENSO on European Precipitation: Observational Analysis. *J. Clim.* 27,  
8 6423–6438. <https://doi.org/10.1175/JCLI-D-14-00008.1>  
9  
10 Shen, C., Wang, W.-C., Gong, W., Hao, Z., 2006. A Pacific Decadal Oscillation record since 1470 AD reconstructed  
11 from proxy data of summer rainfall over eastern China. *Geophys. Res. Lett.* 33.  
12 <https://doi.org/10.1029/2005GL024804>  
13  
14 Shepherd, T.G., 2014. Atmospheric circulation as a source of uncertainty in climate change projections. *Nat. Geosci.*  
15 7, 703–708. <https://doi.org/10.1038/ngeo2253>  
16  
17 Sigl, M., Winstrup, M., McConnell, J.R., Welten, K.C., Plunkett, G., Ludlow, F., Büntgen, U., Caffee, M., Chellman, N.,  
18 Dahl-Jensen, D., Fischer, H., Kipfstuhl, S., Kostick, C., Maselli, O.J., Mekhaldi, F., Mulvaney, R., Muscheler,  
19 R., Pasteris, D.R., Pilcher, J.R., Salzer, M., Schüpbach, S., Steffensen, J.P., Vinther, B.M., Woodruff, T.E.,  
20 2015. Timing and climate forcing of volcanic eruptions for the past 2,500 years. *Nature* 523, 543–549.  
21 <https://doi.org/10.1038/nature14565>  
22  
23 Singh, H.K.A., Hakim, G.J., Tardif, R., Emile-Geay, J., Noone, D.C., 2018. Insights into Atlantic multidecadal  
24 variability using the Last Millennium Reanalysis framework. *Clim. Past* 14, 157–174.  
25 <https://doi.org/10.5194/cp-14-157-2018>  
26  
27 Sjolte, J., Hoffmann, G., Johnsen, S.J., 2014. Modelling the response of stable water isotopes in Greenland  
28 precipitation to orbital configurations of the previous interglacial. *Tellus B Chem. Phys. Meteorol.* 66, 22872.  
29 <https://doi.org/10.3402/tellusb.v66.22872>  
30  
31 Sjolte, J., Sturm, C., Adolphi, F., Vinther, B.M., Werner, M., Lohmann, G., Muscheler, R., 2018. Solar and volcanic  
32 forcing of North Atlantic climate inferred from a process-based reconstruction. *Clim. Past* 14, 1179–1194.  
33 <https://doi.org/10.5194/cp-14-1179-2018>  
34  
35 Slivinski, L.C., Compo, G.P., Whitaker, J.S., Sardeshmukh, P.D., Giese, B.S., McColl, C., Allan, R., Yin, X., Vose, R.,  
36 Titchner, H., Kennedy, J., Spencer, L.J., Ashcroft, L., Brönnimann, S., Brunet, M., Camuffo, D., Cornes, R.,  
37 Cram, T.A., Crouthamel, R., Domínguez-Castro, F., Freeman, J.E., Gergis, J., Hawkins, E., Jones, P.D.,  
38 Jourdain, S., Kaplan, A., Kubota, H., Blancq, F.L., Lee, T.-C., Lorrey, A., Luterbacher, J., Maugeri, M., Mock,  
39 C.J., Moore, G.W.K., Przybylak, R., Pudmenzky, C., Reason, C., Slonosky, V.C., Smith, C.A., Tinz, B., Trewin,  
40 B., Valente, M.A., Wang, X.L., Wilkinson, C., Wood, K., Wyszyński, P., 2019. Towards a more reliable  
41 historical reanalysis: Improvements for version 3 of the Twentieth Century Reanalysis system. *Q. J. R.*  
42 *Meteorol. Soc.* n/a. <https://doi.org/10.1002/qj.3598>  
43  
44 Smerdon, J.E., 2012. Climate models as a test bed for climate reconstruction methods: pseudoproxy experiments.  
45 *WIREs Clim. Change* 3, 63–77. <https://doi.org/10.1002/wcc.149>  
46  
47 Smith, A.C., Wynn, P.M., Barker, P.A., Leng, M.J., Noble, S.R., Tych, W., 2016. North Atlantic forcing of moisture  
48 delivery to Europe throughout the Holocene. *Sci. Rep.* 6, 24745. <https://doi.org/10.1038/srep24745>  
49  
50 Smith, D.M., Booth, B.B.B., Dunstone, N.J., Eade, R., Hermanson, L., Jones, G.S., Scaife, A.A., Sheen, K.L.,  
51 Thompson, V., 2016. Role of volcanic and anthropogenic aerosols in the recent global surface warming  
52 slowdown. *Nat. Clim. Change* 6, 936–940. <https://doi.org/10.1038/nclimate3058>  
53  
54 Smith, D.M., Eade, R., Scaife, A.A., Caron, L.-P., Danabasoglu, G., DelSole, T.M., Delworth, T., Doblas-Reyes, F.J.,  
55 Dunstone, N.J., Hermanson, L., Kharin, V., Kimoto, M., Merryfield, W.J., Mochizuki, T., Müller, W.A.,  
56 Pohlmann, H., Yeager, S., Yang, X., 2019. Robust skill of decadal climate predictions. *Npj Clim. Atmospheric*  
57 *Sci.* 2, 1–10. <https://doi.org/10.1038/s41612-019-0071-y>  
58  
59 Snowball, I., Muscheler, R., Zillén, L., Sandgren, P., Stanton, T., Ljung, K., 2010. Radiocarbon wiggle matching of  
60 Swedish lake varves reveals asynchronous climate changes around the 8.2 kyr cold event. *Boreas* 39, 720–  
61 733. <https://doi.org/10.1111/j.1502-3885.2010.00167.x>  
62  
63 Spahni, R., Chappellaz, J., Stocker, T.F., Loulergue, L., Hausammann, G., Kawamura, K., Flückiger, J., Schwander,  
64 J., Raynaud, D., Masson-Delmotte, V., Jouzel, J., 2005. Atmospheric Methane and Nitrous Oxide of the Late  
65 Pleistocene from Antarctic Ice Cores. *Science* 310, 1317–1321. <https://doi.org/10.1126/science.1120132>  
66  
67 Stahle, D.W., D'Arrigo, R.D., Krusic, P.J., Cleaveland, M.K., Cook, E.R., Allan, R.J., Cole, J.E., Dunbar, R.B.,  
68 Therrell, M.D., Gay, D.A., Moore, M.D., Stokes, M.A., Burns, B.T., Villanueva-Diaz, J., Thompson, L.G., 1998.  
69 Experimental Dendroclimatic Reconstruction of the Southern Oscillation. *Bull. Am. Meteorol. Soc.* 79, 2137–  
70 2152. [https://doi.org/10.1175/1520-0477\(1998\)079<2137:EDROTS>2.0.CO;2](https://doi.org/10.1175/1520-0477(1998)079<2137:EDROTS>2.0.CO;2)  
71  
72 Stansell, N.D., Steinman, B.A., Abbott, M.B., Rubinov, M., Roman-Lacayo, M., 2013. Lacustrine stable isotope record  
73 of precipitation changes in Nicaragua during the Little Ice Age and Medieval Climate Anomaly. *Geology* 41,  
74 151–154. <https://doi.org/10.1130/G33736.1>  
75

- 1  
2  
3 Steiger, N.J., Steig, E.J., Dee, S.G., Roe, G.H., Hakim, G.J., 2017. Climate reconstruction using data assimilation of  
4 water isotope ratios from ice cores. *J. Geophys. Res. Atmospheres* 122, 1545–1568.  
5 <https://doi.org/10.1002/2016JD026011>  
6  
7 Steinhilber, F., Beer, J., Fröhlich, C., 2009. Total solar irradiance during the Holocene. *Geophys. Res. Lett.* 36.  
8 <https://doi.org/10.1029/2009GL040142>  
9  
10 Stephenson, D., Pavan, V., participating CMIP1 modelling groups, 2003. The North Atlantic Oscillation in coupled  
11 climate models: a CMIP1 evaluation. *Clim. Dyn.* 20, 381–399. <https://doi.org/10.1007/s00382-002-0281-5>  
12  
13 Stephenson, D.B., Hannachi, A., O'Neill, A., 2004. On the existence of multiple climate regimes. *Q. J. R. Meteorol.*  
14 *Soc.* 130, 583–605. <https://doi.org/10.1256/qj.02.146>  
15  
16 Stevenson, S., Fasullo, J.T., Otto-Bliesner, B.L., Tomas, R.A., Gao, C., 2017. Role of eruption season in reconciling  
17 model and proxy responses to tropical volcanism. *Proc. Natl. Acad. Sci.* 114, 1822–1826.  
18 <https://doi.org/10.1073/pnas.1612505114>  
19  
20 Stocker, T. (Ed.), 2014. *Climate change 2013: the physical science basis: Working Group I contribution to the Fifth*  
21 *assessment report of the Intergovernmental Panel on Climate Change.* Cambridge University Press, New  
22 York.  
23  
24 Stoffel, M., Khodri, M., Corona, C., Guillet, S., Poulain, V., Bekki, S., Guiot, J., Luckman, B.H., Oppenheimer, C.,  
25 Lebas, N., Beniston, M., Masson-Delmotte, V., 2015. Estimates of volcanic-induced cooling in the Northern  
26 Hemisphere over the past 1,500 years. *Nat. Geosci.* 8, 784–788. <https://doi.org/10.1038/ngeo2526>  
27  
28 Stone, J.R., Fritz, S.C., 2006. Multidecadal drought and Holocene climate instability in the Rocky Mountains. *Geology*  
29 34, 409–412. <https://doi.org/10.1130/G22225.1>  
30  
31 Stuiver, M., Braziunas, T.F., 1993. Modeling Atmospheric <sup>14</sup>C Influences and <sup>14</sup>C Ages of Marine Samples to 10,000  
32 BC. *Radiocarbon* 35, 137–189. <https://doi.org/10.1017/S0033822200013874>  
33  
34 Stuiver, M., Pearson, G.W., Braziunas, T., 1986. Radiocarbon Age Calibration of Marine Samples Back to 9000 Cal  
35 Yr BP. *Radiocarbon* 28, 980–1021. <https://doi.org/10.1017/S0033822200060264>  
36  
37 Sutton, R.T., Hodson, D.L.R., 2005. Atlantic Ocean Forcing of North American and European Summer Climate.  
38 *Science* 309, 115–118. <https://doi.org/10.1126/science.1109496>  
39  
40 Svalgaard, L., Schatten, K.H., 2016. Reconstruction of the Sunspot Group Number: The Backbone Method. *Sol.*  
41 *Phys.* 291, 2653–2684. <https://doi.org/10.1007/s11207-015-0815-8>  
42  
43 Svendsen, L., Hetzinger, S., Keenlyside, N., Gao, Y., 2014. Marine-based multiproxy reconstruction of Atlantic  
44 multidecadal variability. *Geophys. Res. Lett.* 41, 1295–1300. <https://doi.org/10.1002/2013GL059076>  
45  
46 Svensmark, H., Bondo, T., Svensmark, J., 2009. Cosmic ray decreases affect atmospheric aerosols and clouds.  
47 *Geophys. Res. Lett.* 36. <https://doi.org/10.1029/2009GL038429>  
48  
49 Sweeney, J., Salter-Townshend, M., Edwards, T., Buck, C.E., Parnell, A.C., 2018. Statistical challenges in estimating  
50 past climate changes. *Wiley Interdiscip. Rev. Comput. Stat.* 10, e1437. <https://doi.org/10.1002/wics.1437>  
51  
52 Swingedouw, D., Colin, C., Eynaud, F., Ayache, M., Zaragosi, S., 2019. Impact of freshwater release in the  
53 Mediterranean Sea on the North Atlantic climate. *Clim. Dyn.* 53, 3893–3915. <https://doi.org/10.1007/s00382-019-04758-5>  
54  
55 Swingedouw, D., Mignot, J., Ortega, P., Khodri, M., Menegoz, M., Cassou, C., Hanquiez, V., 2017. Impact of  
56 explosive volcanic eruptions on the main climate variability modes. *Glob. Planet. Change* 150, 24–45.  
57 <https://doi.org/10.1016/j.gloplacha.2017.01.006>  
58  
59 Swingedouw, D., Ortega, P., Mignot, J., Guilyardi, E., Masson-Delmotte, V., Butler, P.G., Khodri, M., Séférian, R.,  
60 2015. Bidecadal North Atlantic ocean circulation variability controlled by timing of volcanic eruptions. *Nat.*  
61 *Commun.* 6, 1–12. <https://doi.org/10.1038/ncomms7545>  
62  
63 Swingedouw, D., Terray, L., Cassou, C., Voldoire, A., Salas-Méla, D., Servonnat, J., 2011. Natural forcing of climate  
64 during the last millennium: fingerprint of solar variability. *Clim. Dyn.* 36, 1349–1364.  
65 <https://doi.org/10.1007/s00382-010-0803-5>  
66  
67 Tardif, R., Hakim, G.J., Perkins, W.A., Horlick, K.A., Erb, M.P., Emile-Geay, J., Anderson, D.M., Steig, E.J., Noone,  
68 D., 2019. Last Millennium Reanalysis with an expanded proxy database and seasonal proxy modeling. *Clim.*  
69 *Past* 15, 1251–1273. <https://doi.org/10.5194/cp-15-1251-2019>  
70  
71 Terray, L., 2012. Evidence for multiple drivers of North Atlantic multi-decadal climate variability. *Geophys. Res. Lett.*  
72 39. <https://doi.org/10.1029/2012GL053046>  
73  
74 Thiéblemont, R., Matthes, K., Omrani, N.-E., Kodera, K., Hansen, F., 2015. Solar forcing synchronizes decadal North  
75 Atlantic climate variability. *Nat. Commun.* 6, 8268. <https://doi.org/10.1038/ncomms9268>  
76  
77 Thompson, D.W.J., Solomon, S., 2002. Interpretation of Recent Southern Hemisphere Climate Change. *Science* 296,  
78 895–899. <https://doi.org/10.1126/science.1069270>  
79  
80  
81  
82  
83  
84  
85

- 1  
2  
3 Thompson, D.W.J., Solomon, S., Kushner, P.J., England, M.H., Grise, K.M., Karoly, D.J., 2011. Signatures of the  
4 Antarctic ozone hole in Southern Hemisphere surface climate change. *Nat. Geosci.* 4, 741–749.  
5 <https://doi.org/10.1038/ngeo1296>  
6  
7 Thompson, D.W.J., Wallace, J.M., 2001. Regional Climate Impacts of the Northern Hemisphere Annular Mode.  
8 *Science* 293, 85–89. <https://doi.org/10.1126/science.1058958>  
9  
10 Thompson, D.W.J., Wallace, J.M., 2000. Annular Modes in the Extratropical Circulation. Part I: Month-to-Month  
11 Variability. *J. Clim.* 13, 1000–1016. [https://doi.org/10.1175/1520-0442\(2000\)013<1000:AMITEC>2.0.CO;2](https://doi.org/10.1175/1520-0442(2000)013<1000:AMITEC>2.0.CO;2)  
12  
13 Thompson, V., Dunstone, N.J., Scaife, A.A., Smith, D.M., Slingo, J.M., Brown, S., Belcher, S.E., 2017. High risk of  
14 unprecedented UK rainfall in the current climate. *Nat. Commun.* 8, 1–6. [https://doi.org/10.1038/s41467-017-](https://doi.org/10.1038/s41467-017-00275-3)  
15 [00275-3](https://doi.org/10.1038/s41467-017-00275-3)  
16  
17 Thornalley, D.J.R., Blaschek, M., Davies, F.J., Praetorius, S., Oppo, D.W., McManus, J.F., Hall, I.R., Kleiven, H.,  
18 Renssen, H., McCave, I.N., 2013. Long-term variations in Iceland–Scotland overflow strength during the  
19 Holocene. *Clim. Past* 9, 2073–2084. <https://doi.org/10.5194/cp-9-2073-2013>  
20  
21 Timm, O., Ruprecht, E., Kleppek, S., 2004. Scale-Dependent Reconstruction of the NAO Index. *J. Clim.* 17, 2157–  
22 2169. [https://doi.org/10.1175/1520-0442\(2004\)017<2157:SROTNI>2.0.CO;2](https://doi.org/10.1175/1520-0442(2004)017<2157:SROTNI>2.0.CO;2)  
23  
24 Tingley, M.P., Huybers, P., 2009. A Bayesian Algorithm for Reconstructing Climate Anomalies in Space and Time.  
25 Part I: Development and Applications to Paleoclimate Reconstruction Problems. *J. Clim.* 23, 2759–2781.  
26 <https://doi.org/10.1175/2009JCLI3015.1>  
27  
28 Toohey, M., Krüger, K., Bittner, M., Timmreck, C., Schmidt, H., 2014. The impact of volcanic aerosol on the Northern  
29 Hemisphere stratospheric polar vortex: mechanisms and sensitivity to forcing structure. *Atmospheric Chem.*  
30 *Phys.* 14, 13063–13079. <https://doi.org/10.5194/acp-14-13063-2014>  
31  
32 Toohey, M., Sigl, M., 2017. Volcanic stratospheric sulfur injections and aerosol optical depth from 500 BCE to 1900  
33 CE. *Earth Syst. Sci. Data* 9, 809–831. <https://doi.org/10.5194/essd-9-809-2017>  
34  
35 Tourpali, K., Schuurmans, C.J.E., Dorland, R. van, Steil, B., Brühl, C., Manzini, E., 2005. Solar cycle modulation of  
36 the Arctic Oscillation in a chemistry-climate model. *Geophys. Res. Lett.* 32.  
37 <https://doi.org/10.1029/2005GL023509>  
38  
39 Trenberth, K.E., Dai, A., van der Schrier, G., Jones, P.D., Barichivich, J., Briffa, K.R., Sheffield, J., 2014. Global  
40 warming and changes in drought. *Nat. Clim. Change* 4, 17–22. <https://doi.org/10.1038/nclimate2067>  
41  
42 Trenberth, K.E., Shea, D.J., 2006. Atlantic hurricanes and natural variability in 2005. *Geophys. Res. Lett.* 33.  
43 <https://doi.org/10.1029/2006GL026894>  
44  
45 Trigo, R.M., Valente, M.A., Trigo, I.F., Miranda, P.M.A., Ramos, A.M., Paredes, D., García-Herrera, R., 2008. The  
46 Impact of North Atlantic Wind and Cyclone Trends on European Precipitation and Significant Wave Height in  
47 the Atlantic. *Ann. N. Y. Acad. Sci.* 1146, 212–234. <https://doi.org/10.1196/annals.1446.014>  
48  
49 Trouet, V., Esper, J., Graham, N.E., Baker, A., Scourse, J.D., Frank, D.C., 2009. Persistent Positive North Atlantic  
50 Oscillation Mode Dominated the Medieval Climate Anomaly. *Science* 324, 78–80.  
51 <https://doi.org/10.1126/science.1166349>  
52  
53 Tudhope, A.W., Chilcott, C.P., McCulloch, M.T., Cook, E.R., Chappell, J., Ellam, R.M., Lea, D.W., Lough, J.M.,  
54 Shimmield, G.B., 2001. Variability in the El Niño–Southern Oscillation Through a Glacial–Interglacial Cycle.  
55 *Science* 291, 1511–1517. <https://doi.org/10.1126/science.1057969>  
56  
57 Turney, C.S.M., Wilmshurst, J.M., Jones, R.T., Wood, J.R., Palmer, J.G., Hogg, A.G., Fenwick, P., Crowley, S.F.,  
58 Privat, K., Thomas, Z., 2017. Reconstructing atmospheric circulation over southern New Zealand:  
59 Establishment of modern westerly airflow 5500 years ago and implications for Southern Hemisphere Holocene  
60 climate change. *Quat. Sci. Rev.* 159, 77–87. <https://doi.org/10.1016/j.quascirev.2016.12.017>  
61  
62 Ummenhofer, C.C., Biastoch, A., Böning, C.W., 2016. Multidecadal Indian Ocean Variability Linked to the Pacific and  
63 Implications for Preconditioning Indian Ocean Dipole Events. *J. Clim.* 30, 1739–1751.  
64 <https://doi.org/10.1175/JCLI-D-16-0200.1>  
65  
66 Urban, F.E., Cole, J.E., Overpeck, J.T., 2000. Influence of mean climate change on climate variability from a 155-year  
67 tropical Pacific coral record. *Nature* 407, 989–993. <https://doi.org/10.1038/35039597>  
68  
69 Vance, T.R., Roberts, J.L., Plummer, C.T., Kiem, A.S., van Ommen, T.D., 2015. Interdecadal Pacific variability and  
70 eastern Australian megadroughts over the last millennium. *Geophys. Res. Lett.* 42, 129–137.  
71 <https://doi.org/10.1002/2014GL062447>  
72  
73 Vázquez-Bedoya, L.F., Cohen, A.L., Oppo, D.W., Blanchon, P., 2012. Corals record persistent multidecadal SST  
74 variability in the Atlantic Warm Pool since 1775 AD. *Paleoceanography* 27.  
75 <https://doi.org/10.1029/2012PA002313>

- 1  
2  
3 Verdon, D.C., Franks, S.W., 2006. Long-term behaviour of ENSO: Interactions with the PDO over the past 400 years  
4 inferred from paleoclimate records. *Geophys. Res. Lett.* 33. <https://doi.org/10.1029/2005GL025052>
- 5  
6 Villalba, R., Lara, A., Masiokas, M.H., Urrutia, R., Luckman, B.H., Marshall, G.J., Mundo, I.A., Christie, D.A., Cook,  
7 E.R., Neukom, R., Allen, K., Fenwick, P., Boninsegna, J.A., Srur, A.M., Morales, M.S., Araneo, D., Palmer,  
8 J.G., Cuq, E., Aravena, J.C., Holz, A., LeQuesne, C., 2012. Unusual Southern Hemisphere tree growth  
9 patterns induced by changes in the Southern Annular Mode. *Nat. Geosci.* 5, 793–798.  
10 <https://doi.org/10.1038/ngeo1613>
- 11 Vinther, B.M., Andersen, K.K., Hansen, A.W., Schmith, T., Jones, P.D., 2003a. Improving the Gibraltar/Reykjavik  
12 NAO index. *Geophys. Res. Lett.* 30. <https://doi.org/10.1029/2003GL018220>
- 13 Vinther, B.M., Johnsen, S.J., Andersen, K.K., Clausen, H.B., Hansen, A.W., 2003b. NAO signal recorded in the stable  
14 isotopes of Greenland ice cores. *Geophys. Res. Lett.* 30. <https://doi.org/10.1029/2002GL016193>
- 15 Vinther, B.M., Jones, P.D., Briffa, K.R., Clausen, H.B., Andersen, K.K., Dahl-Jensen, D., Johnsen, S.J., 2010.  
16 Climatic signals in multiple highly resolved stable isotope records from Greenland. *Quat. Sci. Rev.* 29, 522–  
17 538. <https://doi.org/10.1016/j.quascirev.2009.11.002>
- 18 Visbeck, M., 2009. A Station-Based Southern Annular Mode Index from 1884 to 2005. *J. Clim.* 22, 940–950.  
19 <https://doi.org/10.1175/2008JCLI2260.1>
- 20 Voigt, I., Chiessi, C.M., Prange, M., Mulitza, S., Groeneveld, J., Varma, V., Henrich, R., 2015. Holocene shifts of the  
21 southern westerlies across the South Atlantic. *Paleoceanography* 30, 39–51.  
22 <https://doi.org/10.1002/2014PA002677>
- 23 Wang, B., Luo, X., Yang, Y.-M., Sun, W., Cane, M.A., Cai, W., Yeh, S.-W., Liu, J., 2019. Historical change of El Niño  
24 properties sheds light on future changes of extreme El Niño. *Proc. Natl. Acad. Sci.* 116, 22512–22517.  
25 <https://doi.org/10.1073/pnas.1911130116>
- 26 Wang, G., Hendon, H.H., Arblaster, J.M., Lim, E.-P., Abhik, S., van Rensch, P., 2019. Compounding tropical and  
27 stratospheric forcing of the record low Antarctic sea-ice in 2016. *Nat. Commun.* 10, 1–9.  
28 <https://doi.org/10.1038/s41467-018-07689-7>
- 29 Wang, J., Yang, B., Ljungqvist, F.C., Luterbacher, J., Osborn, T.J., Briffa, K.R., Zorita, E., 2017. Internal and external  
30 forcing of multidecadal Atlantic climate variability over the past 1,200 years. *Nat. Geosci.* 10, 512–517.  
31 <https://doi.org/10.1038/ngeo2962>
- 32 Wang, L., Chen, W., Huang, R., 2008. Interdecadal modulation of PDO on the impact of ENSO on the east Asian  
33 winter monsoon. *Geophys. Res. Lett.* 35. <https://doi.org/10.1029/2008GL035287>
- 34 Wang, Y., Cheng, H., Edwards, R.L., He, Y., Kong, X., An, Z., Wu, J., Kelly, M.J., Dykoski, C.A., Li, X., 2005. The  
35 Holocene Asian Monsoon: Links to Solar Changes and North Atlantic Climate. *Science* 308, 854–857.  
36 <https://doi.org/10.1126/science.1106296>
- 37 Wanner, H., Brönnimann, S., Casty, C., Gyalistras, D., Luterbacher, J., Schmutz, C.J., Stephenson, D.B., Xoplaki,  
38 E., 2001. North Atlantic Oscillation - Concepts and studies. *Surv. Geophys.* 22, 321–382.  
39 <https://doi.org/10.1023/A:1014217317898>
- 40 Wanner, H., Solomina, O., Grosjean, M., Ritz, S.P., Jetel, M., 2011. Structure and origin of Holocene cold events.  
41 *Quat. Sci. Rev.* 30, 3109–3123. <https://doi.org/10.1016/j.quascirev.2011.07.010>
- 42 Wassenburg, J.A., Dietrich, S., Fietzke, J., Fohlmeister, J., Jochum, K.P., Scholz, D., Richter, D.K., Sabaoui, A.,  
43 Spötl, C., Lohmann, G., Andreae, M.O., Immenhauser, A., 2016. Reorganization of the North Atlantic  
44 Oscillation during early Holocene deglaciation. *Nat. Geosci.* 9, 602–605. <https://doi.org/10.1038/ngeo2767>
- 45 Watanabe, T.K., Watanabe, T., Yamazaki, A., Pfeiffer, M., Claereboudt, M.R., 2019. Oman coral  $\delta^{18}\text{O}$  seawater  
46 record suggests that Western Indian Ocean upwelling uncouples from the Indian Ocean Dipole during the  
47 global-warming hiatus. *Sci. Rep.* 9, 1–9. <https://doi.org/10.1038/s41598-018-38429-y>
- 48 Wei, M., Qiao, F., Guo, Y., Deng, J., Song, Z., Shu, Q., Yang, X., 2019. Quantifying the importance of interannual,  
49 interdecadal and multidecadal climate natural variabilities in the modulation of global warming rates. *Clim.*  
50 *Dyn.* 53, 6715–6727. <https://doi.org/10.1007/s00382-019-04955-2>
- 51 White, S.M., Ravelo, A.C., Polissar, P.J., 2018. Dampened El Niño in the Early and Mid-Holocene Due To Insolation-  
52 Forced Warming/Deepening of the Thermocline. *Geophys. Res. Lett.* 45, 316–326.  
53 <https://doi.org/10.1002/2017GL075433>
- 54 Wilson, R., Cook, E., D'Arrigo, R., Riedwyl, N., Evans, M.N., Tudhope, A., Allan, R., 2010. Reconstructing ENSO: the  
55 influence of method, proxy data, climate forcing and teleconnections. *J. Quat. Sci.* 25, 62–78.  
56 <https://doi.org/10.1002/jqs.1297>
- 57 Wise, E.K., 2015. Tropical Pacific and Northern Hemisphere influences on the coherence of Pacific Decadal  
58 Oscillation reconstructions. *Int. J. Climatol.* 35, 154–160. <https://doi.org/10.1002/joc.3966>
- 59  
60  
61  
62  
63  
64  
65

- 1  
2  
3 Wittenberg, A.T., 2009. Are historical records sufficient to constrain ENSO simulations? *Geophys. Res. Lett.* 36.  
4 <https://doi.org/10.1029/2009GL038710>
- 5 Woollings, T., Blackburn, M., 2011. The North Atlantic Jet Stream under Climate Change and Its Relation to the NAO  
6 and EA Patterns. *J. Clim.* 25, 886–902. <https://doi.org/10.1175/JCLI-D-11-00087.1>
- 7 Wu, T., Hu, A., Gao, F., Zhang, J., Meehl, G.A., 2019. New insights into natural variability and anthropogenic forcing  
8 of global/regional climate evolution. *Npj Clim. Atmospheric Sci.* 2, 1–13. <https://doi.org/10.1038/s41612-019-0075-7>
- 9  
10 Wulf, S., Dräger, N., Ott, F., Serb, J., Appelt, O., Guðmundsdóttir, E., van den Bogaard, C., Słowiński, M.,  
11 Błaszkiwicz, M., Brauer, A., 2016. Holocene tephrostratigraphy of varved sediment records from Lakes Tiefer  
12 See (NE Germany) and Czechowskie (N Poland). *Quat. Sci. Rev.* 132, 1–14.  
13 <https://doi.org/10.1016/j.quascirev.2015.11.007>
- 14 Wulf, S., Ott, F., Słowiński, M., Noryśkiwicz, A.M., Dräger, N., Martin-Puertas, C., Czymzik, M., Neugebauer, I.,  
15 Dulski, P., Bourne, A.J., Błaszkiwicz, M., Brauer, A., 2013. Tracing the Laacher See Tephra in the varved  
16 sediment record of the Trzechowskie palaeolake in central Northern Poland. *Quat. Sci. Rev.* 76, 129–139.  
17 <https://doi.org/10.1016/j.quascirev.2013.07.010>
- 18 Xoplaki, E., González-Rouco, J.F., Luterbacher, J., Wanner, H., 2004. Wet season Mediterranean precipitation  
19 variability: influence of large-scale dynamics and trends. *Clim. Dyn.* 23, 63–78. <https://doi.org/10.1007/s00382-004-0422-0>
- 20 Xoplaki, E., Luterbacher, J., Paeth, H., Dietrich, D., Steiner, N., Grosjean, M., Wanner, H., 2005. European spring  
21 and autumn temperature variability and change of extremes over the last half millennium. *Geophys. Res. Lett.*  
22 32. <https://doi.org/10.1029/2005GL023424>
- 23 Xoplaki, E., Luterbacher, J., Wagner, S., Zorita, E., Fleitmann, D., Preiser-Kapeller, J., Sargent, A.M., White, S.,  
24 Toreti, A., Haldon, J.F., Mordechai, L., Bozkurt, D., Akçer-Ön, S., Izdebski, A., 2018. Modelling Climate and  
25 Societal Resilience in the Eastern Mediterranean in the Last Millennium. *Hum. Ecol.* 46, 363–379.  
26 <https://doi.org/10.1007/s10745-018-9995-9>
- 27 Yan, H., Sun, L., Wang, Y., Huang, W., Qiu, S., Yang, C., 2011. A record of the Southern Oscillation Index for the  
28 past 2,000 years from precipitation proxies. *Nat. Geosci.* 4, 611–614. <https://doi.org/10.1038/ngeo1231>
- 29 Yao, J., Xiao, L., Gou, M., Li, C., Lian, E., Yang, S., 2018. Pacific decadal oscillation impact on East China  
30 precipitation and its imprint in new geological documents. *Sci. China Earth Sci.* 61, 473–482.  
31 <https://doi.org/10.1007/s11430-016-9146-2>
- 32 Yiou, P., Servonnat, J., Yoshimori, M., Swingedouw, D., Khodri, M., Abe-Ouchi, A., 2012. Stability of weather regimes  
33 during the last millennium from climate simulations. *Geophys. Res. Lett.* 39.  
34 <https://doi.org/10.1029/2012GL051310>
- 35 Zanchettin, D., Bothe, O., Graf, H.F., Lorenz, S.J., Luterbacher, J., Timmreck, C., Jungclaus, J.H., 2013. Background  
36 conditions influence the decadal climate response to strong volcanic eruptions. *J. Geophys. Res.*  
37 *Atmospheres* 118, 4090–4106. <https://doi.org/10.1002/jgrd.50229>
- 38 Zhang, R., Delworth, T.L., 2006. Impact of Atlantic multidecadal oscillations on India/Sahel rainfall and Atlantic  
39 hurricanes. *Geophys. Res. Lett.* 33. <https://doi.org/10.1029/2006GL026267>
- 40 Zhang, R., Sutton, R., Danabasoglu, G., Kwon, Y.-O., Marsh, R., Yeager, S.G., Amrhein, D.E., Little, C.M., 2019. A  
41 Review of the Role of the Atlantic Meridional Overturning Circulation in Atlantic Multidecadal Variability and  
42 Associated Climate Impacts. *Rev. Geophys.* 57, 316–375. <https://doi.org/10.1029/2019RG000644>
- 43 Zhang, T., Sun, D.-Z., 2014. ENSO Asymmetry in CMIP5 Models. *J. Clim.* 27, 4070–4093.  
44 <https://doi.org/10.1175/JCLI-D-13-00454.1>
- 45 Zhang, Z.-Y., Gong, D.-Y., He, X.-Z., Lei, Y.-N., Feng, S.-H., 2010. Statistical Reconstruction of the Antarctic  
46 Oscillation Index Based on Multiple Proxies. *Atmospheric Ocean. Sci. Lett.* 3, 283–287.  
47 <https://doi.org/10.1080/16742834.2010.11446883>
- 48 Zielhofer, C., Fletcher, W.J., Mischke, S., De Batist, M., Campbell, J.F.E., Joannin, S., Tjallingii, R., El Hamouti, N.,  
49 Junginger, A., Stele, A., Bussmann, J., Schneider, B., Lauer, T., Spitzer, K., Strupler, M., Brachert, T., Mikdad,  
50 A., 2017. Atlantic forcing of Western Mediterranean winter rain minima during the last 12,000 years. *Quat. Sci.*  
51 *Rev.* 157, 29–51. <https://doi.org/10.1016/j.quascirev.2016.11.037>
- 52 Zielinski, G.A., Mayewski, P.A., Meeker, L.D., Whitlow, S., Twickler, M.S., Morrison, M., Meese, D.A., Gow, A.J.,  
53 Alley, R.B., 1994. Record of Volcanism Since 7000 B.C. from the GISP2 Greenland Ice Core and Implications  
54 for the Volcano-Climate System. *Science* 264, 948–952. <https://doi.org/10.1126/science.264.5161.948>
- 55 Zolitschka, B., Francus, P., Ojala, A.E.K., Schimmelmann, A., 2015. Varves in lake sediments – a review. *Quat. Sci.*  
56 *Rev.* 117, 1–41. <https://doi.org/10.1016/j.quascirev.2015.03.019>
- 57  
58  
59  
60  
61  
62  
63  
64  
65

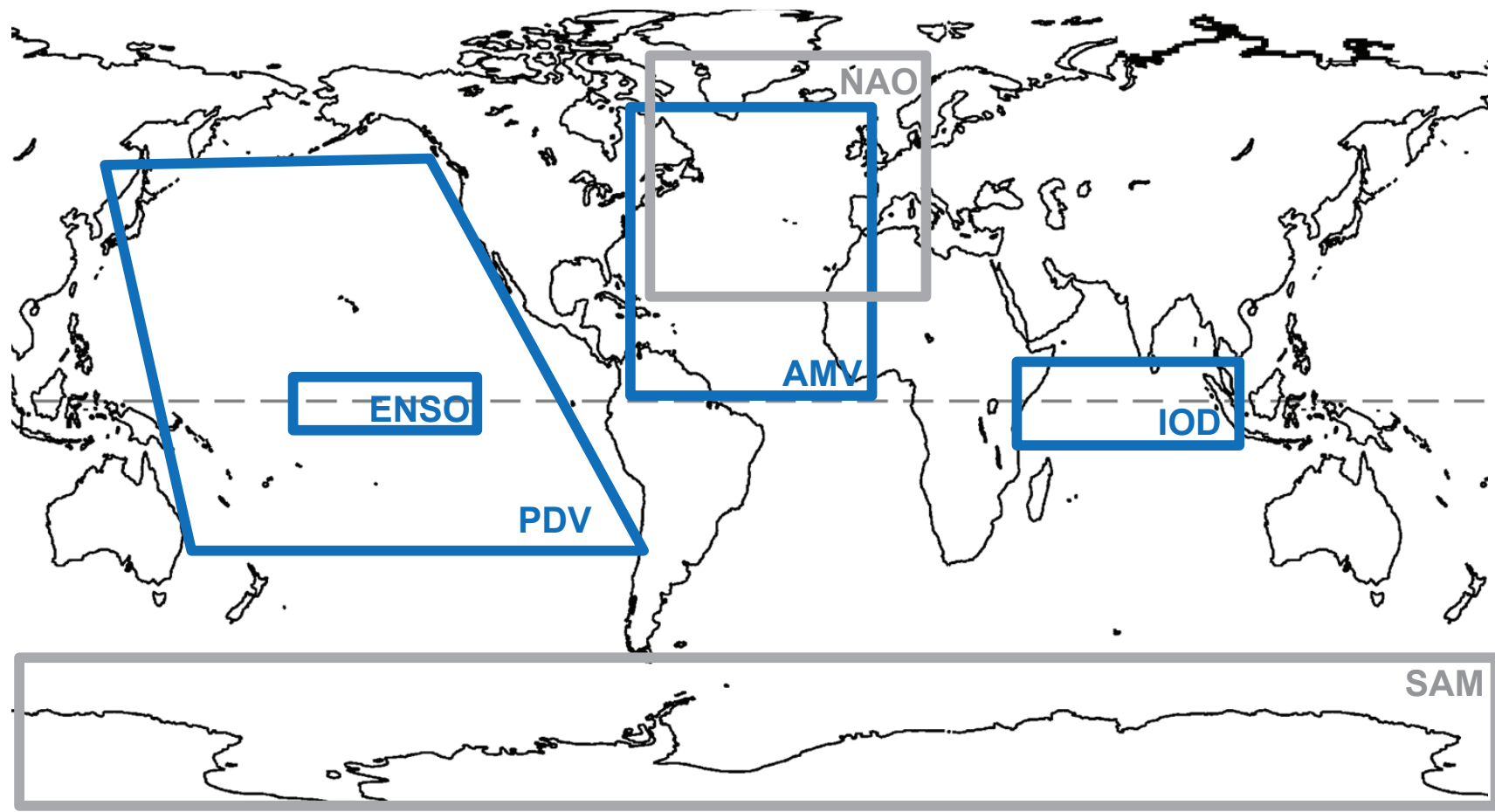
1  
2  
3  
4  
5  
6  
7  
8  
9  
10  
11  
12  
13  
14  
15  
16  
17  
18  
19  
20  
21  
22  
23  
24  
25  
26  
27  
28  
29  
30  
31  
32  
33  
34  
35  
36  
37  
38  
39  
40  
41  
42  
43  
44  
45  
46  
47  
48  
49  
50  
51  
52  
53  
54  
55  
56  
57  
58  
59  
60  
61  
62  
63  
64  
65

Zou, H., Hastie, T., 2005. Regularization and variable selection via the elastic net. *J. R. Stat. Soc. Ser. B Stat. Methodol.* 67, 301–320. <https://doi.org/10.1111/j.1467-9868.2005.00503.x>

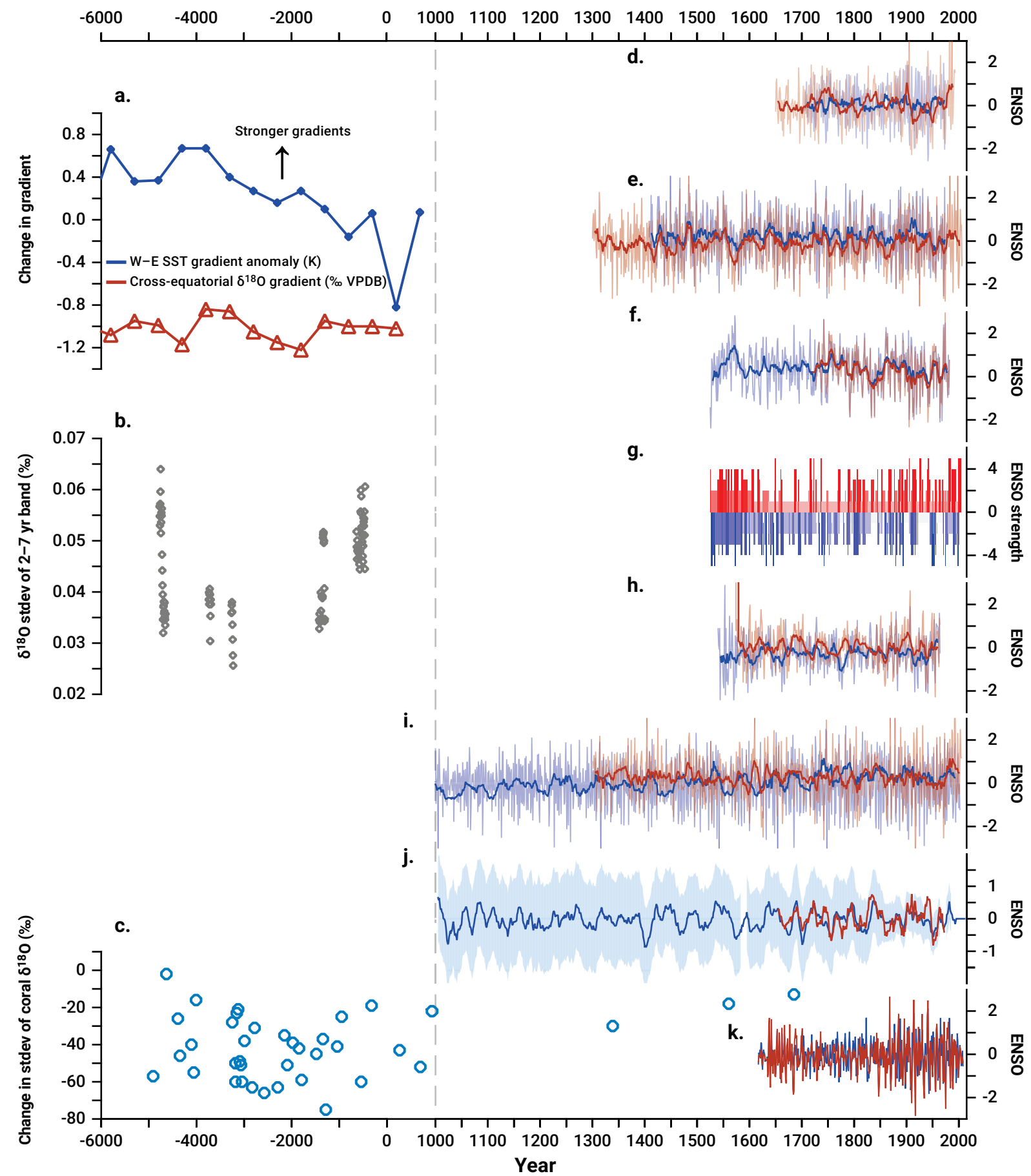
Zubiate, L., McDermott, F., Sweeney, C., O'Malley, M., 2017. Spatial variability in winter NAO–wind speed relationships in western Europe linked to concomitant states of the East Atlantic and Scandinavian patterns. *Q. J. R. Meteorol. Soc.* 143, 552–562. <https://doi.org/10.1002/qj.2943>



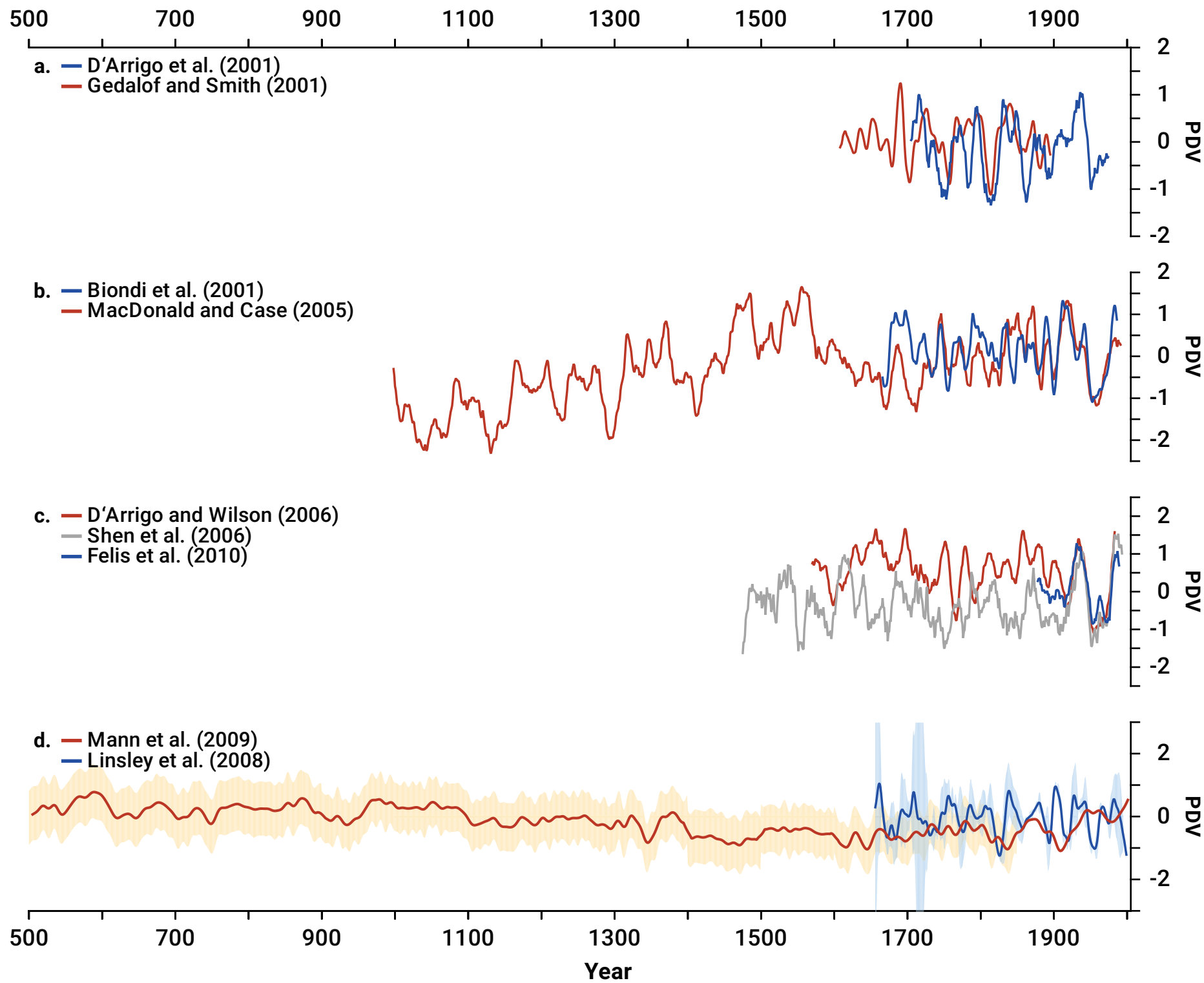
Figure\_1



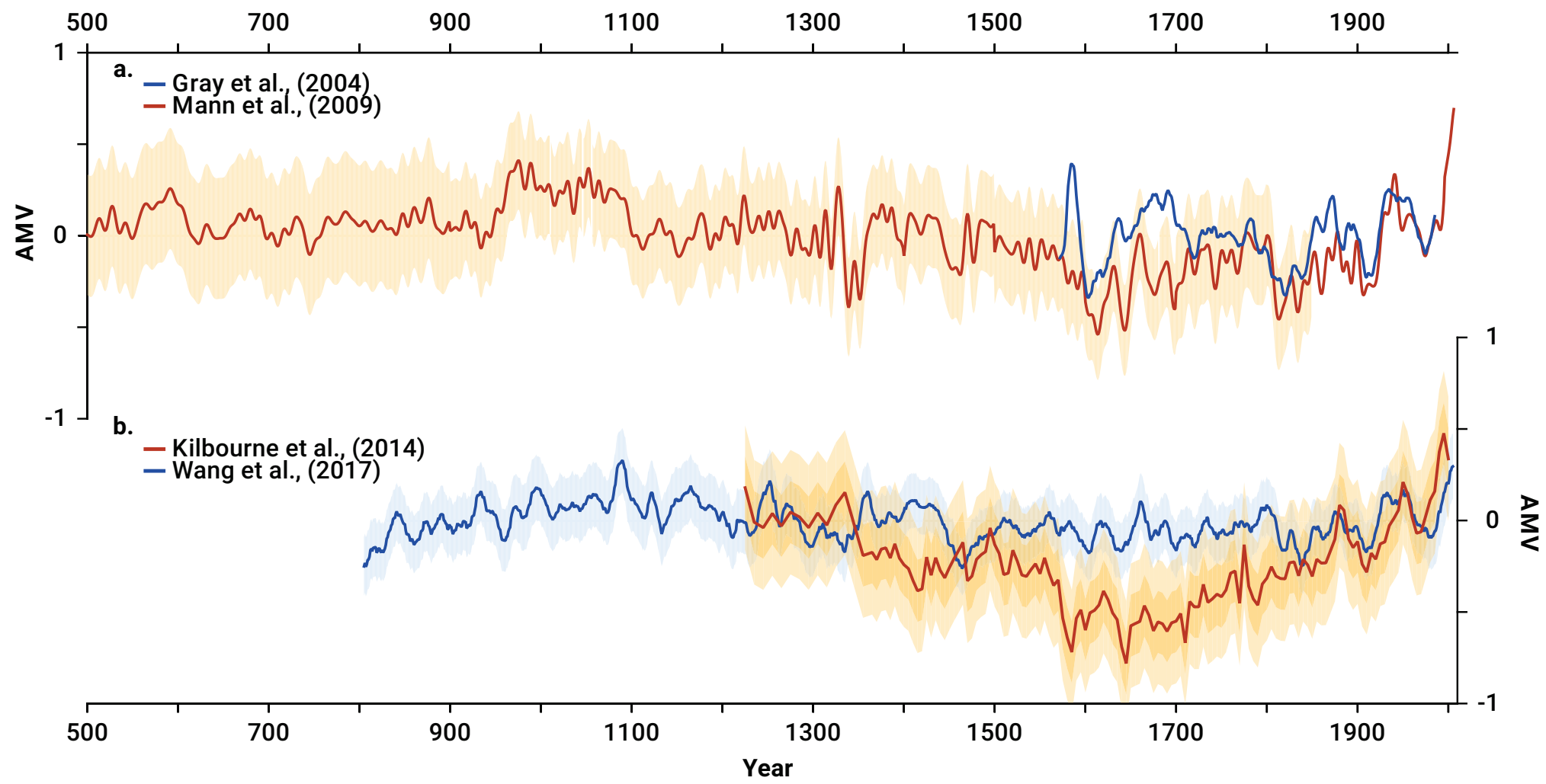
Figure\_2



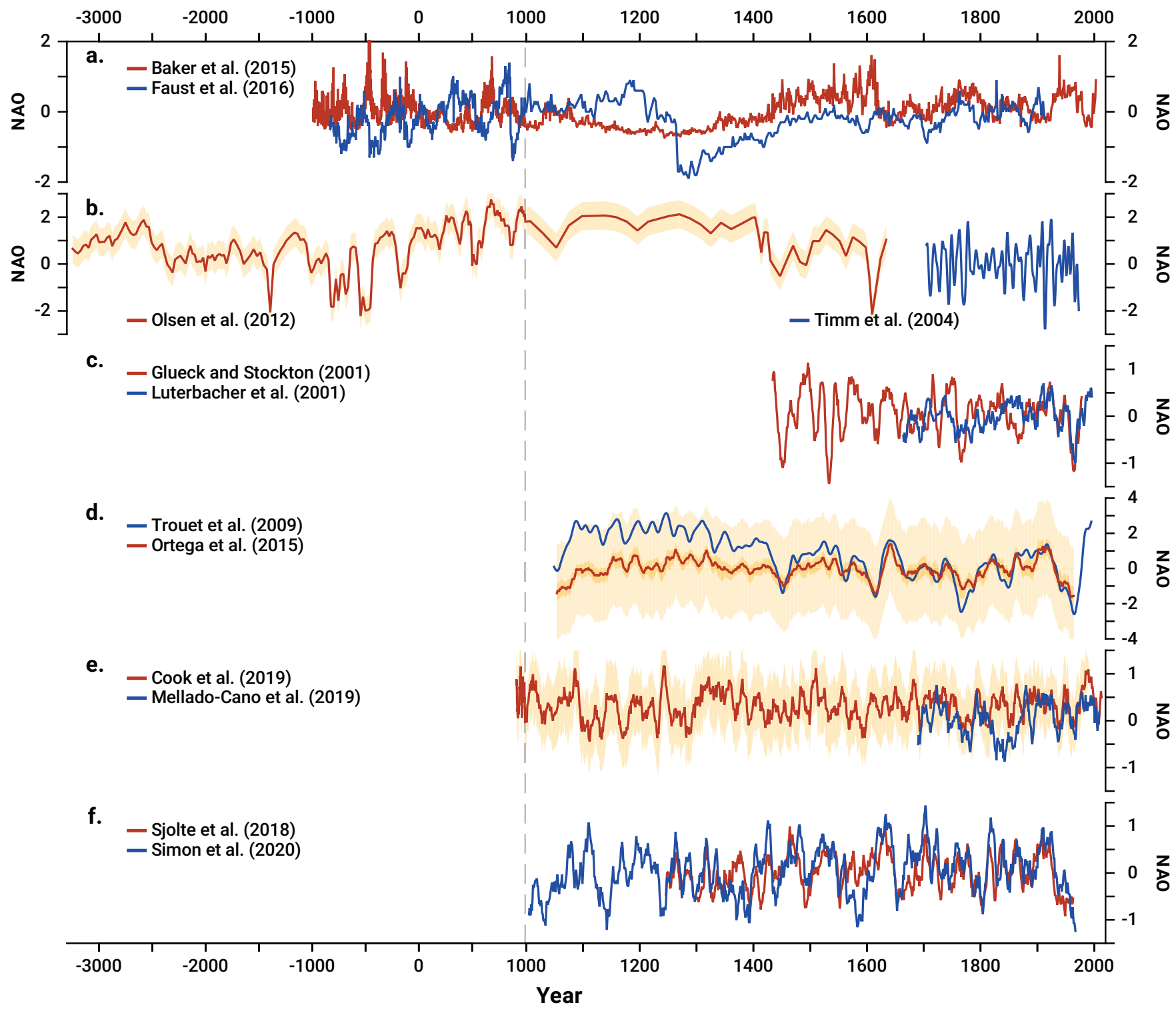
Figure\_3



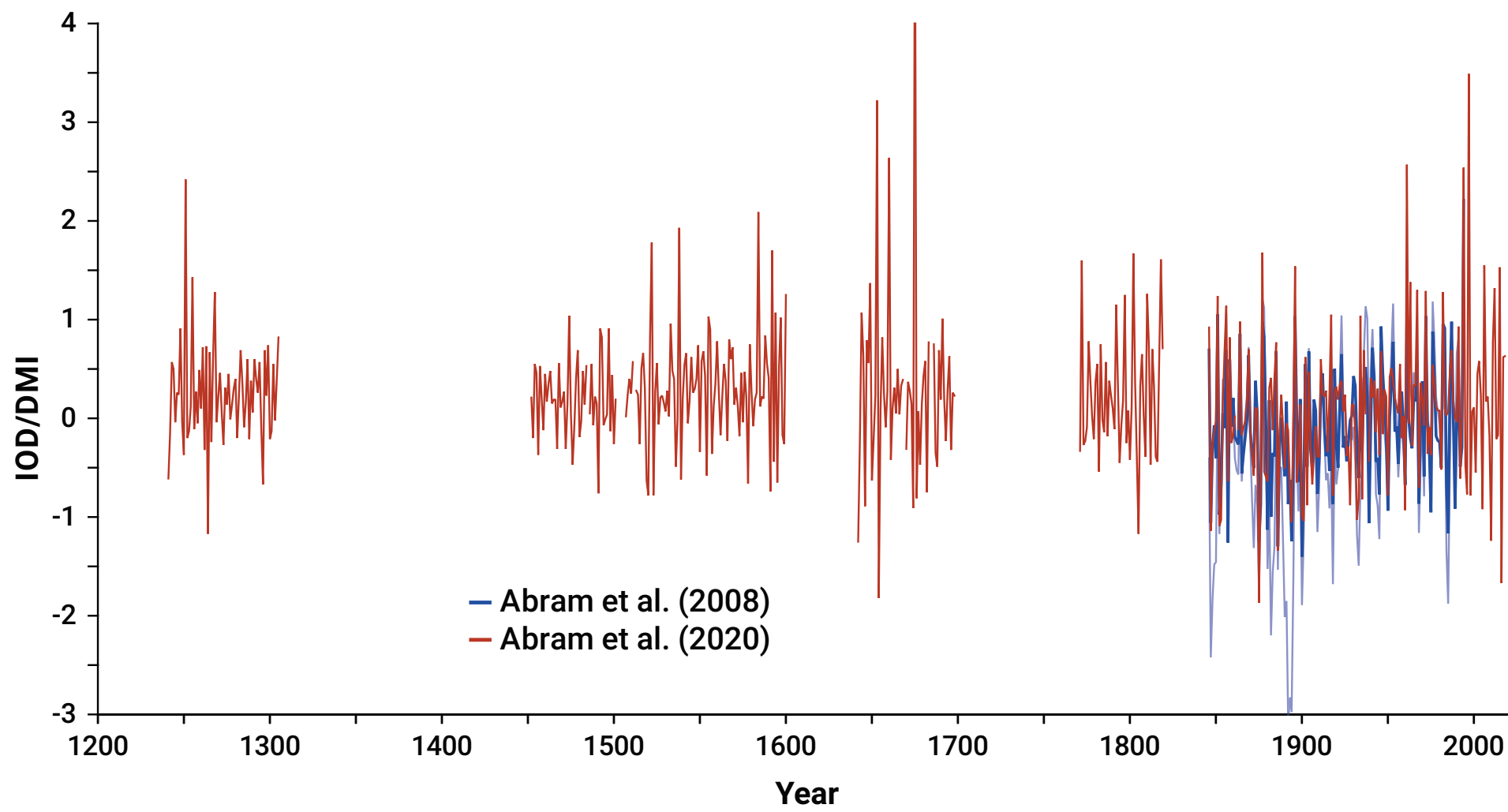
Figure\_4



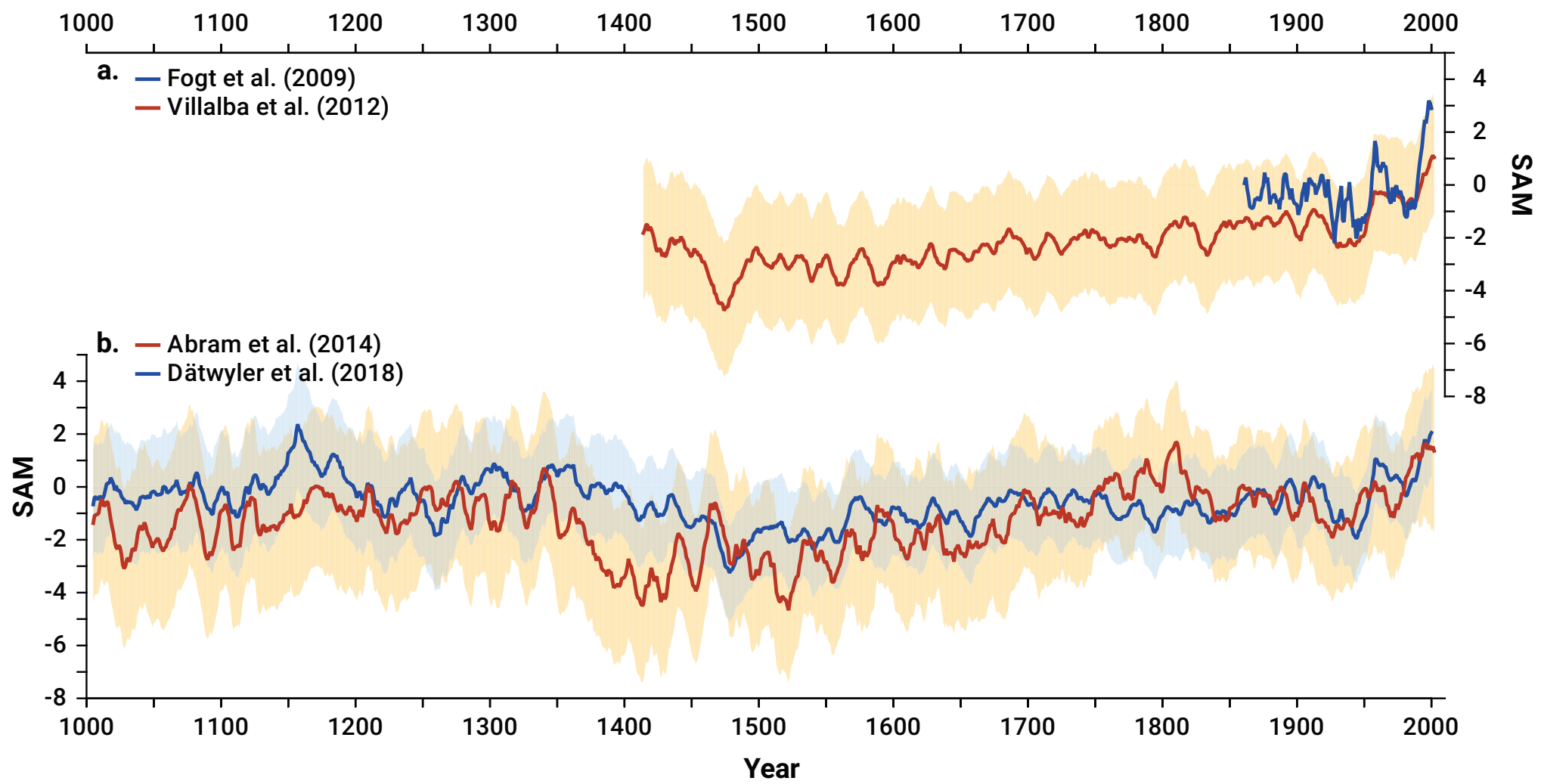
Figure\_5



Figure\_6



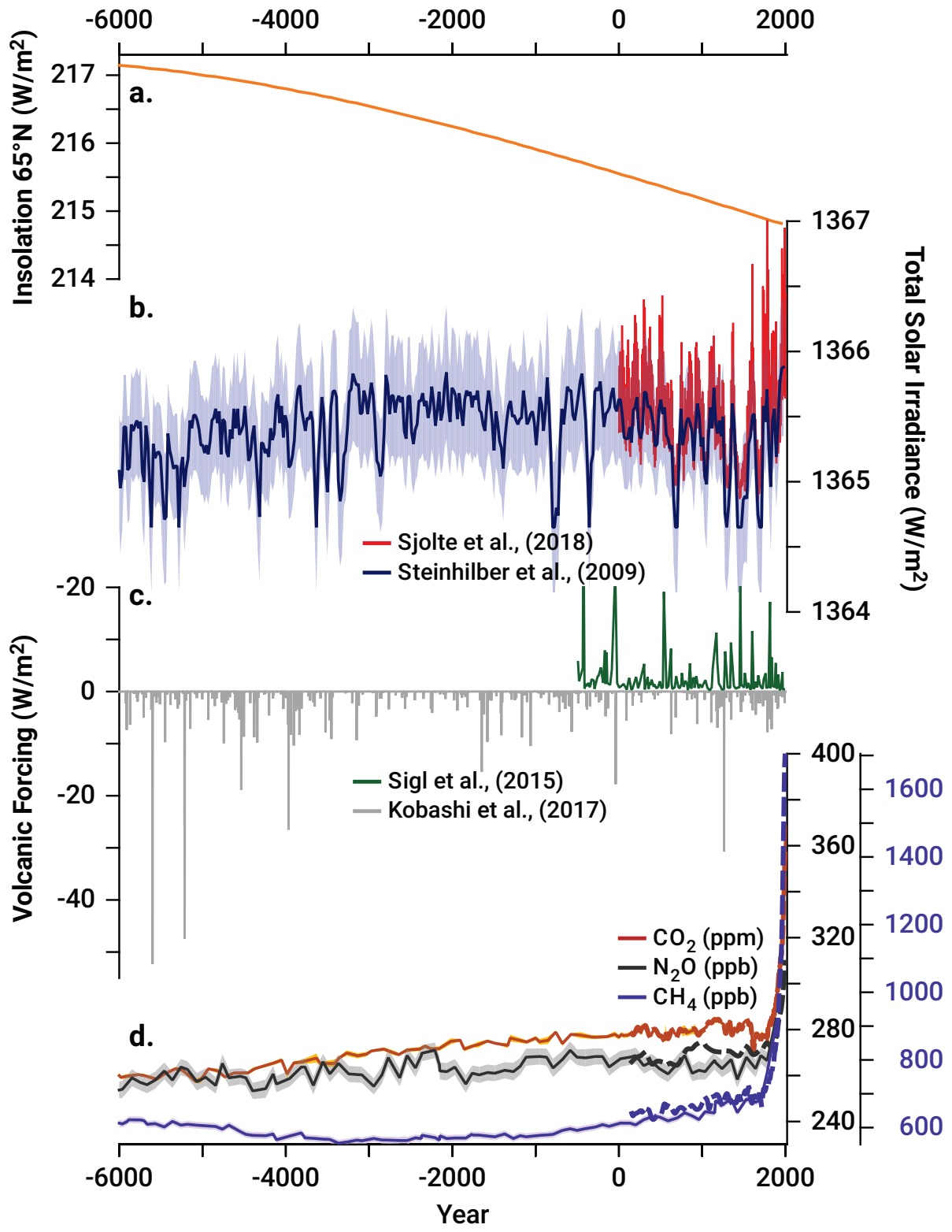
Figure\_7







Figure\_9





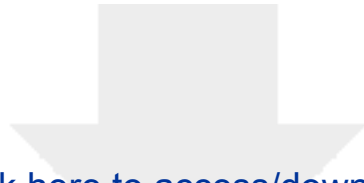
MINISTERIO  
DE CIENCIA, INNOVACIÓN  
Y UNIVERSIDADES



### Declaration of interests

- The authors declare that they have no known competing financial interests or personal relationships that could have appeared to influence the work reported in this paper.
- The authors declare the following financial interests/personal relationships which may be considered as potential competing interests:

Dr Armand Hernández, on behalf of all co-authors



[Click here to access/download](#)

**Supplementary Material**

Modes\_ESR\_AH\_Reviewed\_SupMat.docx

